Technical Report EL-93-25
December 1993

US Army Corps
of Engineers
Waterways Experiment
Station

Microwave Dielectric Behavior of Soils

Report 1
Summary of Related Research and Applications

by *John O. Curtis*
Environmental Laboratory

Approved For Public Release; Distribution Is Unlimited

Prepared for Headquarters, U.S. Army Corps of Engineers

The contents of this report are not to be used for advertising, publication, or promotional purposes. Citation of trade names does not constitute an official endorsement or approval of the use of such commercial products.

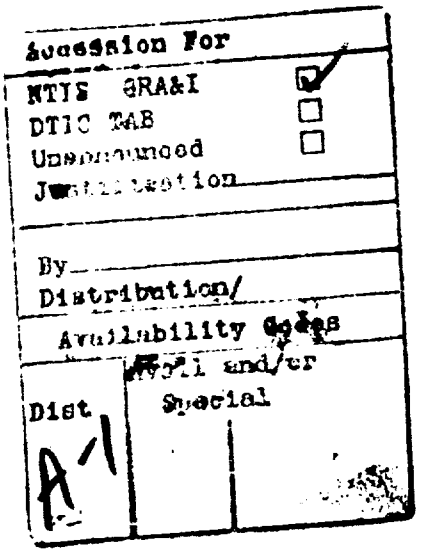

PRINTED ON RECYCLED PAPER

Technical Report EL-93-25
December 1993

Microwave Dielectric Behavior of Soils

Report 1
Summary of Related Research and Applications

by John O. Curtis
Environmental Laboratory

U.S. Army Corps of Engineers
Waterways Experiment Station
3909 Halls Ferry Road
Vicksburg, MS 39180-6199

Report 1 of a series

Prepared for U.S. Army Corps of Engineers
Washington, DC 20314-1000

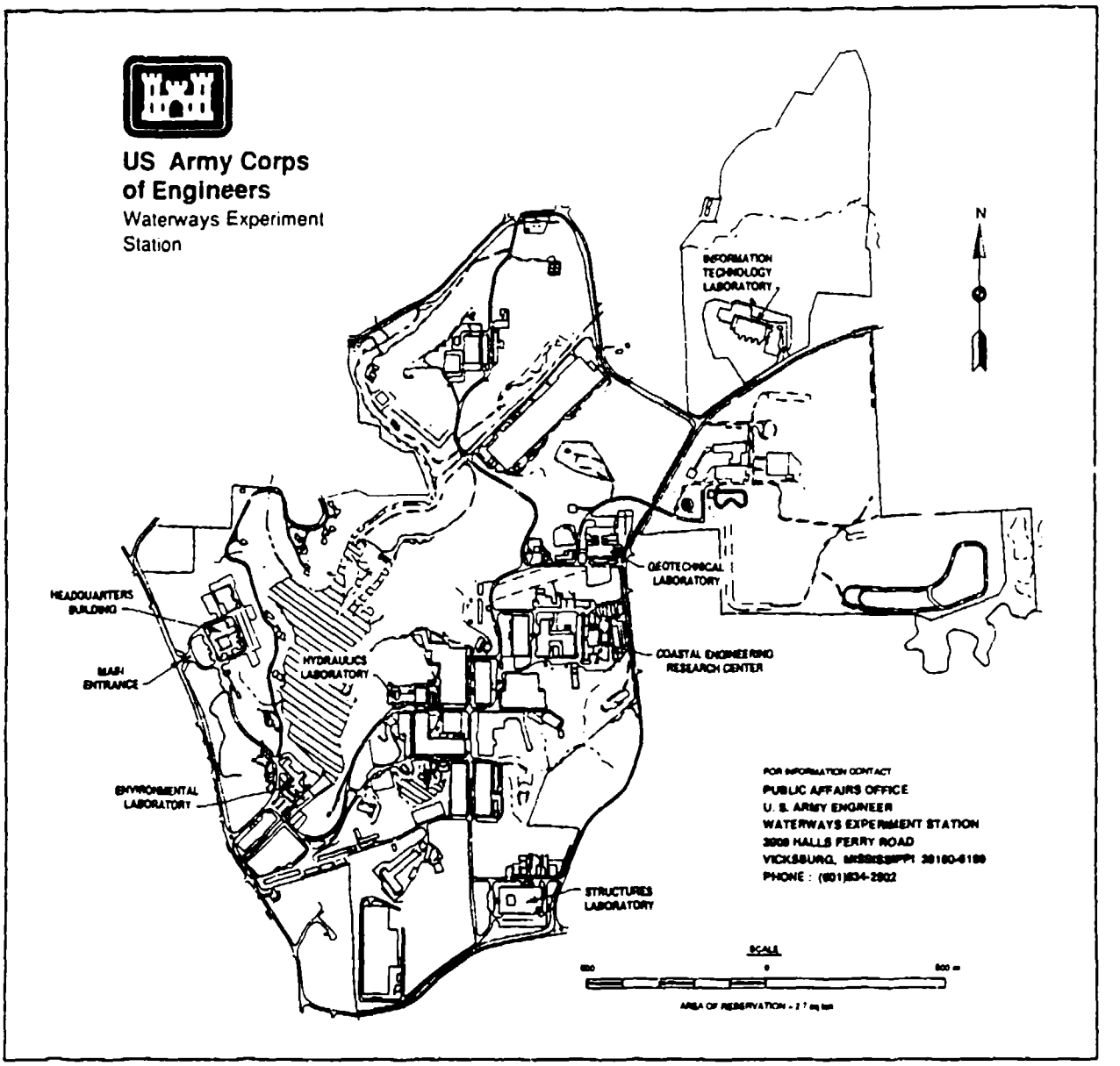

Waterways Experiment Station Cataloging-In-Publication Data

Curtis, John O.

Microwave dielectric behavior of soils / by John O. Curtis ; prepared for U.S. Army Corps of Engineers.

3 v. : ill. ; 28 cm. — (Technical report ; EL-93-25)

Contents: Report 1, Summary of related research and applications — Report 2, A unique coaxial measurement apparatus — Report 3, Measurements and modeling.

Includes bibliographical references.

1. Soils — Electric properties. 2. Dielectric measurements. 3. Microwave measurements. 4. Remote sensing. I. United States. Army. Corps of Engineers. II. U.S. Army Engineer Waterways Experiment Station. III. Title. IV. Series: Technical report (U.S. Army Engineer Waterways Experiment Station) ; EL-93-25.

TA7 W34 no.EL-93-25

Contents

List of Figures

Preface

The study reported herein was conducted within the facilities of the Environmental Laboratory (EL) of the U.S. Army Engineer Waterways Experiment Station (WES) during the period of May 1991 to June 1992 for Headquarters, U.S. Army Corps of Engineers. General supervision was provided by Drs. Daniel Cress and Victor Barber, Acting Chiefs, Environmental Systems Division (ESD), EL, Dr. Raymond L. Montgomery, Chief, Environmental Engineering Division, EL, and Dr. John Harrison, Director, EL.

Dr. John O. Curtis collected the information and prepared the report under the direct supervision of Messrs. Malcolm Keown and Kenneth Hall, Chiefs, Environmental Constraints Group, ESD.

At the time of publication of this report, Director of WES was Dr. Robert W. Whalin. Commander was COL Bruce K. Howard, EN.

This report should be cited as follows:

> Curtis, J. O. (1993). "Microwave dielectric behavior of soils; Report 1, Summary of related research and applications," Technical Report EL-93-25, U.S. Army Engineer Waterways Experiment Station, Vicksburg, MS.

Conversion Factors, Non-SI to SI Units of Measurement

Non-SI units of measurement used in this report can be converted to SI units as follows:

Multiply	By	To Obtain
degrees (angle)	0.01745329	radians
feet	0.3048	meters
inches	2.54	centimeters

1 Introduction

New and improved methods of remote sensing have increased the understanding of Earth's origins, its resources, and those processes that contribute to its dynamic (on a large time scale) nature. Scientists and engineers from many disciplines are constantly exploring new ways to quantify the Earth's properties for their particular applications. Among these methods are measurements of electromagnetic energy in many different wavelength regimes, both passive and active. The development of small powerful sources and ultrasensitive receivers along with improved data processing capabilities has fostered renewed interest in measurements of the Earth within the microwave region of the spectrum, where wavelengths in air range from a few millimeters to several meters.

Natural terrain surfaces consist of bare soils, rocks, vegetation, and water. This study was initiated with the hope of making a meaningful contribution to the understanding of microwave interactions with natural terrain. In particular, the focus here is to summarize what is currently known about the measurement and modeling of the electrical properties of well-characterized soils. Follow-on reports will deal with a new measurement capability recently developed at the U.S. Army Engineer Waterways Experiment Station (WES) in Vicksburg, MS, and the interpretation of data collected at WES using those new measurement resources. Most of the information contained in this series of reports is drawn from a doctoral research program recently completed by the author (Curtis 1992).

Reasons for Studying Electrical Properties of Soils

Soil moisture measurements

The dominant factor that controls the electrical behavior of soils is the presence of water (Topp, Davis, and Annan 1980). Obviously one would hope to take advantage of this experimental fact to develop a means of accurately and quickly measuring the moisture in soils without having to collect numerous samples in the field, weigh them, dry them for extended periods of time, and weigh them again to obtain either a gravimetric (weight of water/weight of dry

soil) moisture content or a more useful volumetric (volume of water/volume of soil sample) moisture content.

Numerous attempts have been made to develop a useful method for measuring soil moisture content. All have met with varying degrees of success and none has proven accurate under all conditions. For example, a technique that involves burying radar transmit and receive antennas in the soil and relating the measurements of attenuated received signals to moisture content (Birchak et al. 1974) is destructive to the soil fabric (the way in which soil particles are arranged), is very much controlled by the fabric and the size distribution of particles, and precludes the use of the same instrument in multiple locations (nature is not homogeneous) as well as the ability to easily repair defective equipment.

Another approach for making field measurements of soil moisture taken by some researchers (that also has numerous application in the biomedical field) is that of measuring the change in fringe capacitance of an open-ended coaxial probe (Thomas 1966; Brunfeldt 1987; Gabriel, Grant, and Young 1986). When pressed against a soil whose properties are unknown, the resulting change in capacitance produced by the impedance mismatch is related to electrical properties through calibration relationships. Problems arising from these measurements include the need to have proper contact between the probe tip and the soil surface, the fact that the volume of material associated with the fringe capacitance is quite small (1 cm^3 or less), and that calibration conditions simply cannot account for all of the dielectric loss mechanisms that exist in natural soils. The losses in moist soils can be highly frequency dependent over a range of several frequency decades on the electromagnetic spectrum. A recent variation on the open-ended probe measurement scheme involves the use of a waveguide section instead of a coaxial device (Parchomchuk, Wallender, and King 1990).

The concern over small sample volumes can be overcome with a redesign of the open-ended coaxial probe that replaces the solid outer conductor with several pointed tines (Campbell 1988) which allows for the probe to be pushed into the surface of soft soils. The volume of soil enclosed by such probes can easily be tens of cubic centimeters. The tined coaxial probes that have been built to date operate in a frequency range that is very much subject to the material-dependent loss mechanisms alluded to above. Research continues that is directed to better understanding these various mechanisms and to fabricate a probe that operates in a frequency range that is not subject to such material-dependent anomalies.

Subterranean Investigations

Many types of electrical measurements in soils (and rocks) are used to understand what lies beneath the Earth's surface (Telford et al. 1984). Among these are various schemes for measuring soil resistivity as well as the attenuation of propagating electromagnetic waves.

Resistivity measurements. Resistivity data in soils are collected by injecting known currents (usually of a frequency less than 60 Hz: alternating current (AC) required to minimize effects of charge buildup on the probe) into the ground and measuring potential differences across pairs of nearby electrodes. Assuming homogeneous media and uniform resistivity, it is possible to calculate from the potential differences an apparent resistivity of the earth material. These measurements will be affected by the presence of water in the soil or rock, by the presence of mineral compounds that could go into ionic solution with available water, and by the physical structure of the subsurface terrain itself. This being the case, resistivity measurements are useful as a measure of subsurface water volume, the locations of mineral deposits, and subsurface structure.

Electromagnetic wave propagation. Another method of making electrical subsurface measurements involves the transmission of electromagnetic waves into the soil and detection of energy that results from waves reflected from subsurface anomalies. Having the ability to track wave propagation in time, either by pulsing the source or sweeping over a known frequency band in some controlled manner, means that electromagnetic wave propagation methods of subterranean investigations are particularly useful for locating the depth of electrical anomalies such as the water table in sandy soil (Olhoeft 1983; Stewart 1982; Wright, Olhoeft, and Watts 1984), buried pipes or wires, or cavities such as tunnels or caves (Ballard 1983). Other applications include the delineation of stratified media (Lundien 1972) and determination of the thickness of ice and frost layers (Jakkula, Ylinen, and Tiuri 1980; O'Neill and Arcone 1991).

There are some practical bounds on the utility of radio frequency systems to conduct subterranean investigations due to the phenomenon of "skin depth" (Appendix A), a measure of the attenuation of the electromagnetic energy as it travels through the medium. For relatively low-frequency sources (about 200 MHz), it can be shown that low-loss soils such as dry sands can possess a skin depth of about 10 to 15 m, while high-loss soils such as wet silts and clays may have skin depths of only a few centimeters. Modern radio frequency receivers are extremely sensitive devices, often having a dynamic range of 50 to 100 db. The signal at skin depth represents about an 8.7-db loss in power or a two-way loss at the receiver for reflected signals of about 17.4-db. It is certainly not inconceivable that radio frequency receivers should be capable of successfully detecting reflected signals from subterranean anomalies at depths of two to three skin depths or more.

Remote sensing of environment

Virtually all remote sensing of the environment from airborne or spaceborne platforms involves the measurement of electromagnetic radiation from the Earth's surface and/or atmosphere. Passive surveillance involves measurements of emitted radiation and that reflected from natural sources such as the sun, the atmosphere, and surrounding terrain. Active remote sensing

measurement systems include a source for illuminating the target of interest. Whether passive or active, whether visual, thermal infrared, microwave, or millimeter wave sensors are utilized, remote sensing is the collection and interpretation of electromagnetic radiation and, as such, demands an understanding of the dielectric properties of those materials being observed.

Environmental remote sensing applications form a list that grows yearly as electronic components are improved and data collection and processing hardware and software become faster, more reliable, and less costly. For example, satellites can provide worldwide surveys of land-use patterns to monitor the threat of urbanization, waste disposal, and erosion of the land (Colwell 1983). Similar systems (including those mounted in aircraft) can monitor the health of vegetation to keep abreast of such things as loss of forest and the potential for food shortages. Sea traffic in the far northern and southern shipping lanes can be made safer through the use of airborne and spaceborne sensors to detect ice hazards.

One of the more obvious applications for microwave remote sensing devices is that of conducting surface moisture surveys to help predict groundwater availability and the potential for flooding. Attempts have been made to relate soil moisture to both laboratory reflectance data (Lundien 1966) and to airborne sensor backscatter measurements (Ulaby, Cihlar, and Moore 1974; John 1992). Careful airborne sensor measurements might provide a first approximation to the complex dielectric constant of the soil near the surface.

Because of the difference in dielectric behavior of liquid water and various forms of ice, it may be possible to use airborne sensors to detect freezing and thawing (Wegmuller 1990) in remote locations that could be used to predict spring runoff conditions and all that encompasses for agricultural applications, the effects on the fishing industry, and the anticipation of flooding in built-up areas. Military analysts are concerned about soil moisture conditions because of its impact on trafficability, the ability of vehicles to move effectively over natural terrain.

Another remote sensing application is the mapping of exposed soils and rocks in remote areas of the world from high-flying aircraft or satellites, which might prove useful for geomorphological studies (Swanson et al. 1988) or even mineral exploration. A less obvious but recent application of microwave remote sensing in soils dealt with archeological surveys in desert areas (Berlin et al. 1986; McCauley et al. 1986).

Others

While the above paragraphs emphasize some of the most obvious and useful applications of a better understanding of soil electrical properties, others have been noted in the literature. For example, some researchers have attempted to relate electrical property measurements to the physical properties of soils (Campbell and Ulrichs 1969, Hayre 1970; Arulanandan and Smith

1973; Madden 1974). Of course, nothing has been said about the military's need to better understand the microwave response of soils that form the backgrounds to military targets; i.e., when and why does clutter become a source of target-like signatures. Outside the topic of soils, studies of the microwave response of foodstuffs have direct application to quality control concerns in the food industry (Nelson 1973, 1983).

Another new application of this technology that is closely related to the discussion on soil moisture is that of detecting liquid ground contaminants, either near the surface or at arbitrary depths using a specially fabricated probe. If, as will be argued later, polarizable liquids can be characterized by a unique frequency of peak losses due to the dielectric relaxation phenomenon, then a probe could be designed to measure losses over a frequency span that is broad enough to detect a peak loss frequency and, coupled with the results of a thorough experimental program, to identify the particular contaminant.

Complex Dielectric Constant

Background information for this study would not be complete without a definition of terms that will be used. Consider, for the moment, Ampere's law written for linear, isotropic materials and for current density divided into a component due to the motion of free charges such as electrons and ions and one due to other factors such as time variation of polarization and magnetization (Gaussian units are used throughout the text. For other units see the excellent Appendix on Units and Dimensions in Jackson (1975)).

$$\nabla \times \vec{H} = \left(\frac{4\pi}{c}\right)\vec{J}_f + \left(\frac{1}{c}\right)\frac{\partial \vec{D}}{\partial t} \tag{1}$$

where

H = the magnetic field

c = the speed of light in a vacuum

$\vec{J}_f$ = the current density due to free charges

$\vec{D}$ = the electric displacement.

If one also assumes that the magnetic contribution to free charge forces is small relative to that of the electric field, $\vec{E}$, then one can rewrite Equation 1 using Ohm's law.

$$\vec{J}_f = \sigma\vec{E} \tag{2}$$

where σ is the conductivity of the medium. Furthermore, having assumed a linear isotropic material, one can write the electric displacement in terms of the electric field as

$$\vec{D} = \varepsilon \vec{E} \tag{3}$$

where ε is the electric permittivity of the material. (It is understood that if ε is frequency dependent, Equation 3 is not rigorously correct in the time domain, but rather that the electric displacement and electric field are related through Fourier transforms of the frequency-dependent permittivity (Jackson 1975, p. 307). Adding this notational complexity would only serve to cloud the qualitative development intended within this section.) Then Ampere's law can be written as

$$\nabla \times \vec{H} = \frac{4\pi\sigma}{c}\vec{E} + \frac{\varepsilon}{c}\frac{\partial \vec{E}}{\partial t} \tag{4}$$

Thus, the flow of current in a medium is both proportional to the applied electric field and to the time rate of change of that field. By analogy with simple electrical circuits, permittivity is a measure of the electrical capacity or capacitance of the media, that is, its ability to store charge. Capacitor plates in a vacuum collect and give up charge; thus, there is a permittivity of free space, ε_0 (unity in Gaussian units). Capacitor plates filled with a polarizable material exhibit a higher capacitance due to material polarization such that the material permittivity can be written as

$$\varepsilon = \varepsilon_0(1 + 4\pi X_e) \tag{5}$$

where X_e is the electric susceptibility for linear materials and relates the material polarization to electric field. The value of material permittivity normalized to the permittivity of free space is what is called the dielectric constant (or relative permittivity).

$$\varepsilon \equiv \frac{\varepsilon}{\varepsilon_0} = 1 + 4\pi X_e \tag{6}$$

From this point on in the text, ε will refer to the relative permittivity.

As will be shown by the data, the dielectric constant of real materials is frequency dependent (a characteristic referred to as "dispersion"). At relatively low frequencies, polarizable particles, which are effectively electric dipoles, are able to rotate or align themselves with the changing electric field with little loss in energy. However, as will be discussed later, several other mechanisms are at work that do result in electrical energy losses, particularly at frequencies less than 100 MHz. As the frequency goes up, the dipoles cannot keep up

completely with the electric field, resulting in a phase shift in current that peaks in the 10 to 20 GHz frequency range and is quite temperature dependent. Finally, at frequencies well above the peak loss range, the dipoles do not even respond, resulting in a reduction of real capacitance to its optical value that is due to electronic polarizability (Feynman, Leighton, and Sands 1964). This frequency-dependent loss mechanism can be modeled by a complex dielectric constant

$$\varepsilon = \varepsilon' + i\varepsilon'' \tag{7}$$

where ε'' reflects the phase lag in the particle motion. Finally, then, Ampere's law could be written as

$$\nabla \times \vec{H} = \frac{4\pi\sigma}{c}\vec{E} + \left(\frac{\varepsilon'}{c} + i\,\frac{\varepsilon''}{c}\right)\frac{\partial \vec{E}}{\partial t} \tag{8}$$

If one further assumes that the material is subjected to a sinusoidal electric field

$$\vec{E} = \vec{E}_0 e^{-i\omega t} \tag{9}$$

then

$$\nabla \times \vec{H} = \left(\frac{4\pi\sigma}{c} + \frac{\omega\varepsilon''}{c} - i\,\frac{\omega\varepsilon'}{c}\right)\vec{E}, \tag{10}$$

The first two terms on the right hand side of Equation 10 represent the conductive nature of the material, the flow of energy that is associated with losses. The third term is a measure of its energy flow due to its polarizability. All of the terms within the square brackets are collectively referred to as the admittance of the material, being the ratio of current to voltage. The first two terms represent the conductance of the material, and the last term represents its susceptance. It is clear, then, that $\omega\varepsilon''/4\pi$ can be thought of as a dielectric conductivity.

It appears that electrical property measurements reported in the literature seldom, if at all, distinguish between the two physically different loss mechanisms. In fact, the terms ε'' and $4\pi\sigma/\omega$ are often used interchangeably. This observation, coupled with the fact that the engineering community uses a notational and sign convention for dealing with dielectric properties that is different from that used by physicists and chemists, makes reading of the literature often quite burdensome.

2 Electrical Properties of Water

Certainly, over the range of the electromagnetic spectrum from direct current (DC) to millimeter waves, the single most important factor in determining the electrical behavior of soils is the presence of water. Whether as a solvent that provides a medium and path for ionic conduction, or as particles that bond to clay changing the electrochemical characteristics of the soil, or as a source of dipoles that lead to high-frequency residual dielectric conduction, water has a major impact on how the moist soil interacts with electromagnetic fields. For these reasons, a study of the electrical properties of moist soils should include a study of the electrical properties of water.

Summary of Data on Pure Water

The available literature on electrical measurements of water show a consensus on several points. First, the so-called static (frequency <100 MHz) dielectric behavior of pure, deionized water is very well defined over a broad range of temperatures (Hasted 1973). Second, there is a loss mechanism (dipole relaxation) at higher frequencies (greater than 1 GHz) that can be modeled in a rather simple fashion and for which data is highly repeatable (Kaatze 1986). Third, fresh water exhibits low-frequency conductivity losses. Finally, seawater and saline solutions have low-frequency losses that are a couple of orders of magnitude higher than fresh water. There seems to be little, if any, information on the electrical behavior of pure, deionized water in the frequency range between 100 MHz and 1 GHz.

Figure 1 is a graphical representation of the complex dielectric constant for liquid fresh water as a function of temperature. These curves were plotted from empirical relationships developed by Ray (1972), for which excellent correlation between the empirical fits and actual data was clearly demonstrated. A description of the models for losses at higher frequencies follows.

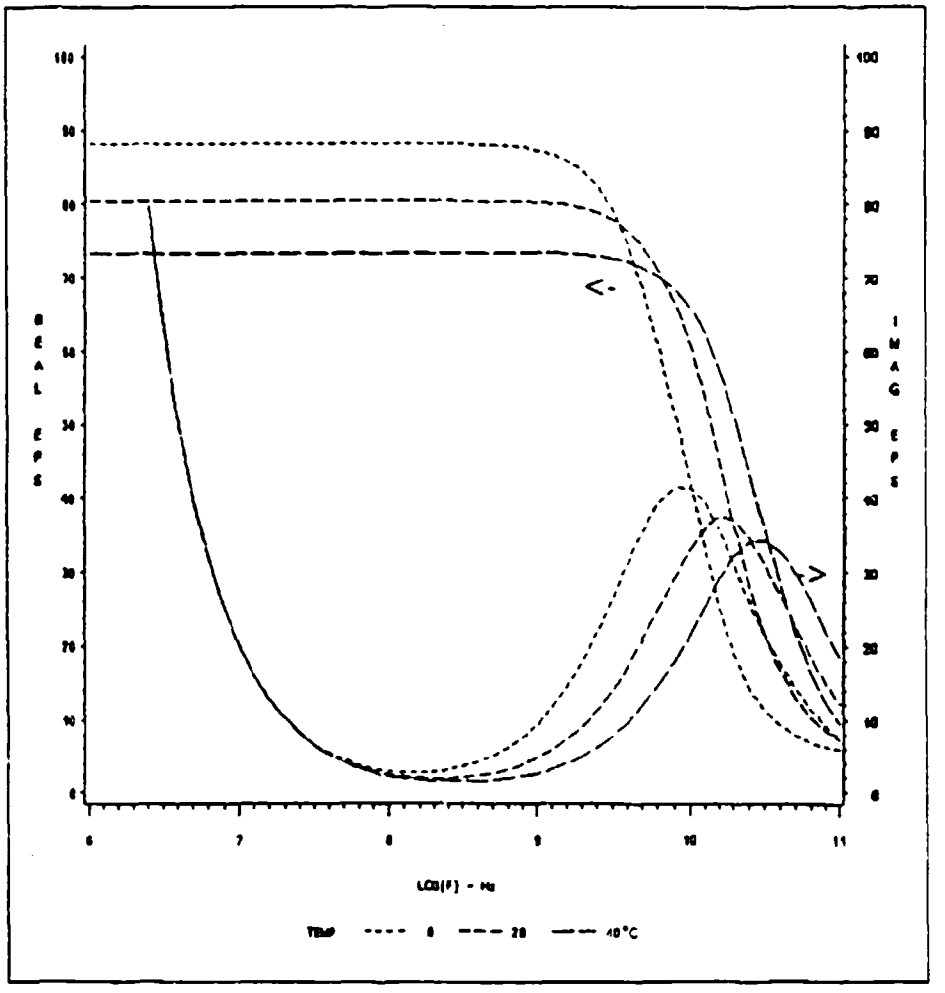

Figure 1. Complex dielectric constant for liquid water as a function of temperature (analytical models after Ray (1972))

Microwave Frequency Loss Mechanisms

Breaking of hydrogen bonds

The precise physical structure of liquid water is unknown. A physical model of free water molecules (H_2O) is accepted as consisting of two hydrogen atoms bonded to an oxygen atom in a V-shape with an angle of 104.5 deg[1] formed by lines through the hydrogen protons and meeting at the center of the oxygen nucleus. Viewing such a molecule along the normal to the plane through the bond angle using the point charge model of the water molecule

[1] A table of factors for converting non-SI units of measurement to SI units is presented on page viii.

shown in Figure 2, one can compute that the free water molecule has a dipole moment with a value of 1.83×10^{-18} electrostatic units. The molecule has two positively charged "corners" at the hydrogen protons and two negatively charged corners at the electron pairs that are not shared.

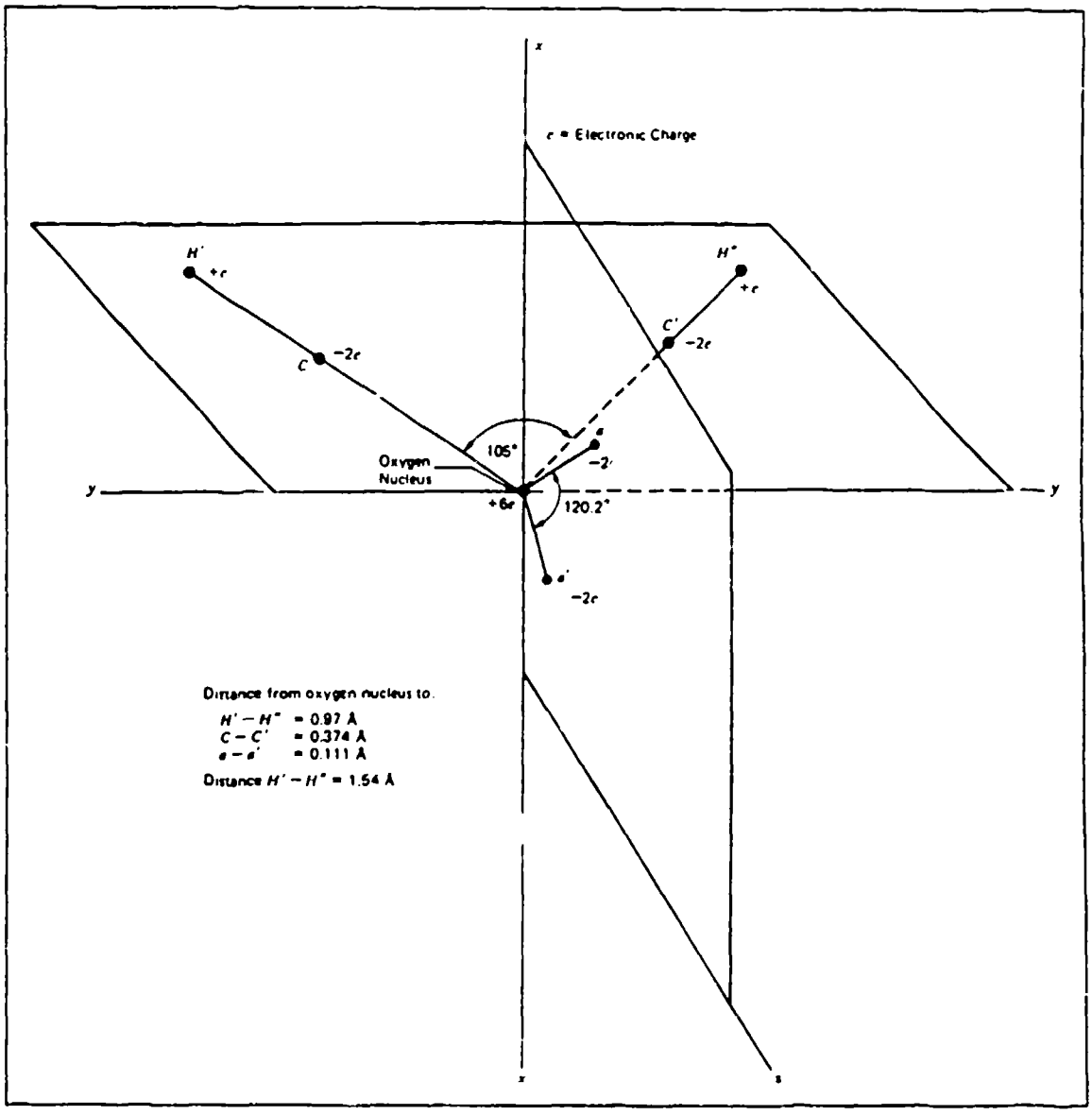

Figure 2. Point charge model of free water molecule (from Mitchell (1976))

Hydrogen bonds are formed when one of these positive corners bonds to the negative corner of a neighboring molecule with the resultant sharing of a hydrogen proton. Each free molecule, therefore, has the capability of having four neighboring molecules bonded to it. In fact, this model might predict that all of the H_2O molecules might be bonded together. Of course this cannot be so because of the liquid nature of water. This is not even true for ice (Hasted

1973). Further experimental evidence is needed to help postulate a reasonable pure liquid water physical structure.

Given that the individual water molecules are dipoles (which is supported by the fact that pure water does exhibit a relatively high static permittivity of around 80), then one could reasonably assume that the dominant high-frequency loss mechanism shown in Figure 1 is, in fact, associated with the dipoles not being able to keep up with the rapidly changing electric field. Switching off a static electric field applied to a sample of water would produce a finite, albeit small, delay in the material returning to an unpolarized state (relaxation). Such behavior could be modeled by

$$P \propto e^{-t/\tau} \tag{11}$$

where

P = the polarization of the material

t = time

τ = a characteristic of the material called its relaxation time

The rate of change of polarization is then

$$\frac{dP}{dt} \propto \frac{1}{\tau} P \tag{12}$$

Carrying this argument a bit further, one can assume that the relaxation process behaves as a temperature dependent chemical reaction for which

$$rate\ of\ reaction = k\,[S] \tag{13}$$

where

k = the rate constant, or the probability of the reaction taking place

$[S]$ = the concentration of reacting material

Now, Arrhenius postulated that the rate constant goes like (Grimshaw 1971)

$$k = Ce^{-\frac{A}{RT}} \tag{14}$$

where

A = the activation energy, or the energy needed to overcome some equilibrium state

R = the universal gas constant

T = the absolute temperature

Drawing parallels between the hypothesized time rate of change of material polarization and Arrhenius' rate of chemical reaction by thinking of polarization as concentration and the inverse of the relaxation time as the rate constant, one could write that

$$\frac{1}{\tau} = Ce^{-\frac{A}{RT}} \tag{15}$$

or

$$\ln\left(\frac{1}{\tau}\right) \alpha - \frac{A}{R}\left(\frac{1}{T}\right) \tag{16}$$

If measurements of $1/\tau$ (model developments in the next section will show that $1/\tau$ is the radial frequency at peak loss) as a function of temperature plotted semilogarithmically as a straight line, then one could estimate the activation energy required for that process to take place from the slope of the curve.

Ray's empirical fit for liquid water includes a relationship between the relaxation wavelength and temperature that looks just like Equation 15. A simple calculation results in an estimate for activation energy of water to be about 5.4 kcal/mole, which is about the energy required to break a hydrogen bond (Cotton and Wilkinson 1972). In other words, hydrogen bond breaking becomes a likely candidate for describing the relaxation process in liquid water and is, therefore, an indication of water structure.

Debye relaxation model

The experimental data on the electrical behavior of water clearly demonstrate a frequency-dependent response or an anomalous dispersion within the 1- to 100-GHz frequency range. The preceding section indicated that the structure of liquid water includes a collection of permanent dipoles; i.e., particles subject to realignment in the presence of an oscillating electromagnetic field. An obvious analogy found in classical mechanics for an oscillating particle whose behavior changes with frequency is the harmonic oscillator. What follows is the development of a simple model for the dipole relaxation loss seen in liquid water based on the harmonic oscillator.

Using the notation and following (with some extension) the treatment of optical dispersion in materials presented by Reitz, Milford, and Christy (1980), one can consider the dipole to behave like a one-dimensional, damped, forced oscillator where the positive charge e moves and the negative charge remains fixed.

$$m \frac{d^2x}{dt^2} + G \frac{dx}{dt} + Cx = eE_m \tag{17}$$

where

x = a measure of the displacement

G = a viscosity coefficient

C = a spring resistance coefficient

e = the value of charge at each end of the dipole

E_m = the local electric field

If the driving force were zero and the particle were given some initial displacement, x_o, then

$$x(t) = x_0 e^{-\frac{Ct}{G}} = x_0 e^{-\frac{t}{\tau}} \tag{18}$$

which is consistent with the previous description of relaxation behavior and activation energies.

Now assume that both the driving force (the local electric field) and the resulting displacement vary sinusoidally with amplitudes A_E and A_X,

respectively, and that the inertia forces are negligible. One can then write the equation of motion as

$$G\left(-i\omega A_x e^{-i\omega t}\right) + CA_x e^{-i\omega t} = eA_E e^{-i\omega t} \tag{19}$$

or

$$A_x = \frac{eA_E}{C - iG\omega} \tag{20}$$

For the single dipole, the dipole moment is eA_x. Therefore, the polarization of the material P, which is the number of dipole moments per unit volume and is proportional to the amplitude of the driving force through the susceptability χ, goes like

$$P = NeA_x = \chi A_E \tag{21}$$

where N = the number of dipoles/unit volume.

Then one has

$$\chi = \frac{\frac{Ne^2}{C}}{1 - i\omega\tau} \tag{22}$$

which shows that the electric susceptibility of the medium is both complex and frequency dependent. But to model this behavior in terms of the dielectric constant, one must then pose the relationship between dielectric constant and susceptibility as

$$\varepsilon = \varepsilon_\infty + 4\pi\chi \tag{23}$$

where ε_∞ replaces the unity term in the usual definition for linear dielectrics and represents the high-frequency limit on the real part of the dielectric constant. Combining the last two expressions, one can now write

$$\varepsilon - \varepsilon_{\infty} = \frac{\frac{4\pi N e^2}{C}}{1 - i\omega\tau} \tag{24}$$

Referring to the static ($\omega = 0$) dielectric constant as ε_0, one then has that

$$\frac{4\pi N e^2}{C} = \varepsilon_0 - \varepsilon_{\infty} \tag{25}$$

or finally,

$$\varepsilon - \varepsilon_{\infty} = \frac{\varepsilon_0 - \varepsilon_{\infty}}{1 - i\omega\tau} \tag{26}$$

Recalling that

$$\varepsilon = \varepsilon' + i\varepsilon''$$

the above expression can be solved for ε' and ε''.

$$\varepsilon' = \varepsilon_{\infty} + \frac{\varepsilon_0 - \varepsilon_{\infty}}{1 + (\omega\tau)^2} \tag{27}$$

$$\varepsilon'' = \frac{(\varepsilon_0 - \varepsilon_{\infty})\omega\tau}{1 + (\omega\tau)^2} \tag{28}$$

These are the often-referenced Debye equations (Debye 1929) for modeling the dielectric behavior of materials made up of polar molecules. Plotted on semilogarithmic scales, these equations approximate the anomalous behavior shown for liquid water on Figure 1. At $\omega\tau = 1$, ε'' is maximized, which says that the maximum loss due to the dielectric relaxation mechanism occurs at a frequency equal to the inverse of the relaxation time.

Eliminating $\omega\tau$ from these equations allows one to write the expression

$$\left[\varepsilon' - \frac{(\varepsilon_0 + \varepsilon_\infty)}{2}\right]^2 + [\varepsilon'']^2 = \left[\frac{\varepsilon_0 - \varepsilon_\infty}{2}\right]^2 \qquad (29)$$

Thus, the Debye equations, when drawn in ε', ε'' space, result in a circle centered at

$$\varepsilon' = \frac{(\varepsilon_0 + \varepsilon_\infty)}{2}, \quad \varepsilon'' = 0$$

and having a radius of $(\varepsilon_0 - \varepsilon_\infty)/2$. Such a plot, shown in Figure 3, is known as a Cole-Cole diagram. Three different relaxation frequencies representing the three temperatures shown in the figure were chosen using Ray's empirical model. One should further note that at $\omega = 1/\tau$ (the inverse of the relaxation time)

$$\varepsilon' = \varepsilon_\infty + \frac{(\varepsilon_0 - \varepsilon_\infty)}{2} = \frac{\varepsilon_0 + \varepsilon_\infty}{2}$$

and

$$\varepsilon'' = \frac{\varepsilon_0 - \varepsilon_\infty}{2}$$

i.e., the peak relaxation loss is represented by the point at the top of the Cole-Cole diagram.

What has been demonstrated in the preceding paragraphs is that a simple mechanical model can do a very good job in representing the high-frequency dispersive dielectric behavior of liquid water. Of course, a simple electrical analog can also be developed. In terms of simple circuit elements, the equivalent circuit that precisely models the Debye equations is shown in Figure 4 (Cole and Cole 1941) where $\varepsilon = \varepsilon' + i\varepsilon''$ is the equivalent capacitance of the circuit (Equation 26). Simple models like this will prove to be very helpful in analyzing the behavior of the complex dielectric constant in moist soils.

Cole-Cole relaxation model

Cole and Cole (1941) observed that a good bit of experimental data on both polar liquids and polar solids were not fit by the semicircular ε', ε''

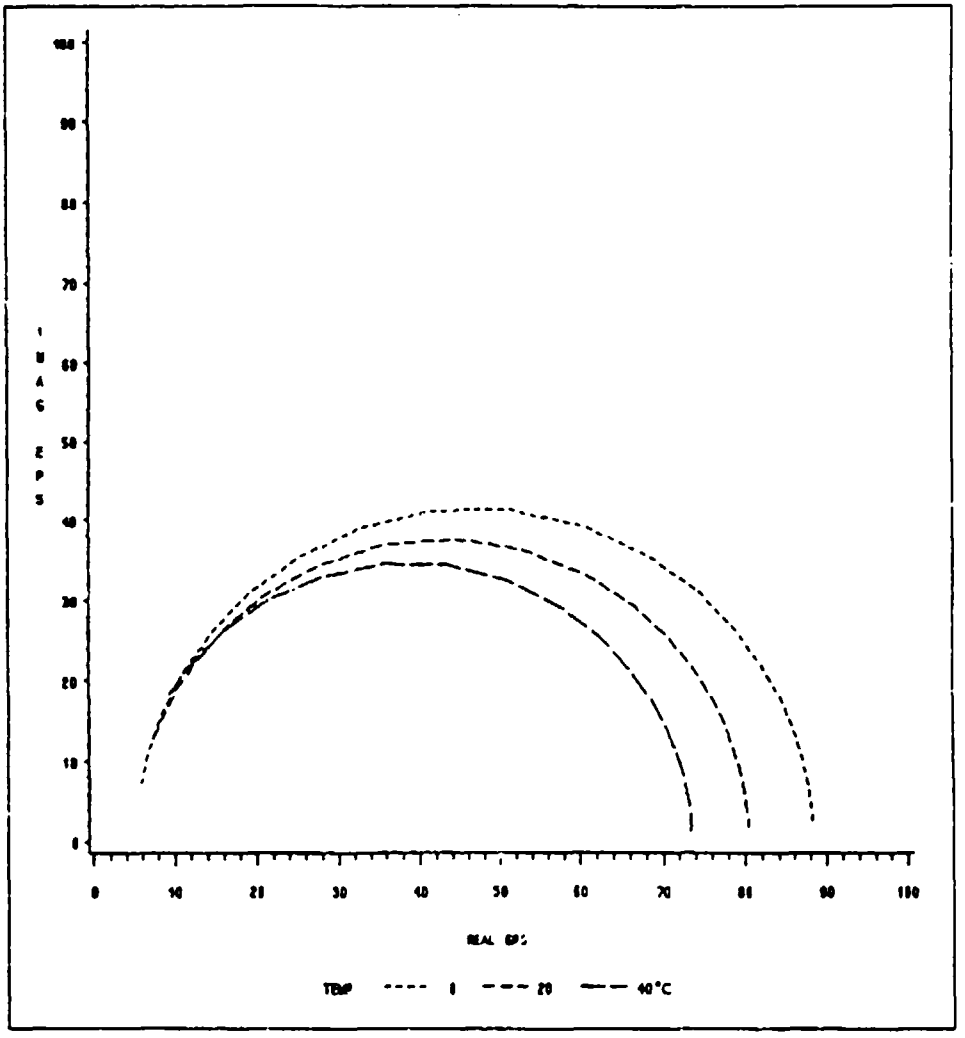

Figure 3. Graphical representation of Debye equations in ε', ε'' space

space predictions of Debye's equations. Rather, it seemed that over large frequency intervals, the data seemed to be best fit by circular arcs; i.e., pieces of circles in ε', ε'' space that were centered below the $\varepsilon'' = 0$ line. Using a series of geometrical and analytical arguments, the authors showed that linear materials that behaved in this manner can be described by the relationship

$$\varepsilon - \varepsilon_\infty = \frac{\varepsilon_0 - \varepsilon_\infty}{1 - (i\omega\tau)^{1-\alpha}} \tag{30}$$

Expressions for ε' and ε'' found by substituting

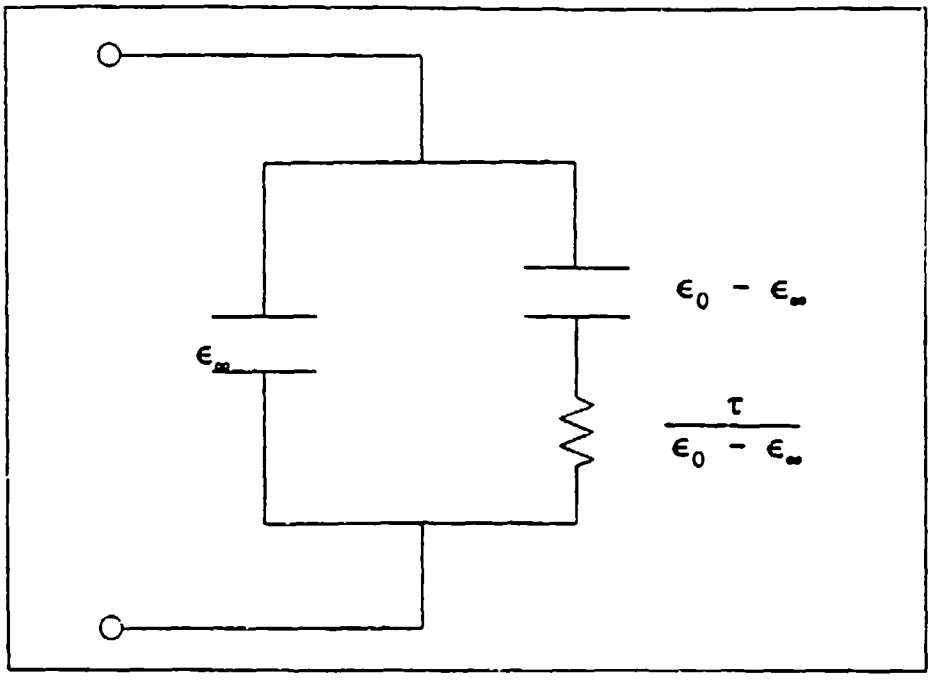

Figure 4. Equivalent circuit for Debye model

$$i^{-\alpha} = e^{-i\frac{\alpha\pi}{2}} = \cos\left(\frac{\alpha\pi}{2}\right) - i\sin\left(\frac{\alpha\pi}{2}\right)$$

are those slightly modified by Ray (1972) to produce the curves in Figure 1.

Furthermore, it is clear from the form of Equation 30 that a simple equivalent circuit can still be drawn for materials that follow the behavior described above. Figure 5 shows that the resistance in the Debye equivalent circuit now becomes a complex impedance. Representative plots of the Cole-Cole relaxation model are shown on Figure 6. These curves were derived from Ray's empirical model for which artificially large alpha values were selected. The vertical lines on the figure reflect the contribution of the conductivity term added to the Cole-Cole model by Ray and were not part of the original development. They do, however, give an indication of the way real material responses may look.

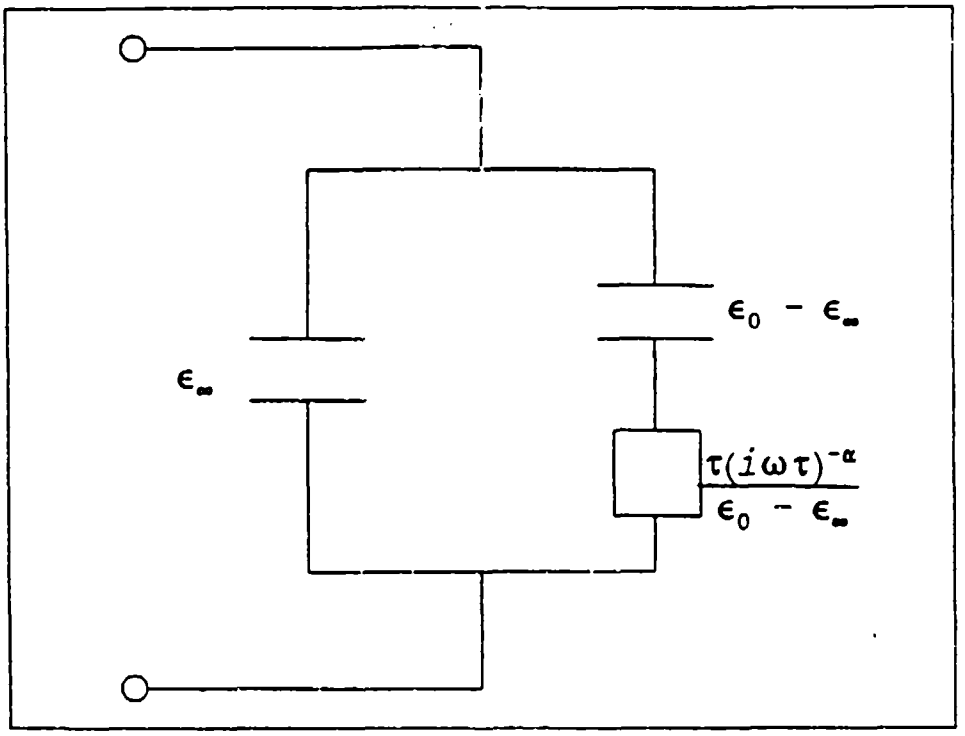

Figure 5. Equivalent circuit for Cole-Cole model

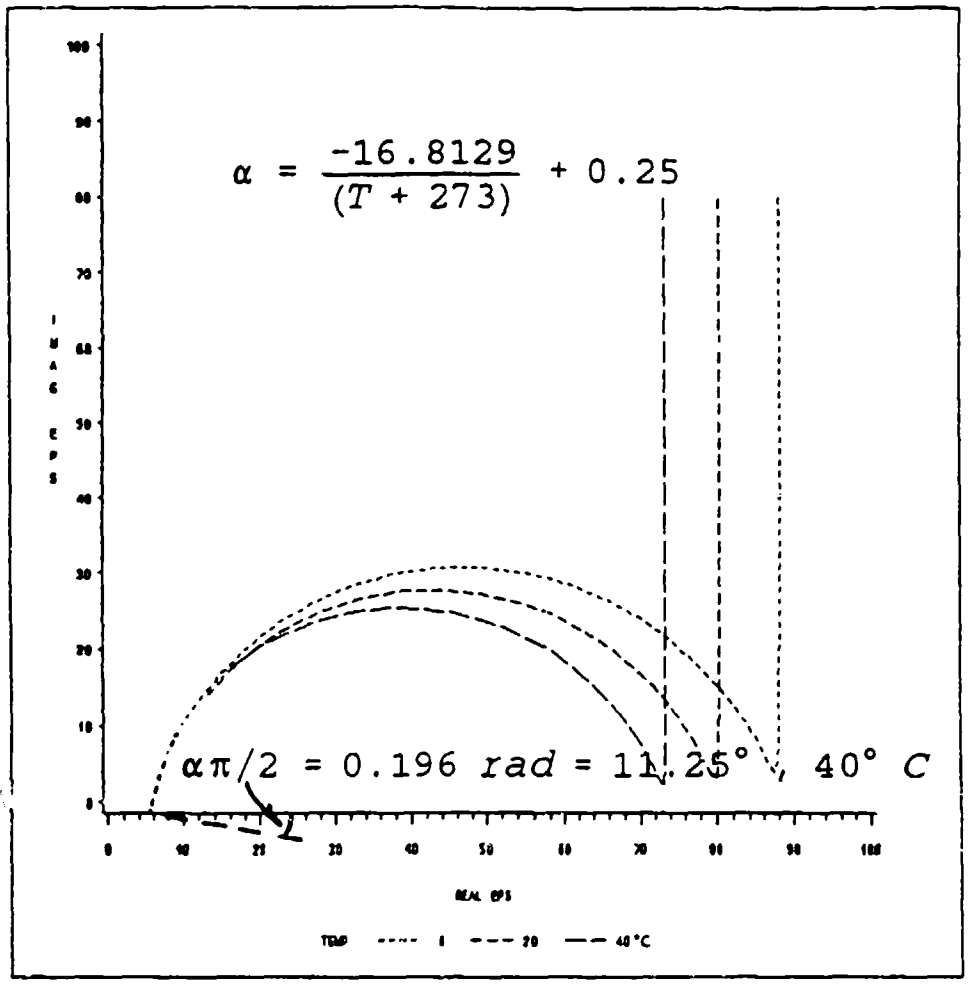

Figure 6. Representative Cole-Cole plots

3 Electrical Properties of Moist Soils

A quick review of available dielectric data on dry soils and wet soils leads to the conclusion that the dominant factor that controls the electrical behavior of soils is the presence of water. Over a broad frequency range, the real part of the complex relative dielectric constant (referred to in this text as permittivity) of dry soil minerals changes very little, covering a range of values from about 2 to about 6 (Nelson, Lindroth, and Blake 1989; Ulaby et al. 1990). However, when considered from the perspective of the idealized electromagnetic wave reflection phenomenon for lossless materials as described in Appendix B, this can translate into reflection coefficients that vary from -0.17 to -0.42. In terms of power (which is proportional to radar backscatter coefficients), these small variations in dry soil properties result in reflectances that span values from 0.029 to 0.176, or a range of about 8 db.

When water is added to the soil fabric, further substantial changes in reflectance at the soil/air interface can take place Take the permittivity of water to be about 80 (at low frequencies). Then for normal incidence electromagnetic waves and lossless media, one can calculate a reflection coefficient of about -0.8 and a reflectance of about 0.64. Now, take the permittivity of a very moist soil to be about 20. Then under ideal conditions, its reflectance at normal incidence could be as much as 0.4. In other words, a very moist soil could theoretically reflect more than thirteen times the power (or more than 11 db) than can the driest soils. While airborne scatterometers may easily see this much variation in measurements over large areas of so-called homogeneous terrain due to surface roughness effects and interference phenomena, these differences in electrical properties of soils could be quite significant for close-up measurements with ground-based electromagnetic devices.

As an example of the effect of soil moisture on real-world situations, consider the data reported by Ulaby, Cihlar, and Moore (1974) that was collected with a ground-based radar scatterometer located in an unplanted, plowed field of clay loam soil. As shown in Figure 7, the power returned to the scatterometer while looking nearly straight down at the soil surface (0-deg incidence) increased by 20 db as moisture contents increased from 4.3 to 36.3 percent (average values in the first 5 cm). Twenty decibels means a 100-fold increase

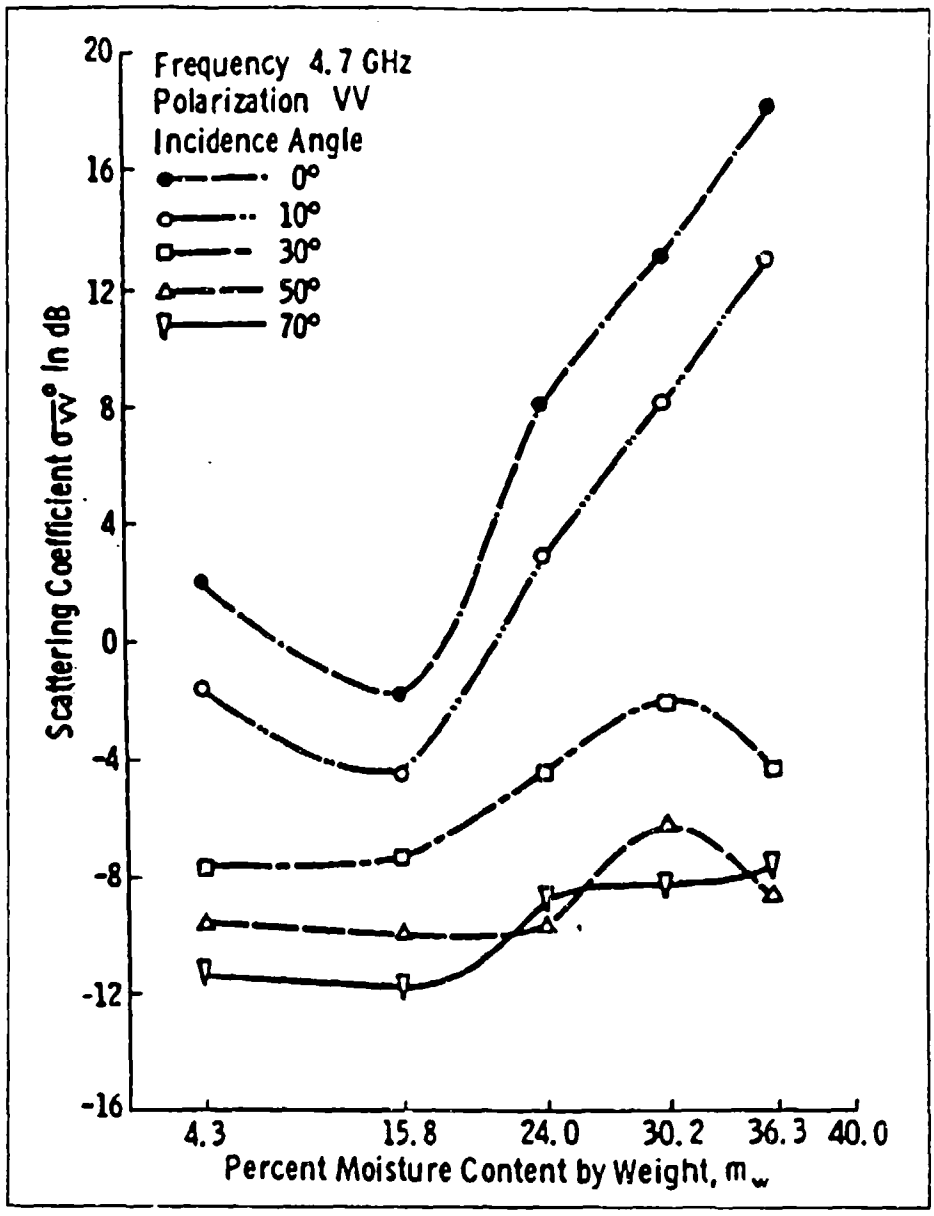

Figure 7. Radar backscatter coefficient versus moisture content (from Ulaby, Cihlar, and Moore (1974))

in power. The arguments above would indicate an anticipated bound of about 11 or 12 db increase. It is possible that surface roughness effects and/or constructive interferences could account for the larger field measurement numbers.

Data on Variations in Frequency, Moisture, and Temperature

At this point, it would be prudent to assess what is already known about the electrical behavior of moist soils. What are the conditions under which data have already been collected? What kinds of soils have been studied? Is there general agreement on results of previous measurements? Have the measurements led to any insight as to the loss mechanisms involved?

While the governing equations for the propagation of electromagnetic waves in linear, homogeneous, isotropic media have been accepted since the late 1800s, only in the last 30 years or so has any serious attention been given to the complex dielectric response of heterogeneous mixtures such as soils. Nevertheless, all measurements of soil electrical properties are still interpreted in a macroscopic sense as if the soil is truly homogeneous and isotropic. Table 1 identifies some of the most relevant work on measuring the electrical response of materials that ultimately apply to this study on the response of soils. No such list could ever hope to be complete, but it does serve to provide a historical perspective and a proper point of departure for the work to be conducted in this and future studies. Paragraphs that follow will highlight several of these contributions.

Structure of clay minerals

Although this section may seem out of place, it is important to set the stage for discussions of soil electrical behavior by briefly addressing the structure of the soil elements that probably are most influential in determining their electrical response; namely, the clay minerals.

Clay minerals are layered silicates whose fundamental building blocks are tetrahedral sheets in which the tetrahedra are linked at their corners and octahedral sheets in which the octahedra are linked along their edges (Moore and Reynolds 1989). Each tetrahedron is formed from four oxygen ions normally surrounding Si^{4+} cations (which can also be replaced by Al^{3+} or Fe^{3+} cations). Each octahedron is formed from six oxygen ions (or hydroxyl ions) surrounding a cation that is normally either Al^{3+}, Mg^{2+}, Fe^{2+}, or Fe^{3+}.

Most clay minerals fit into structural classifications referred to as 1:1 or 2:1. A 1:1 structure is comprised of a tetrahedral sheet joined to an octahedral sheet. The mechanism for this bonding is that the apical oxygens of the tetrahedra replace two out of every three anions in the octahedral sheet. The 2:1 structure is generated by a second tetrahedral sheet bonding to the opposite side of the octahedral sheet. Slight differences in sheet dimensions (or anion spacing) due to various combinations of cations can cause distortions of the layered structure, sometimes so severe as to result in tubular geometries.

Table 1
Electrical Property Measurements

Author(s)	Year	Material(s)	Frequency(ies)	Technique(s)	Motivation/Interpretation
Lane, Saxton	1952	Water, alcohols	9.35, 24, 48 GHz	Waveguide	Alcohols and water are polarizable
Grant, Buchanan, Cook	1957	Water	0.58, 1.74, 3.0 3.65, 9.3, 23.8 GHz	Coaxial line	Cole-Cole model fits
Lundien	1966	Sand, silt, clay	0.3, 9.4, 34.5 GHz	Reflectance	Depth-of-penetration studies
de Loor	1968	Moist organics	1.2, 3.0, 3.8, 6.0 8.6, 9.4, 11.5, 16 GHz	------	Bound water versus free water studies; develop test materials with known complex electrical properties
Carroll, Eberle, Cunningham	1969	Desert soils	0-3 Hz .001-100 MHz	Resistivity array Capacitance cell	-----
Campbell, Ulrichs	1969	Lunar soil	100 Hz - 1 MHz	Capacitance cell	Elevated temperature behavior
Saint-Amant, Strangway	1970	Dry rocks, powdered rocks	50 Hz - 2 MHz	Capacitance cell	Maxwell-Wagner losses observed in dry minerals
Lundien	1971	Sand, silt, clay	1.07-1.5 GHz	Free-space transmission	Establish correlations between moisture content and permittivity
Hoekstra, Doyle	1971	Na-montmorillonite	100 Hz, 9.8 GHz	Slotted waveguide	Low-frequency free charge losses, high-frequency mechanisms: proton mobility, dipole rotations, H-bond ruptures
Smith	1971	Kaolinite, illite montmorillonite	2-60 MHz	Capacitance cell	Maxwell-Wagner loss mechanism

(Sheet 1 of 3)

Table 1 (Continued)

Author(s)	Year	Material(s)	Frequency(ies)	Technique(s)	Motivation/Interpretation
Nelson	1972	Fruits	8-12 GHz	Slotted waveguide	Moisture content relationships
Strangway, et al.	1972	Lunar soil	100 Hz - 1 MHz	Capacitance cell	Impact of residual moisture
Olhoeft, Frisillo, Strangway	1974	Lunar soil	100 Hz - 1 MHz	Capacitance cell	Behavior at elevated temperatures
Olhoeft	1977	Illite-rich permafrost	10 Hz - 1 MHz	Capacitance cell	Multiple loss mechanisms in unfrozen water
Hall, Rose	1978	Kaolinite	.0002-10 MHz	Capacitance cell	Attributed peak losses to Debye relaxation mechanism
Topp, Davis, Annan	1980	Soils, glass beads	1 MHz - 1 GHz	Time-domain reflection	Moisture is the dominant factor
Delaney, Arcone	1982	Silt, sand	0.1-5.0 GHz	Time-domain reflection	Looking for attenuation properties
Waite, Sadeghi, Scott	1984	Silt	1.5, 6 GHz	Bistatic reflectance	Reflectance increases w/moisture
[illegible], et al.	1985	Silts, sandy loam	1-2, 4-6 GHz; select frequencies from 4-18 GHz	Waveguide; free-space transmission	Soil texture is a factor; liquid water exists at subzero temperatures
Pissis	1985	Cellulose	DC	Thermal depolarization	Attempts to distinguish free from bound water response
Ulaby, El-Rayes	1986, 1987	Vegetation	0.2-20 GHz	Open-ended coaxial (fringe capacitance)	Rapid data collection

(Sheet 2 of 3)

Table 1 (Concluded)

Author(s)	Year	Material(s)	Frequency(ies)	Technique(s)	Motivation/Interpretation
Bidadi, Schroeder, Pinnavaia	1988	Na-,Li-montmorillonites	30-100 Hz	Capacitance cell	Low-water content Maxwell-Wagner behavior
Campbell	1988	Sand, silt, clay	.001-1.5 GHz	Coaxial probe, resonant cavity	Low-frequency ionic conductivity losses; fractal long-range connectivity
Nelson, Lindroth, Blake	1989	Mineral powders	1.0, 2.45, 5.5, 11.7, 22.0 GHz	Slotted waveguide	Observed some dispersion in dry minerals
Ulaby, et al	1990	Dry rocks	0.5-18 GHz	Open-ended coaxial (fringe capacitance)	Non-dispersive permittivity; loss factor decreases

(Sheet 3 of 3)

Clay mineral layers formed by the tetrahedral and octahedral sheets are sometimes electrically neutral, but most often are somewhat negatively charged due to the substitution of lesser valence cations for Si^{4+} in the tetrahedral sheet and/or Al^{3+} in the octahedral sheet. Furthermore, because of the finite lateral dimensions of clay mineral crystals, unsatisfied bonds exist at the edges of the layers that also result in layer charge imbalance.

The following simplified descriptions of the clay minerals that will be referred to in this study can now be given. Kaolinite is a 1:1 structure mineral which, if in a very pure form, will have little or no layer charge due to cation exchange, but will attract ions or polar molecules such as water to its edges. Illite, montmorillonite, and hectorite are 2:1 minerals. Many opinions seem to exist regarding what illite really is in terms of a structural formula, but it is generally accepted that it is a mica material whose layers have a half-unit-cell charge imbalance of about 0.8 and whose interlayer spaces are occupied by cations (usually potassium) whose spatial distribution nearly balances the layer charges. Montmorillonite and hectorite have smaller layer charge imbalances; the interlayer cations can attract water, which results in a swelling of the layered structure and the creation of hydrogen bonds between the water molecules and the anions of the tetrahedral sheet surfaces (Moore and Reynolds 1989). These swelling clays have a greater affinity for water, which should cause much different electrical responses than for the nonswelling kaolinite.

Dispersive behavior in moist soils

Smith (1971) conducted a series of tests on the electrical behavior of saturated clays up to a maximum frequency of about 60 MHz using a capacitive bridge measurement apparatus. He looked at three distinct clay types: a montmorillonite, an illite, and a kaolinite.

A representative set of Smith's measurement results is given in Figure 8 in terms of the real part of the dielectric constant and conductivity versus frequency. Of particular interest is the observation that clays with higher basic structural water content have larger complex dielectric constants than those with less water. Conclusions should not be drawn from consolidation differences. Density should clearly affect the dielectric properties of the basic mineral themselves by providing varying degrees of particle contact and, hence, varying electrical path lengths through the matrix; however, the degree of effect is not currently understood.

Lundien (1971) reported permittivity and conductivity measurements over a range of frequencies between 10 MHz and 1.5 GHz. At the lowest frequencies, he used a capacitive bridge setup. Data at about 300 MHz were collected from radar reflectance measurements. The higher frequency data were collected using what was referred to as a microwave interferometer, but was, in fact, a free-space transmission measurement apparatus with the sample faces tilted to the radar path.

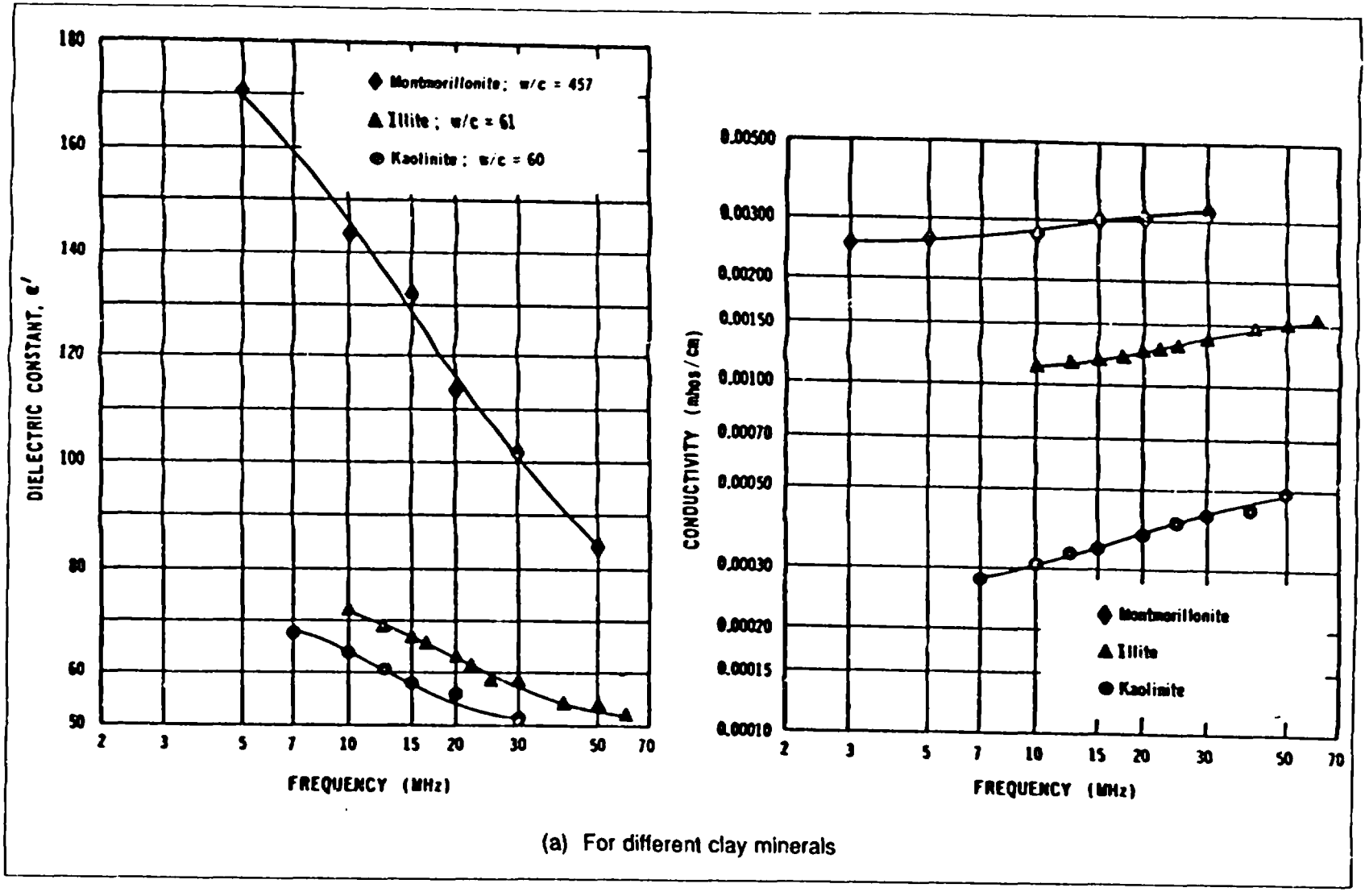

Figure 8. Dielectric constant of clays versus frequency (from Smith (1971)) (Sheet 1 of 3)

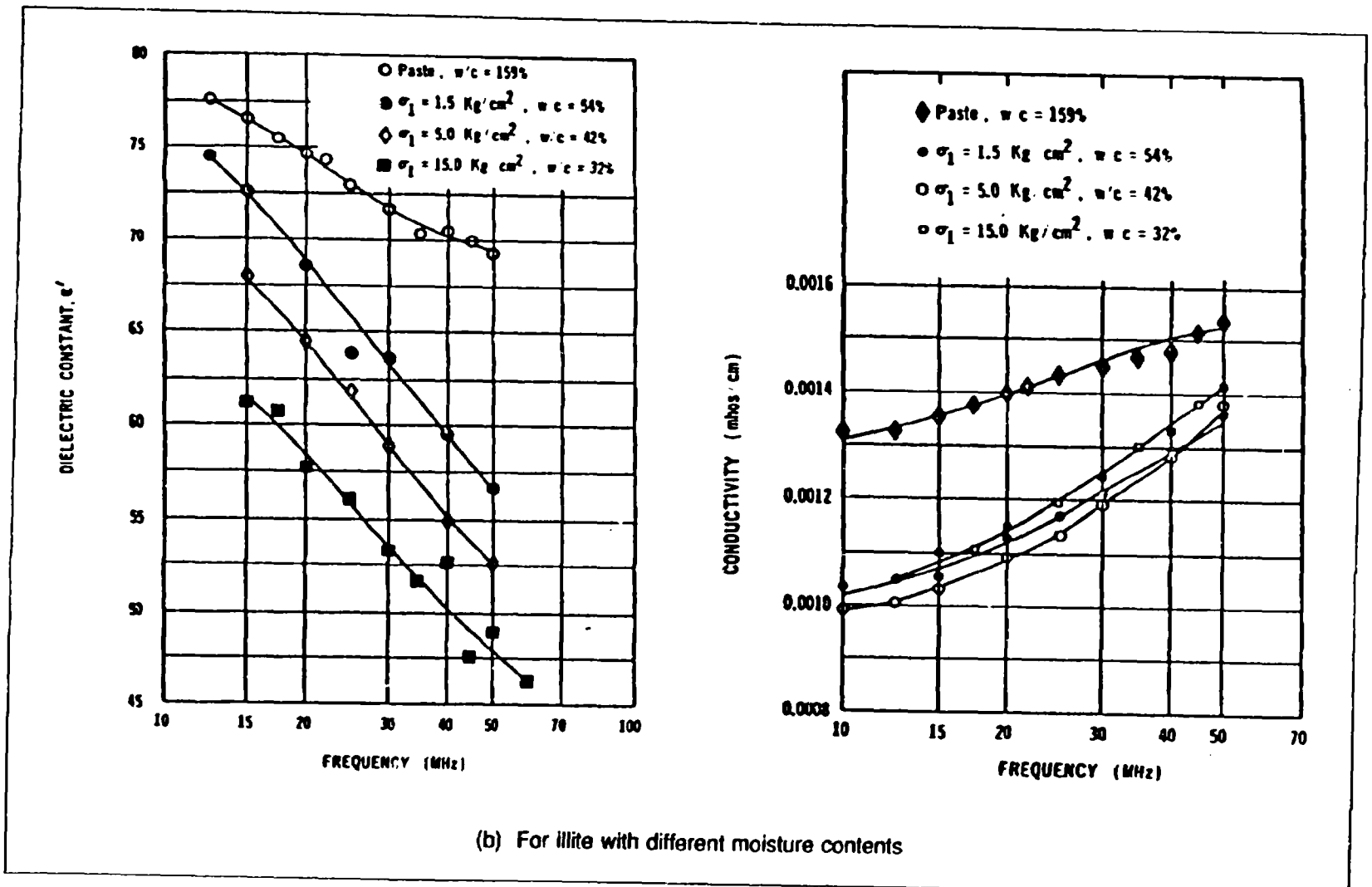

(b) For illite with different moisture contents

Figure 8. (Sheet 2 of 3)

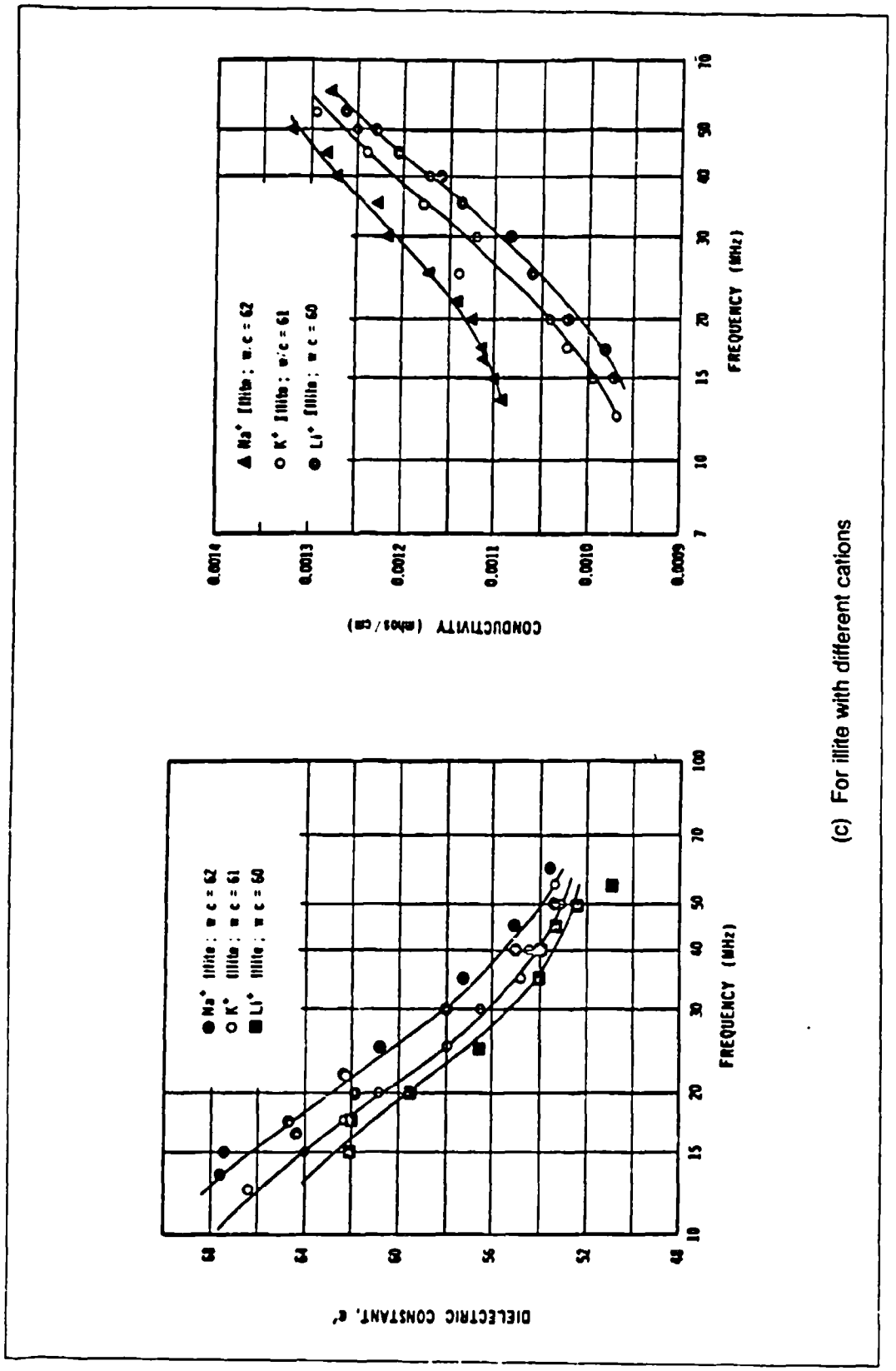

(c) For illite with different cations

Figure 8. (Sheet 3 of 3)

Lundien's results are shown in Figure 9 for three types of soil: a very poorly graded sand, a well-graded silt, and a high clay content locally available soil (50 percent of particles by weight <.0075 mm). Conclusions are difficult to draw, because the data include a broad range of moisture levels. The Long Lake clay is described by Lundien as being composed mostly of montmorillonite particles.

A very nice set of moist soil electrical measurements over a broad range of frequencies was collected by Hoekstra and Delaney (1974) using a 7-mm coaxial line for frequencies up to about 3 GHz and a series of slotted waveguide devices from about 5 GHz to about 20 GHz. Copies of their reported data as a function of frequency are shown in Figures 10 and 11 for two different clays. Figure 10 (a) shows data for one gravimetric moisture content and two temperatures, while Figure 10 (b) shows data for temperature and two moisture conditions. Qualitatively they observed a Debye-like dispersion in the moist soils, but at a lower frequency than for bulk liquid water. They also observed that increasing temperatures reduced the frequency of maximum dielectric loss (which is inconsistent with the response of water) as did increasing water content. They further attempted to fit a modified Debye relaxation equation to the data for one of the clays (Figure 11) with partial success. They concluded that there was no difference between the relaxation of water in sandy soil and that for clays, which contradicts the thesis that chemical bonding of the water dipoles to clay particles should cause a shift of the relaxation frequency.

Hallikainen et al. (1985) collected dispersion data using waveguide transmission techniques in the 1- to 2- and 4- to 6-GHz bands and a free space transmission technique at eight selected frequencies between 4 and 18 GHz. They conducted measurements on soil types ranging from sand loam (51 percent sand and 13 percent clay) to a silty clay (5 percent sand and 47 percent clay). Figure 12 contains their published results for one soil (42 percent sand, 49.5 percent silt, and 8.5 percent clay) collected at an ambient temperature of about 23 °C.

Another set of frequency-dependent data is that collected by Campbell (1988) using a tined coaxial probe and a device for precisely controlling sample moisture content and sample temperature. Frequency was limited to 50 MHz for these measurements. The objective of these studies was to examine the low-frequency dielectric loss mechanisms in moist soils.

Figure 13 is a summary of Campbell's measurements for one type of silty soil that shows the low-frequency dispersion of this soil as a function of volumetric water content. Obviously, one is not able to ascertain the changes in Debye type relaxation because of the frequency limitations of these data. Of particular note was the conclusion drawn by Campbell that the predominant loss mechanism in this frequency range was that of ionic conductivity and not the Maxwell-Wagner effect hypothesized by Smith (1971). These mechanisms will be discussed in a later section.

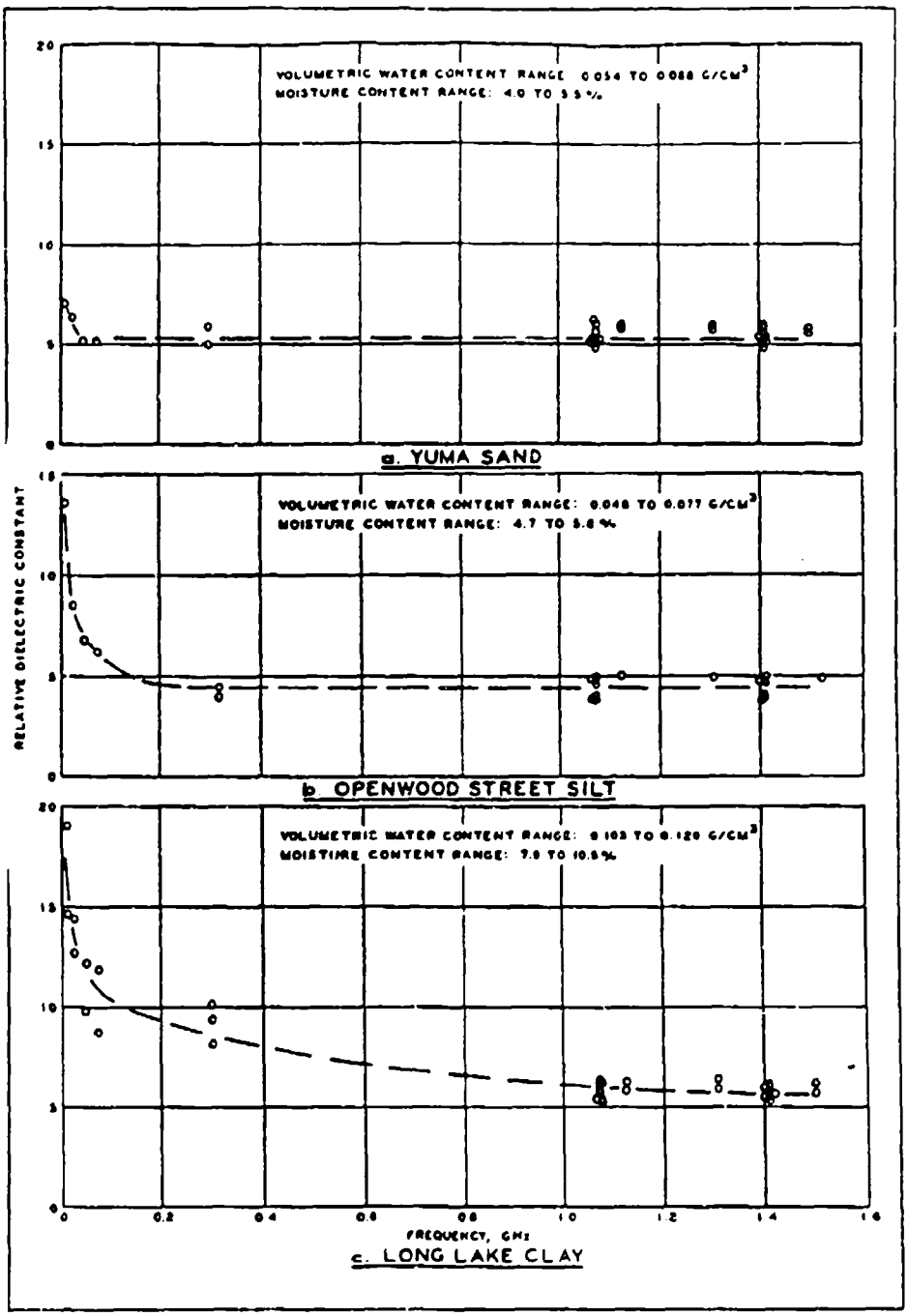

Figure 9. Dielectric constant of soils versus frequency (from Lundien (1971)) (Continued)

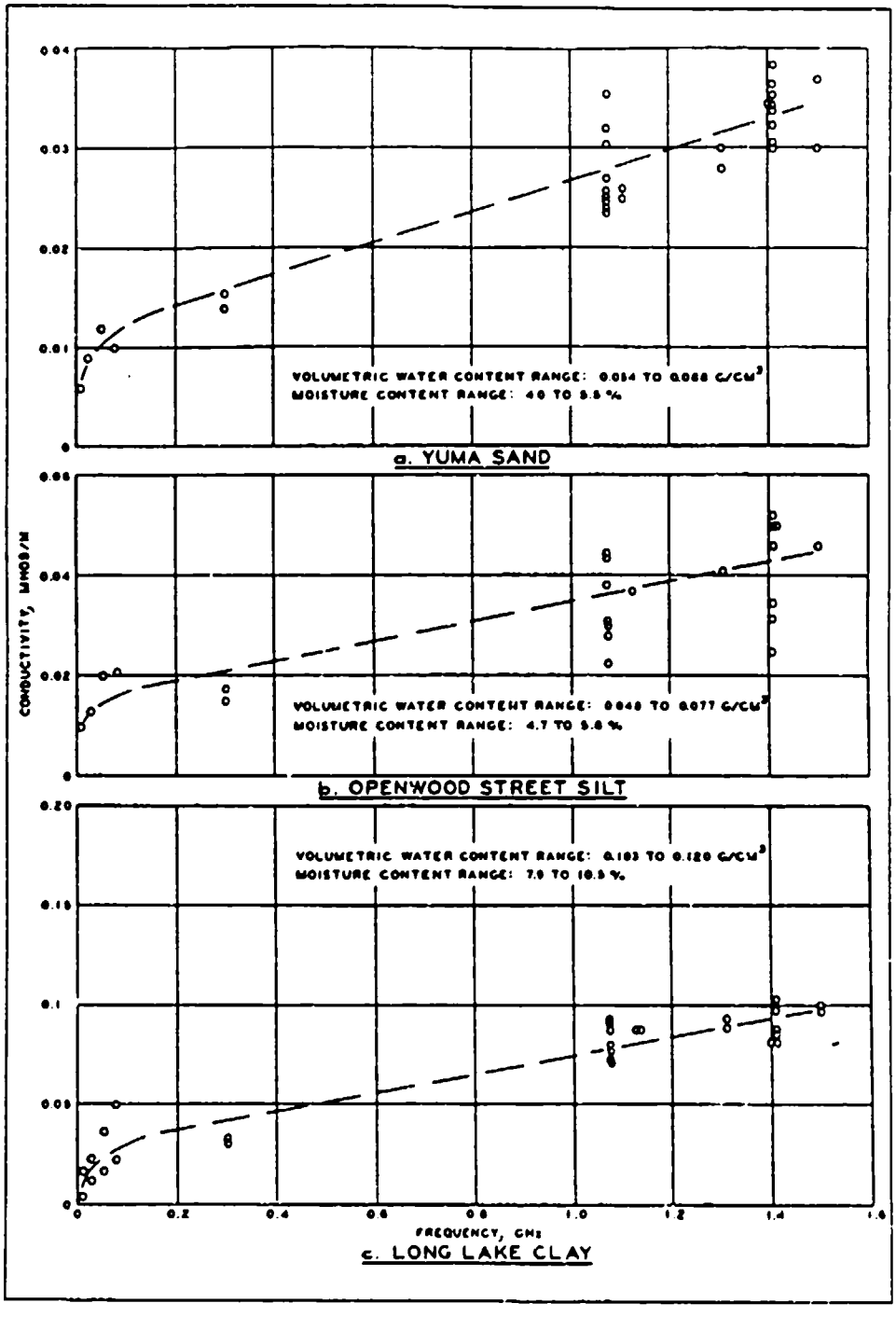

Figure 9. (Concluded)

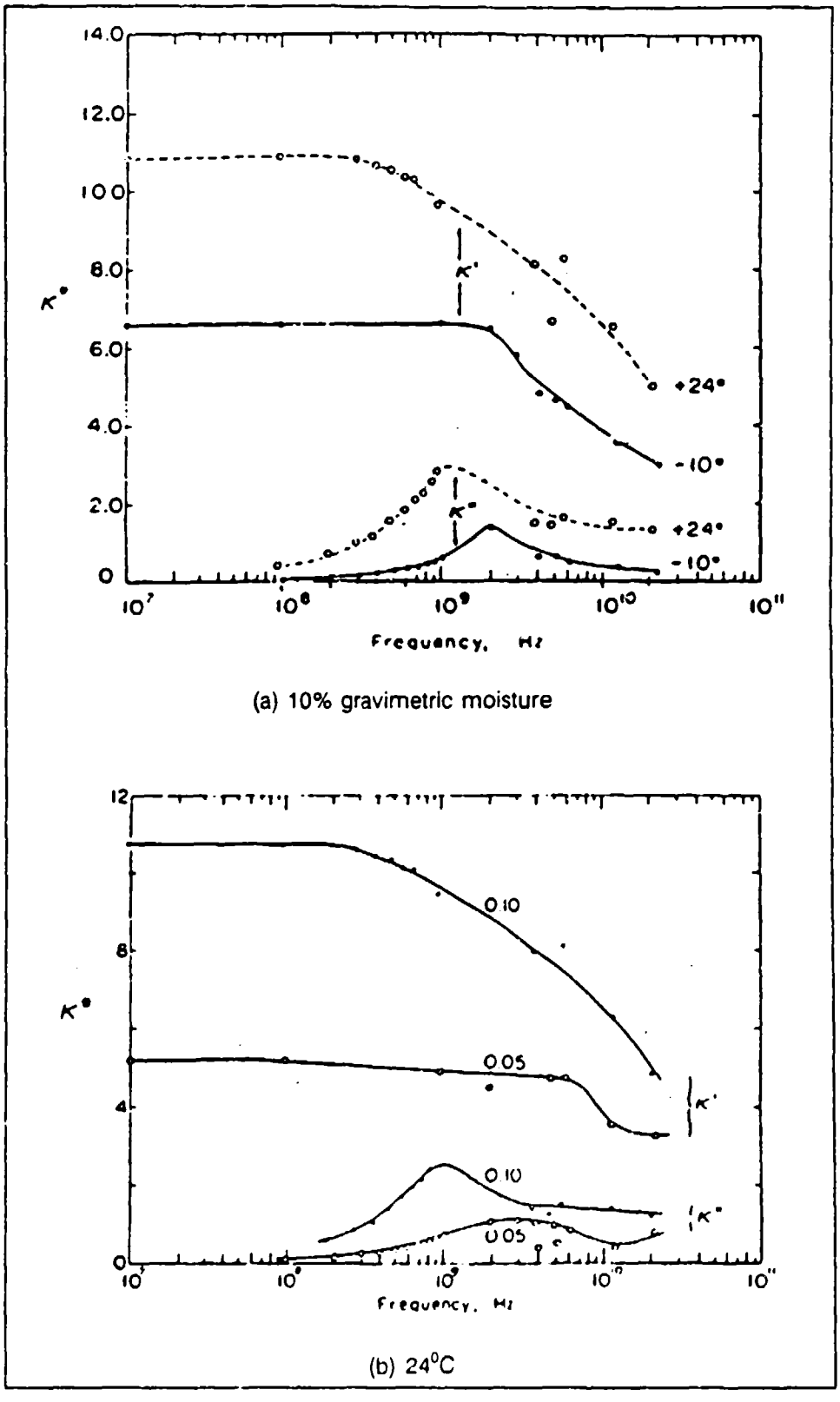

Figure 10. Dielectric constant of Goodrich clay (from Hoekstra and Delaney (1974))

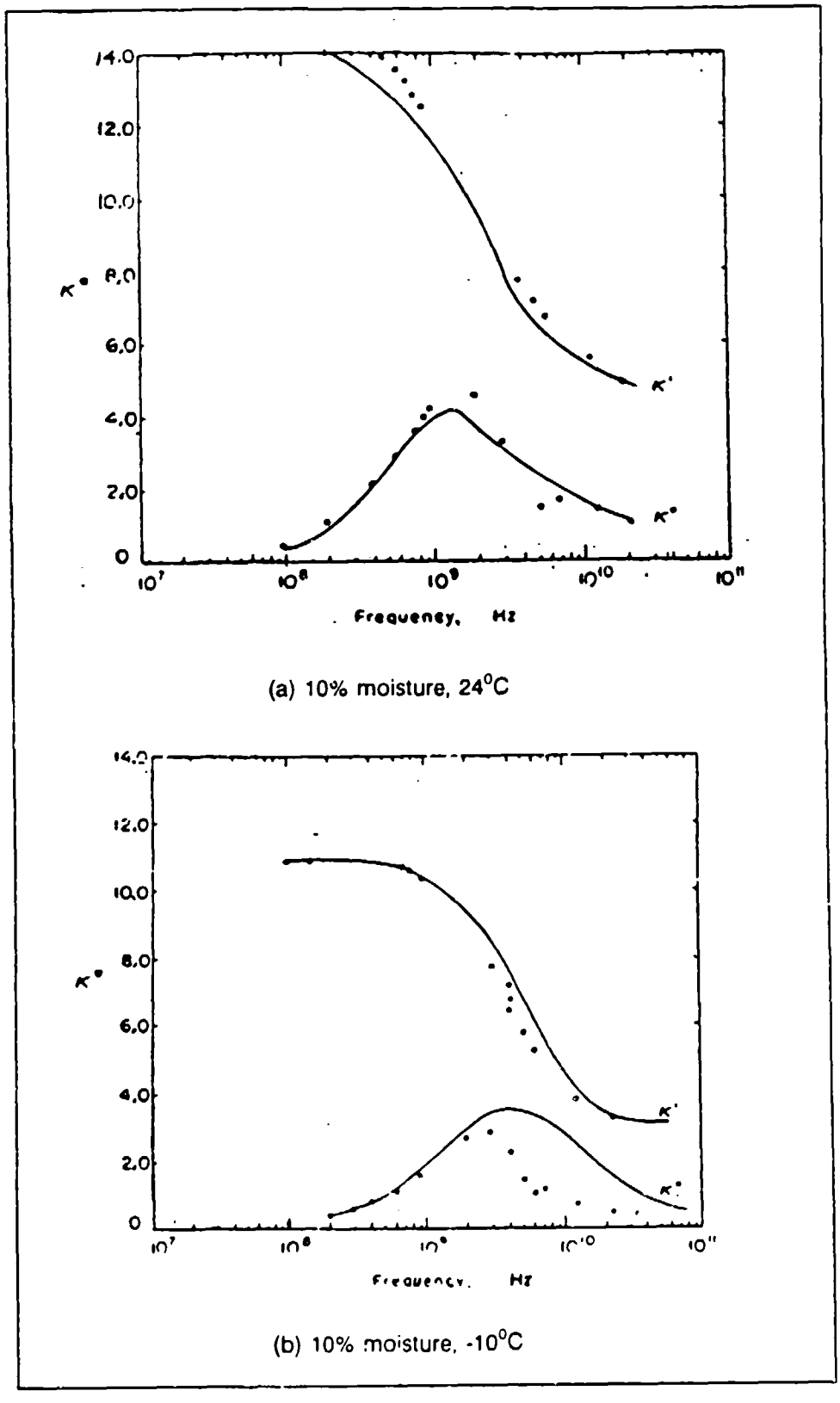

Figure 11. Dielectric constant of Suffield silty clay (from Hoekstra and Delaney (1974))

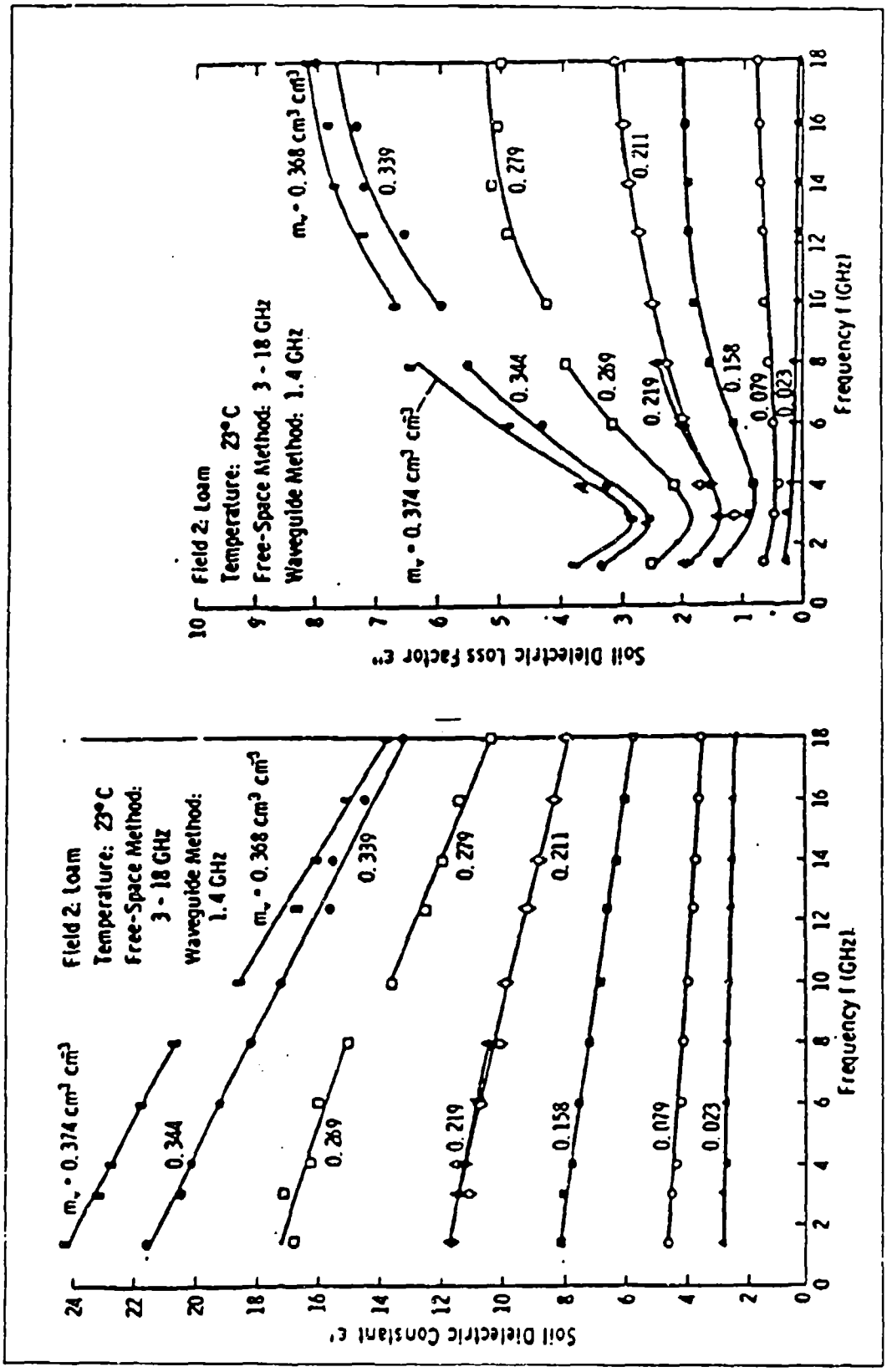

Figure 12. Dielectric constant of loam versus frequency (from Hallikainen et al. (1985))

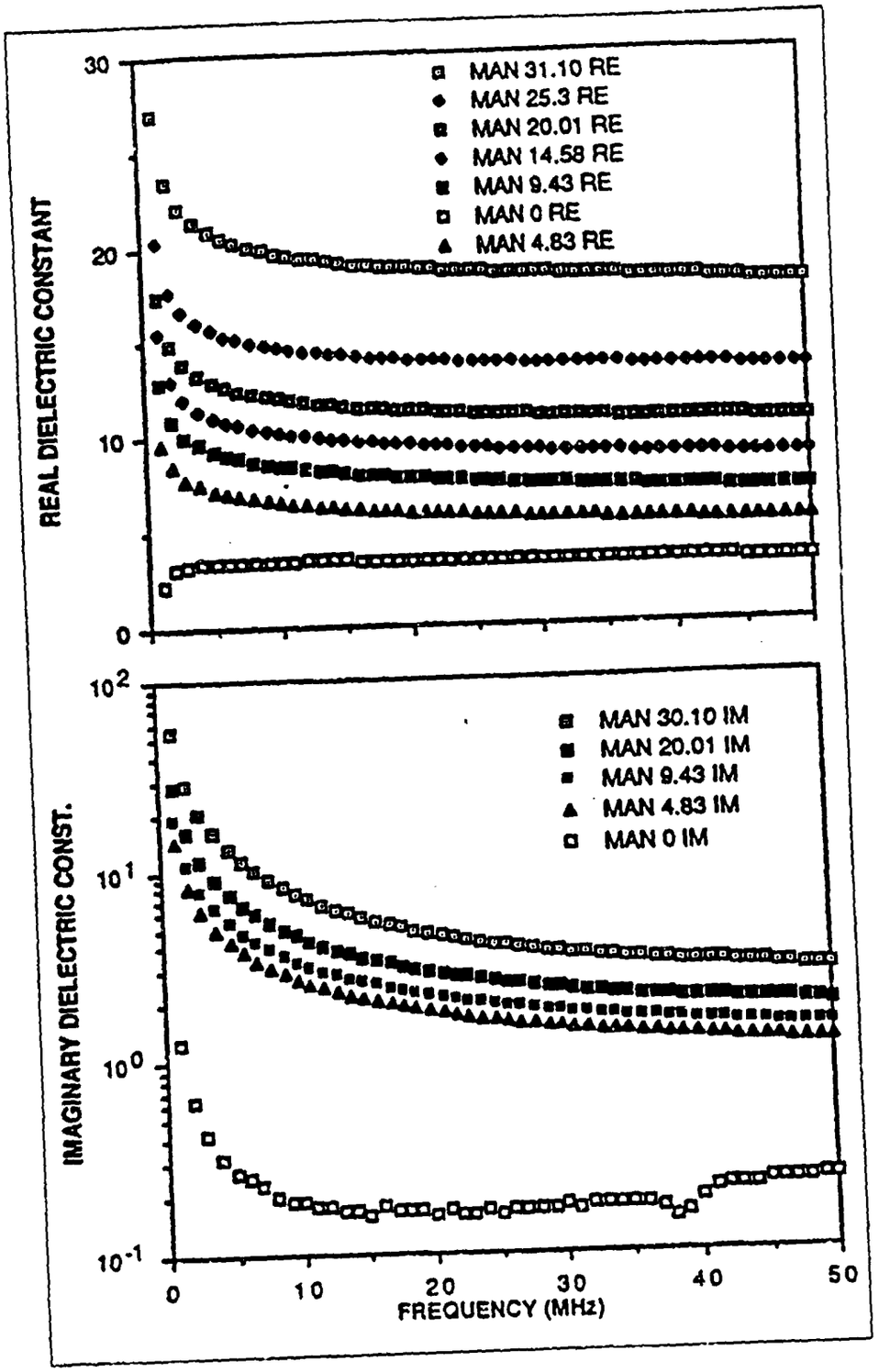

Figure 13. Dielectric constant of Manchester silt (from Campbell (1988))

Existing data on effects of moisture content

Because of the obvious applications of remote sensing technology to the determination of soil moisture levels, considerable data have been collected and reported in the literature. An early example is that of Lundien (1966) in which he used four different radar scatterometers and large specially prepared soil samples to measure the apparent dielectric constant. "Apparent" in this context means that the dielectric constant was computed from the square of the Fresnel coefficients (Appendix B) assuming no imaginary components (no losses). Lundien's results for two soil types are shown in Figures 14 and 15 in which he suggests an exponential fit might be in order. The data are limited in quantity because of the difficulty of sample preparation and, as such, do not reveal what later researchers believe to be a bilinear type of response.

Lundien's later work (1971) using free space transmission measurement techniques is summarized in Figures 16, 17, and 18. The moisture content reported here is volumetric (volume of water/volume of sample) as opposed to his earlier gravimetric (weight of water in sample/dry weight of soil in sample; $m_v = m_g \rho_{dry}/\rho_{water}$) data. Polarization labels on these figures refer to the orientation of the antennas with regard to the horizon. The data show no polarization effects, even for the clay, which under compaction can assume a somewhat regular platelet structure or fabric. The quantity of data collected is much more substantial than the previous results reported above, and in some cases, shows a bilinear response. One can argue from these data that soil fabric does not play a major role in determining the complex dielectric response of moist soils.

Hoekstra and Delaney (1974) also found little difference in the dielectric response of their sand, silt, and clay samples as shown in the data on Figure 19. From an engineering perspective, their conclusion is valid. However, if one wishes to examine the physical mechanisms behind the electrical losses in moist soils, one would have to have more data on each soil type than is shown in Figure 19.

Hallikainen et al. (1985) reported results of measurements on five different soil types. Figure 20 shows curves of dielectric constant versus volumetric water content drawn from polynomial fits to the available data. One could easily argue that these results indicate some differences in electrical behavior due to soil texture at relatively low frequencies (<5 GHz), but hardly any differences at higher frequencies. Their assumption of a polynomial fit (second order in volumetric moisture content) precludes any discussion of bilinear behavior.

Another source of experimental data on moisture content variation is that reported by Campbell (1988) and shown in Figure 21 for three different soils. Clearly, at low frequencies (< 50 MHz) dielectric energy loss goes up with moisture content and is very dependent upon soil type at the upper end of the frequency range of these experiments.

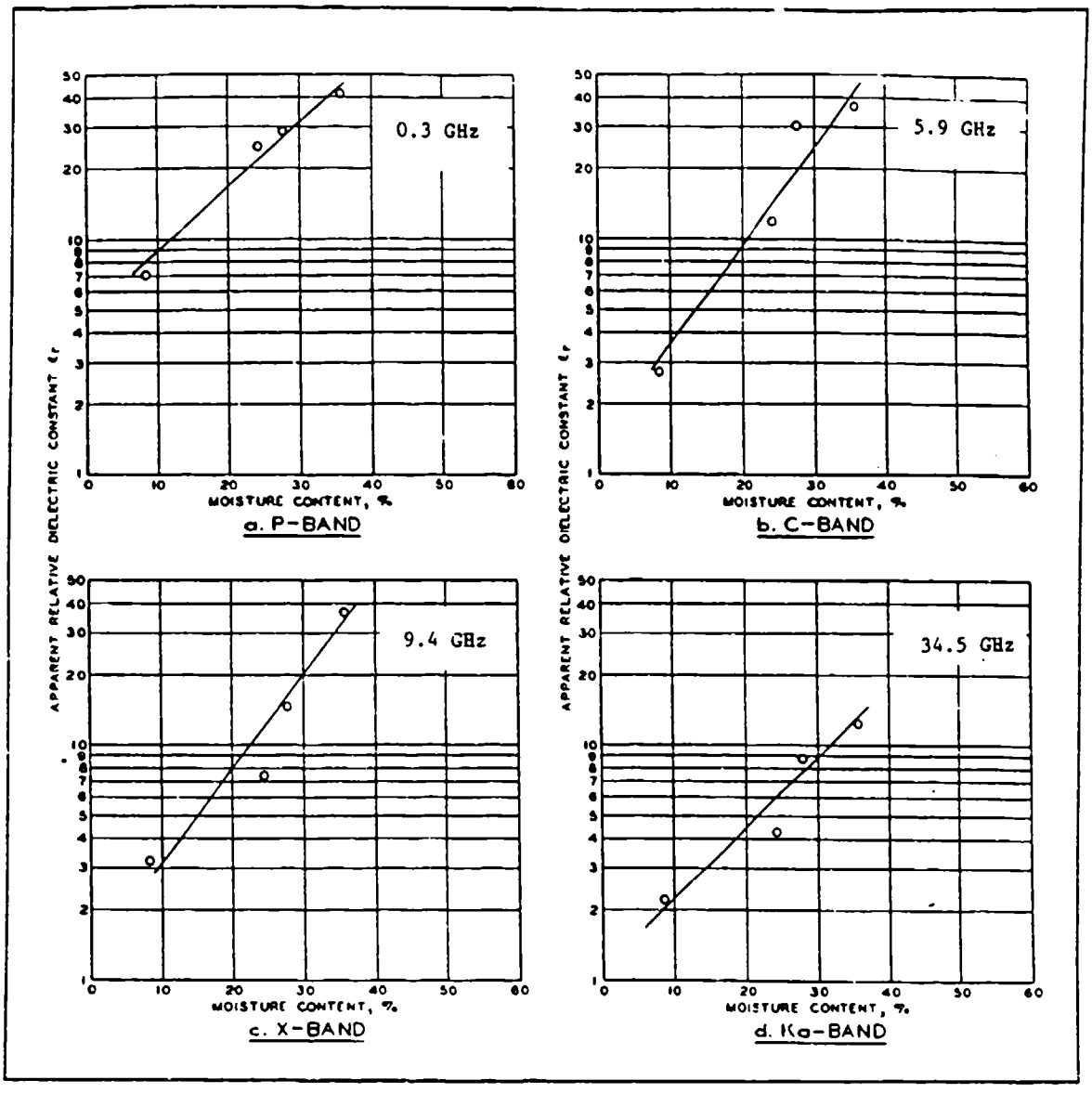

Figure 14. Apparent dielectric constant of a silt loam versus gravimetric moisture (from Lundien (1966))

Effects of sample temperature on dielectric properties

While several of the preceding figures contain information on the effects of sample temperature on dielectric properties, special attention should be given to the work done by Hoekstra and Delaney (1974). While they were not able to conclude anything on the temperature dependence of the characteristic frequency of Debye-type relaxation, they did report on some very interesting dielectric behavior near the freezing point of water. Figure 22 shows how frozen soils, in general, have a lower dielectric response than do unfrozen soils, and that increasing moisture content reveals some very anomalous

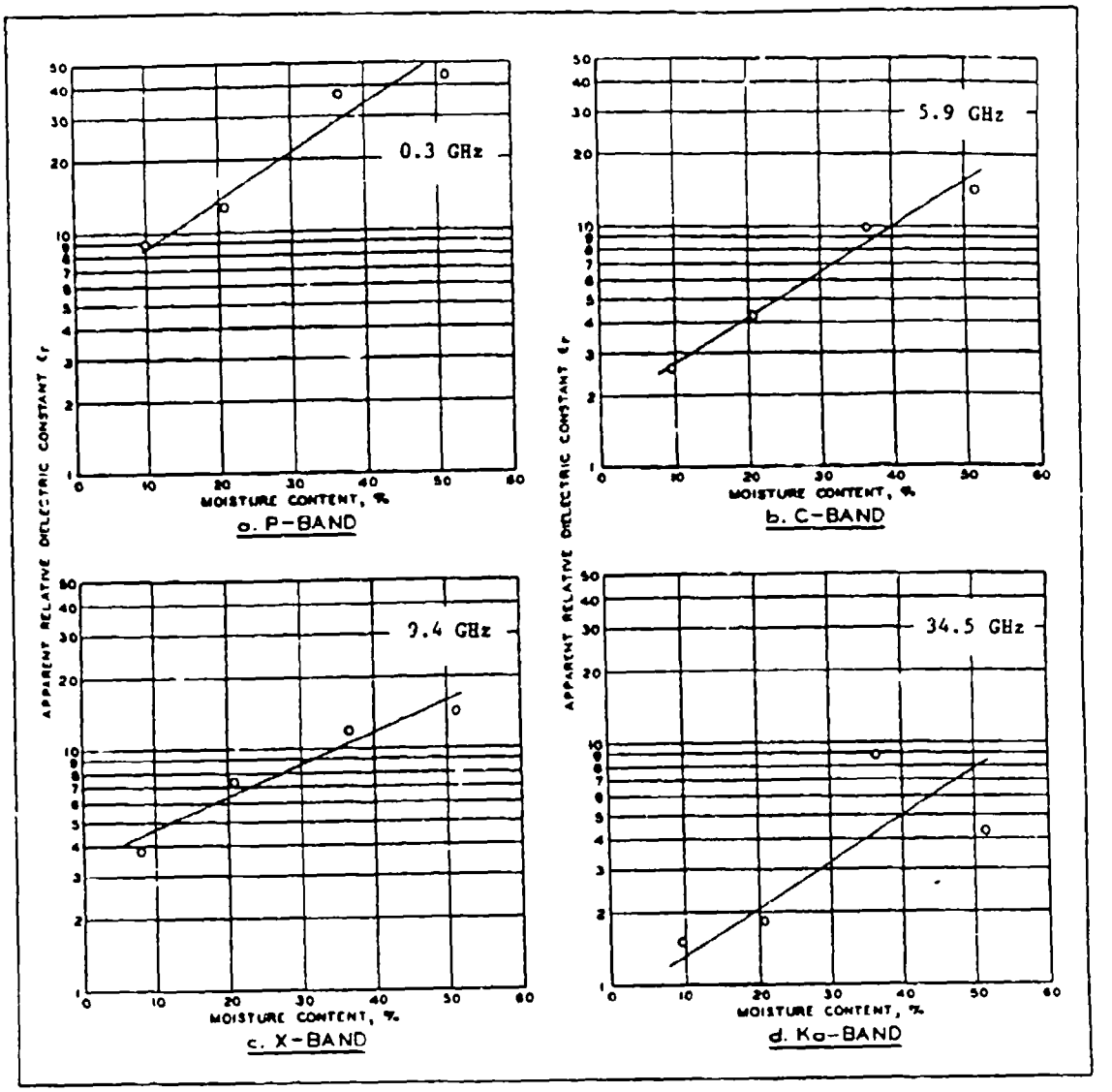

Figure 15. Apparent dielectric constant of a clay versus gravimetric moisture (from Lundien (1966))

behavior near 0 °C. Some earlier results reported by Hoekstra and Doyle (1971) support the same contention.

Another very informative study was carried out by Delaney and Arcone (1982) that involved the cross-plotting of extensive time domain reflectometry data to produce the curves shown in Figure 23 for a silt and a sand.

Hallikainen et al. (1985) also reported measurements made at four different sample temperatures ranging from +23 to -24 °C. Their results, shown in Figure 24, reveal the same relative insensitivity to temperature at subfreezing conditions as was reported by others.

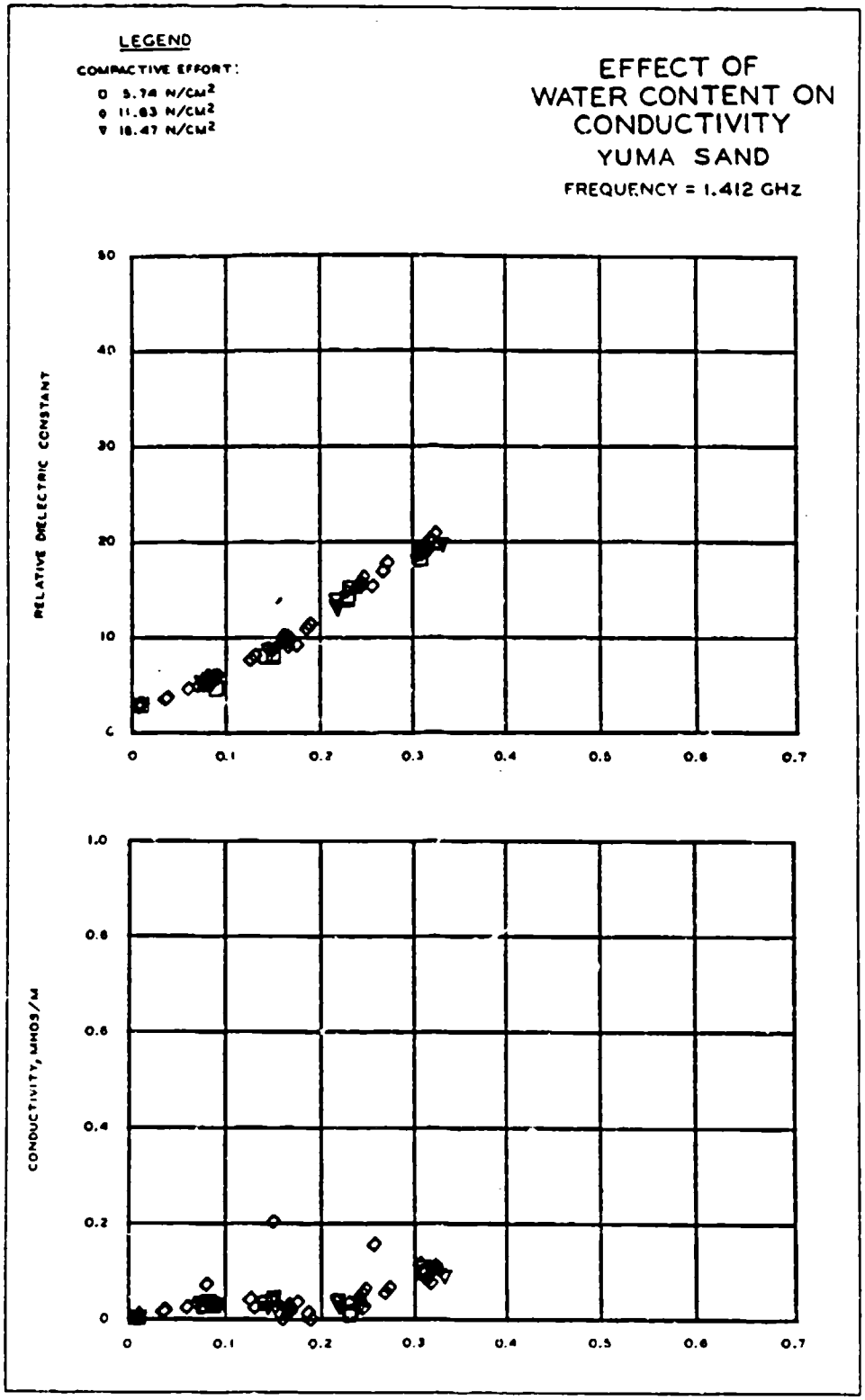

Figure 16. Dielectric constant of a sand versus volumetric moisture (from Lundien (1971))

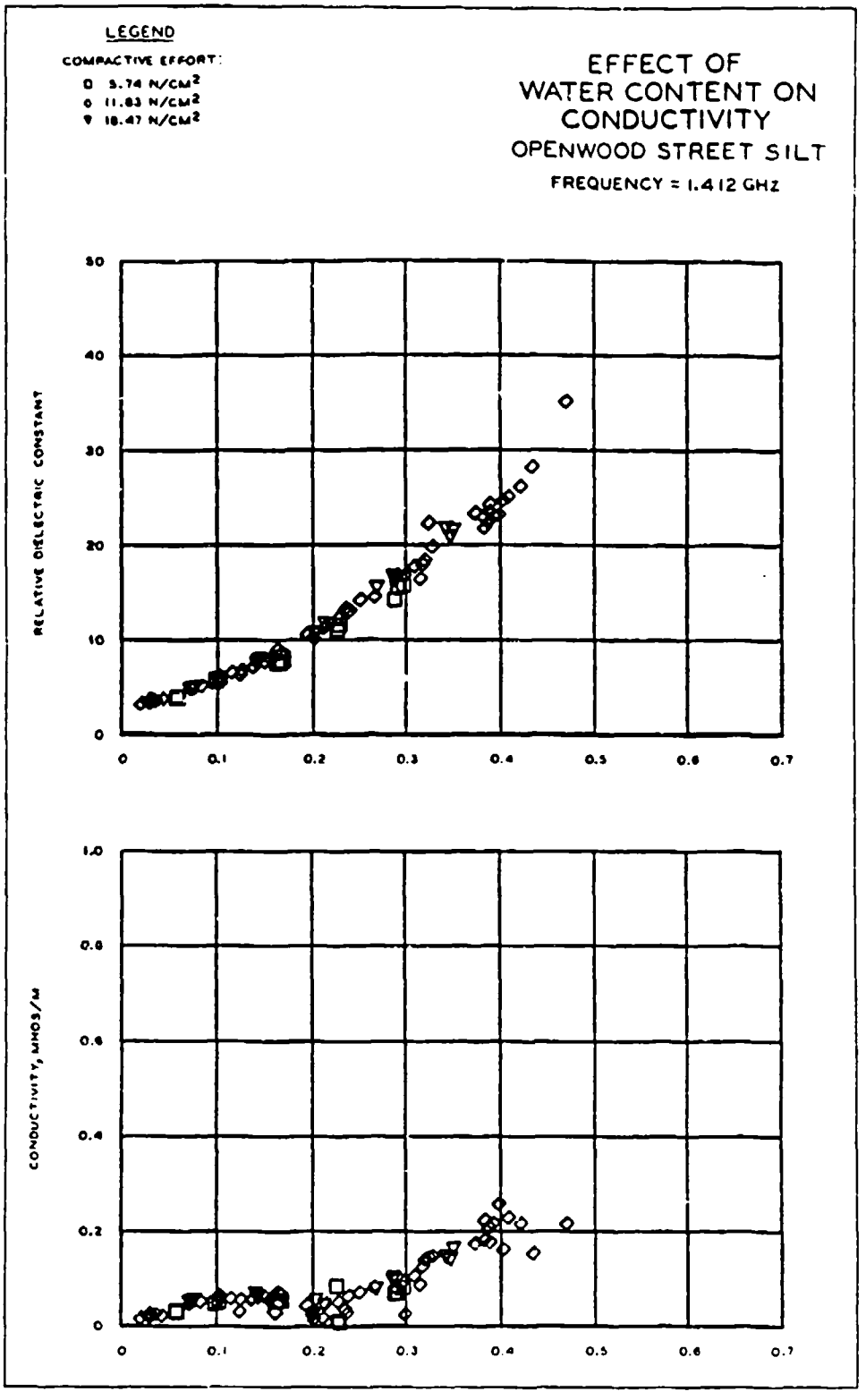

Figure 17. Dielectric constant of a silt versus volumetric moisture (from Lundien (1971))

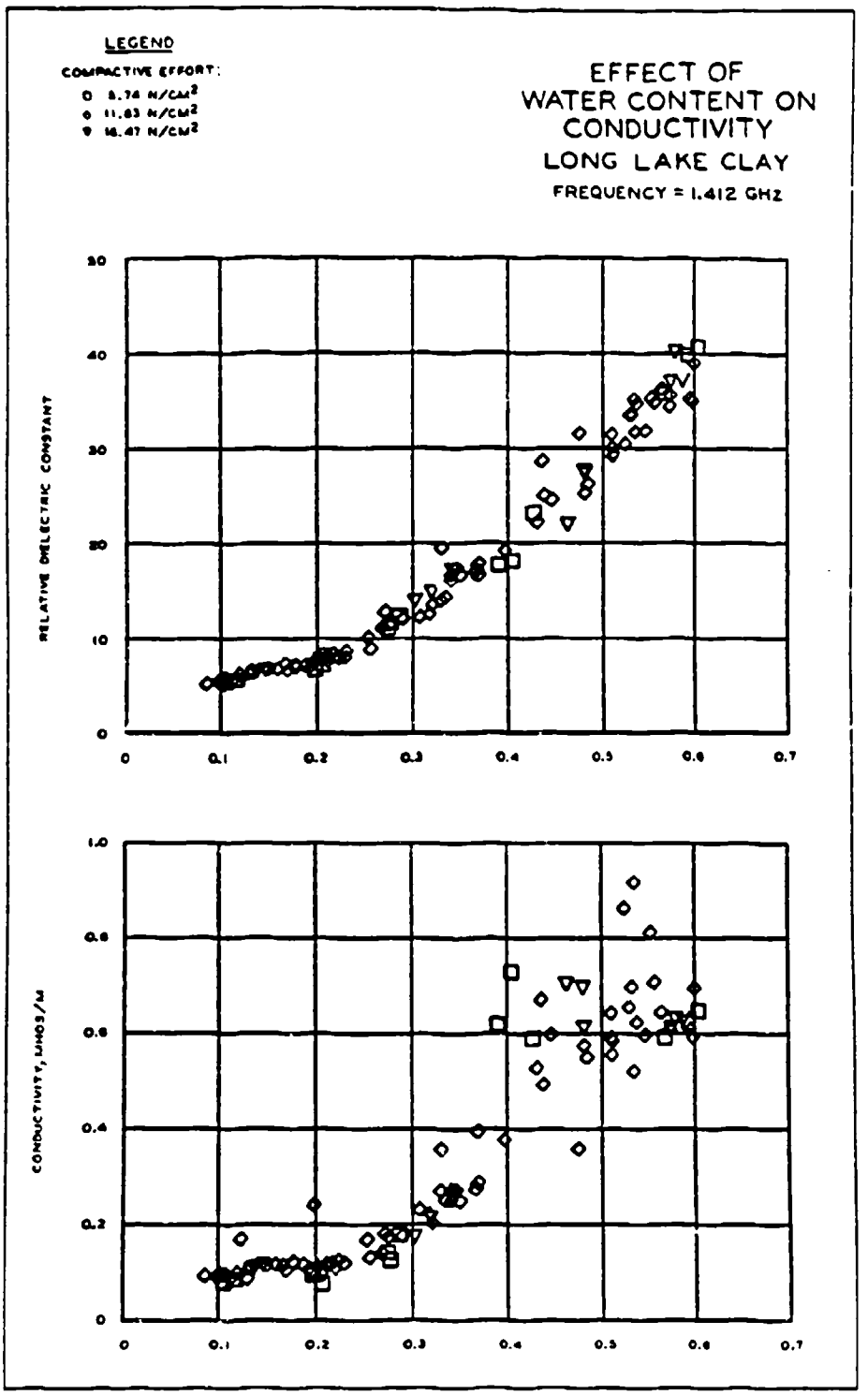

Figure 18. Dielectric constant of a clay versus volumetric moisture content (from Lundien (1971))

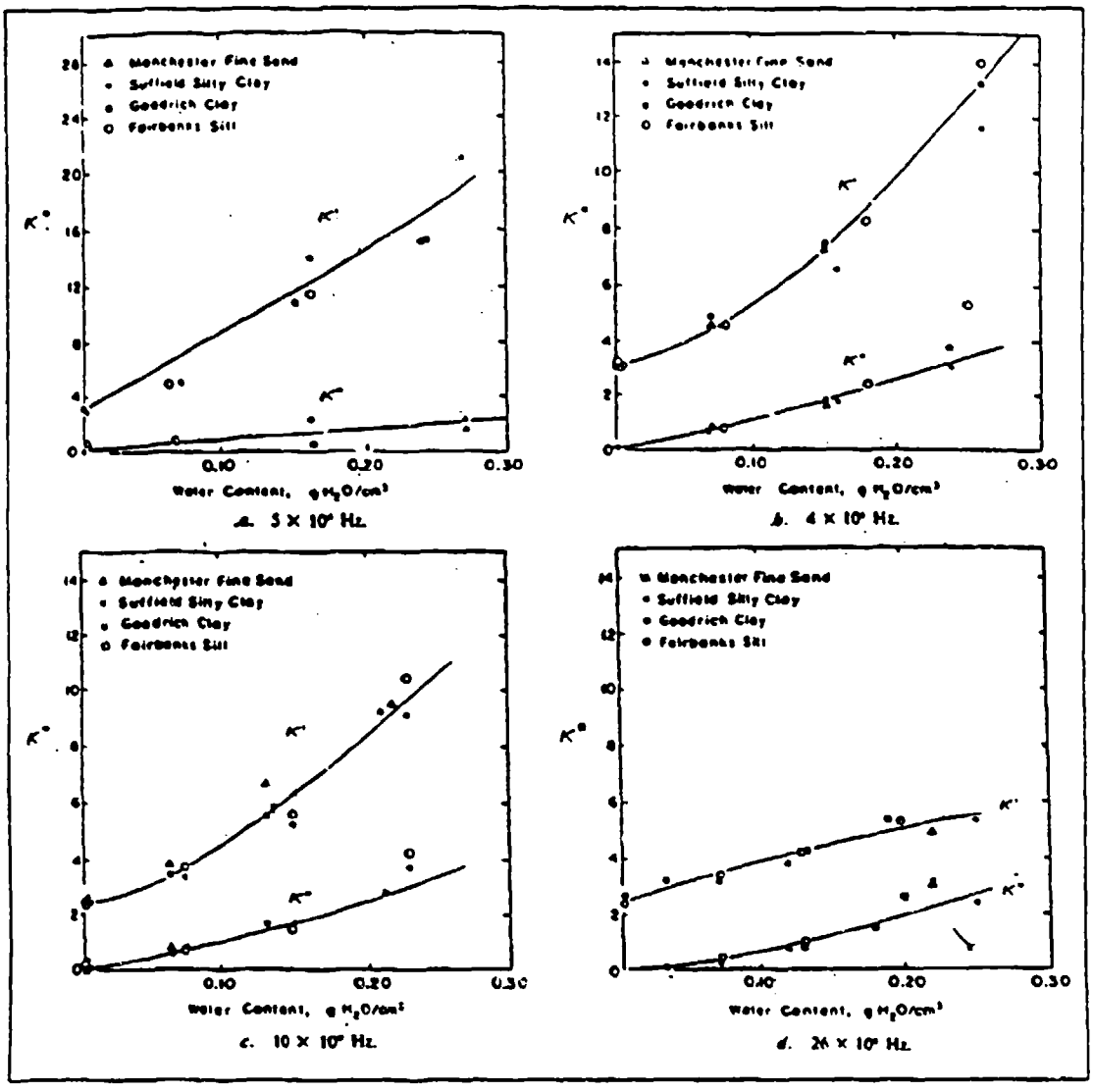

Figure 19. Dielectric constant of soils versus volumetric moisture at 10 °C (from Hoekstra and Delaney (1974))

Bound versus Free Water

In spite of conflicting conclusions regarding the dependence of soil dielectric response on soil texture, many researchers contend that the dependence is there (Wang and Smugge 1980).

If moist soils with different textures do, in fact, possess different dielectric properties for the same levels of moisture content, it must be because of different soil-water bonding mechanisms. Clay particles offer a relatively large amount of electrostatically charged surface area (van Olphen 1963; Dobson et

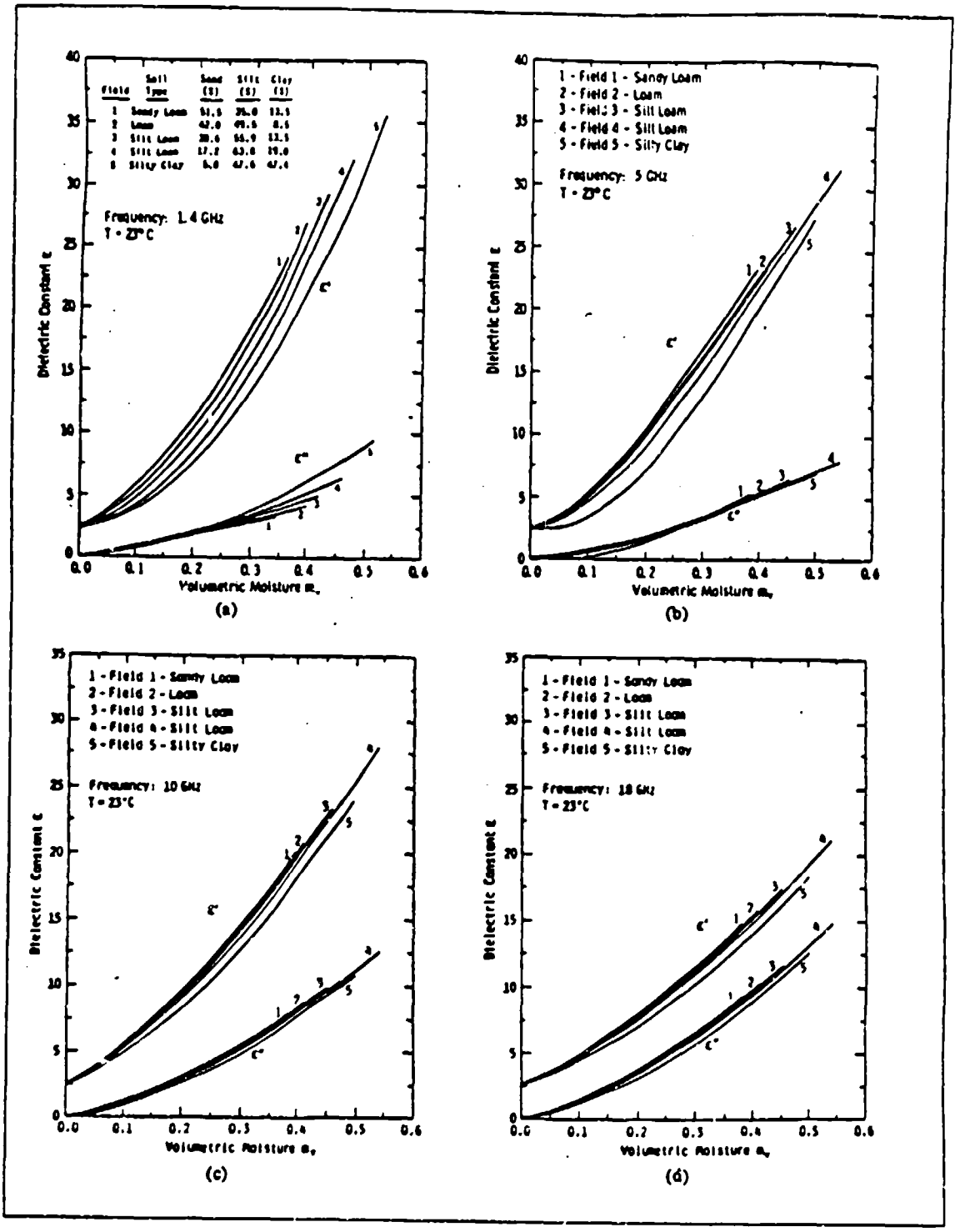

Figure 20. Dielectric constant of soils versus volumetric moisture (from Hallikainen et al. (1985))

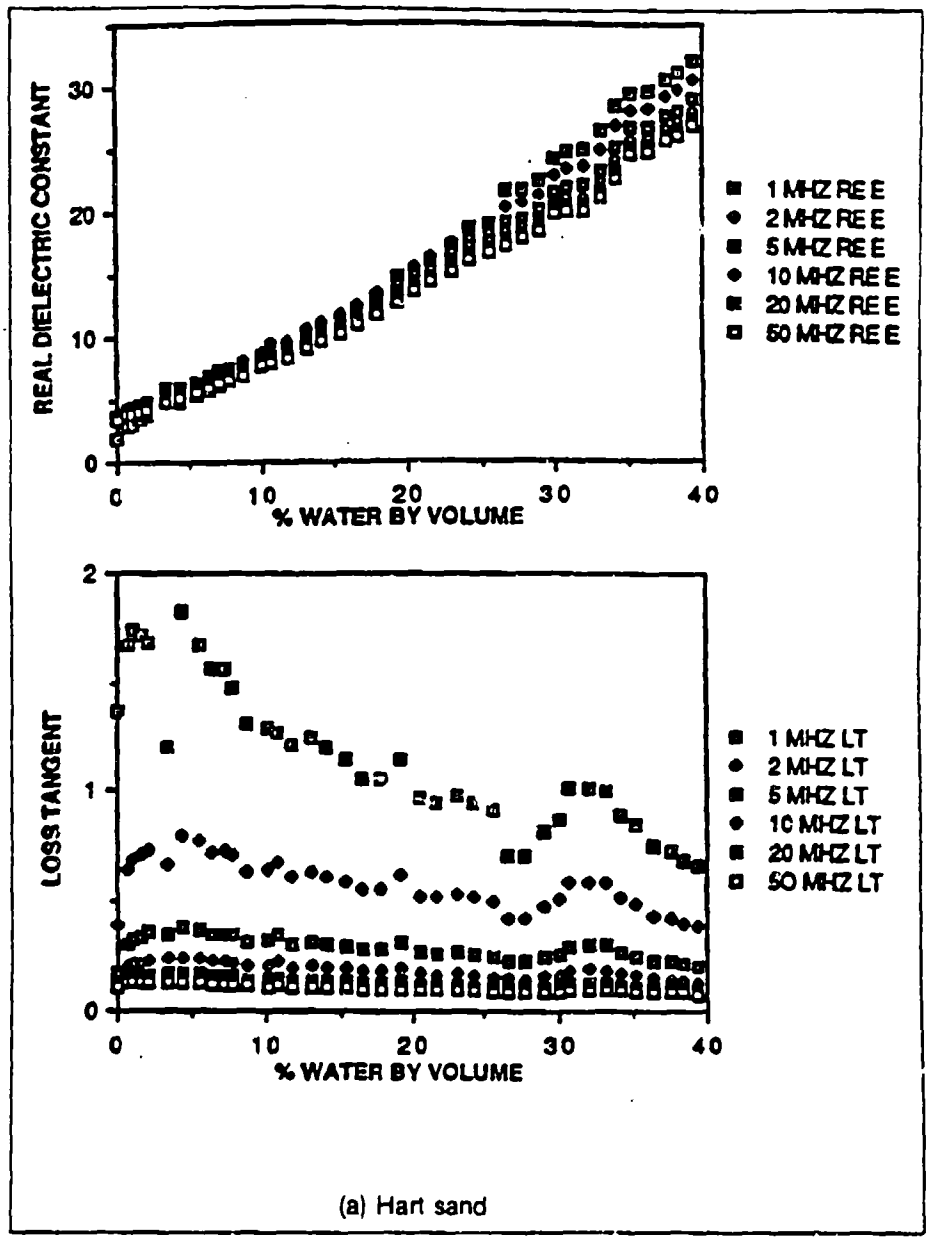

Figure 21. Dielectric constant for soils versus volumetric moisture (from Campbell (1988)) (Sheet 1 of 3)

al. 1985) that could support numerous bonding mechanisms. The unique structure of clayey soils also present many opportunities to alter the dielectric response of the soil as a whole by the creation of microscopic capacitive elements. Even if the surface charge density of sand particles is not significantly different from that of clay particles (van Olphen 1963), the rounded shape of the sand particles and their smaller specific surface area (square meters/gram) must lead to different mechanical as well as electrical behavior.

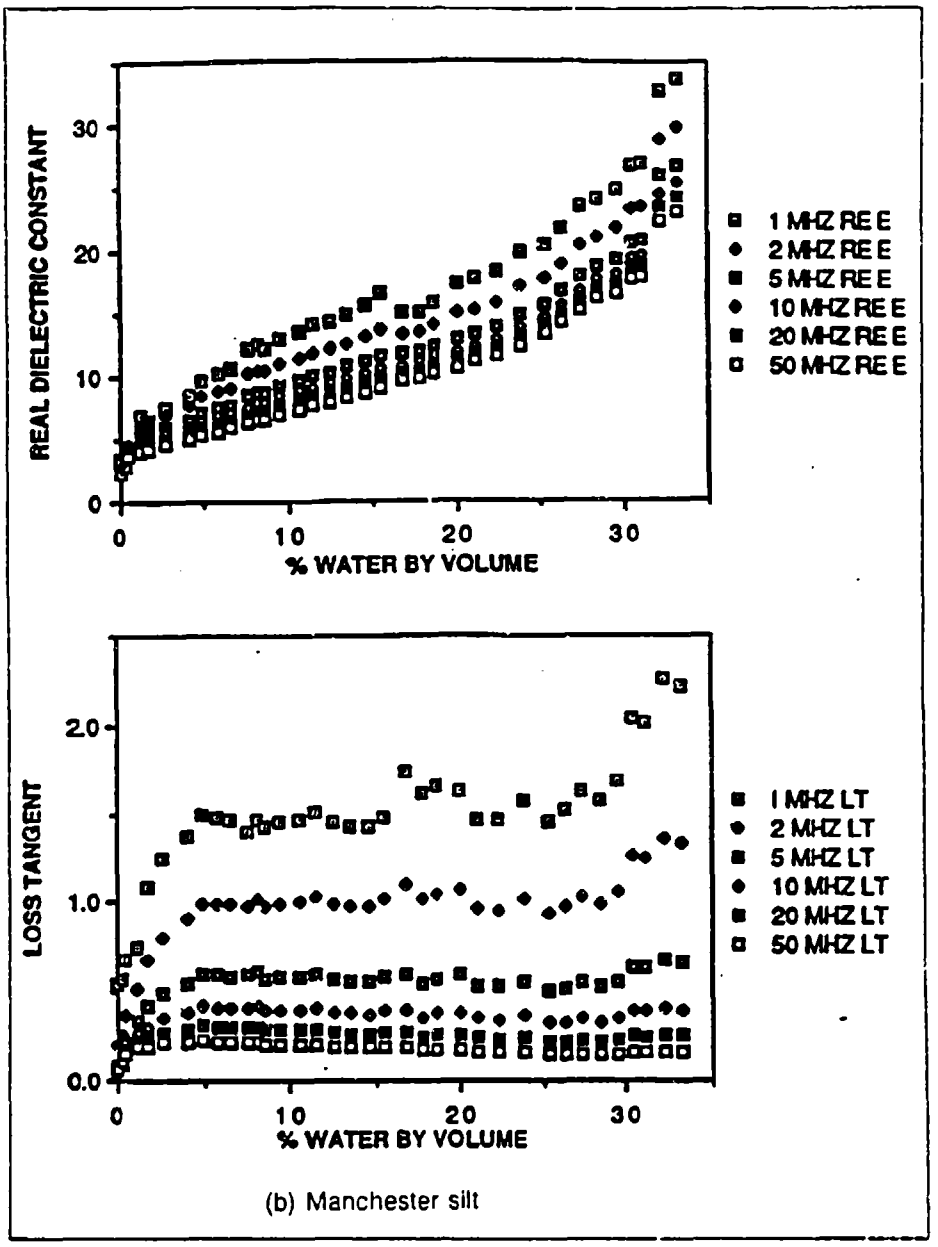

Figure 21. (Sheet 2 of 3)

Relating the physical behavior of moist soil to its dielectric response may even be possible. For example, soil scientists have long associated varying levels of soil tension, reflected in the pressure required to force water from a sample, with varying degrees of soil water bonding. Wang and Smugge (1980) took the concept of soil tension a bit further by correlating a particular level of tension, known as the wilting point, to something called the transition moisture content in moist soils. The transition moisture content is the break point in the bilinear dielectric response referred to in an earlier section.

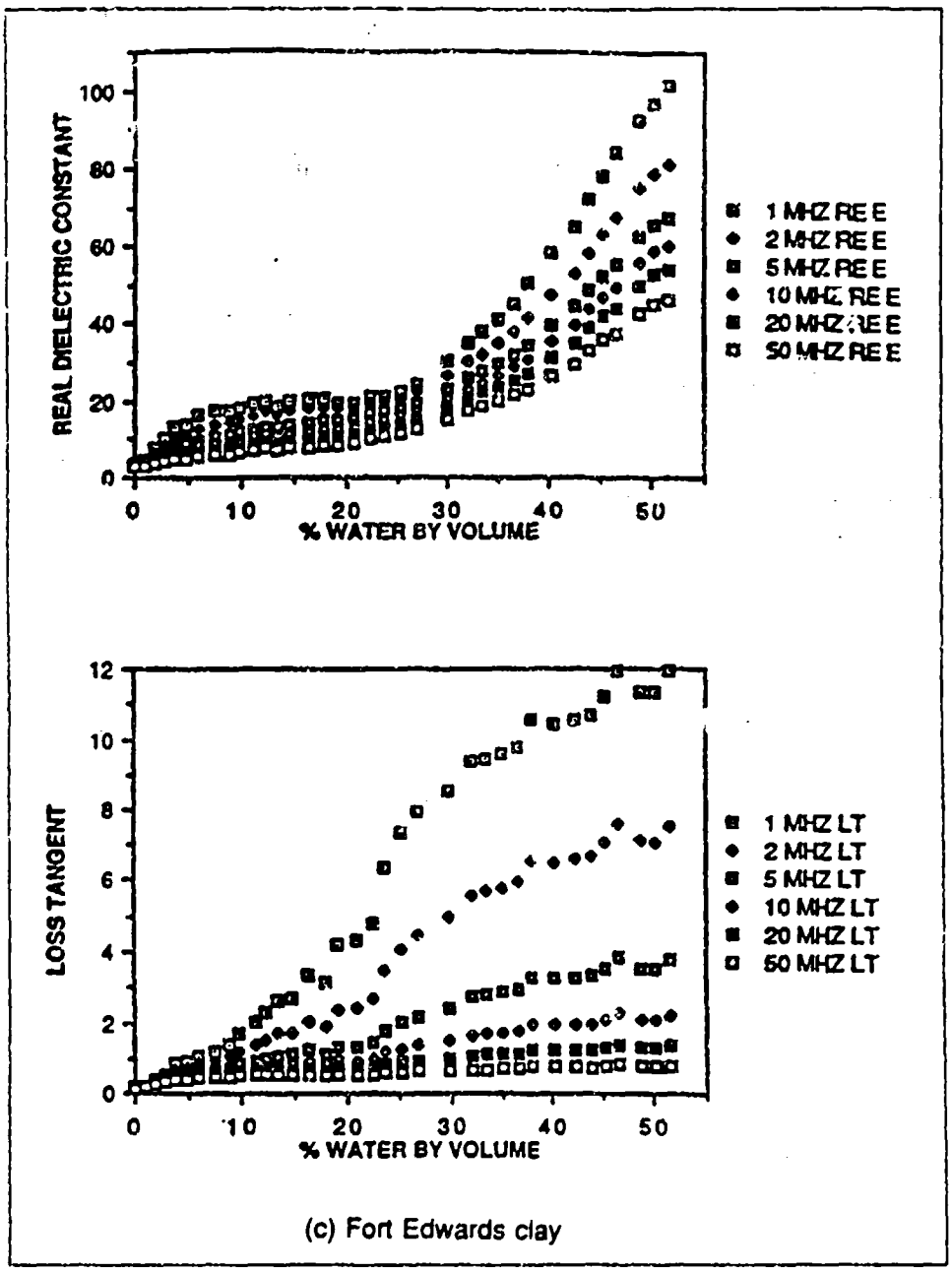

Figure 21. (Sheet 3 of 3)

Universal agreement on a single mechanism for soil-water bonding does not exist. Rather, several hypotheses are offered, each of which can be both supported and refuted by experimental evidence (Mitchell 1974).

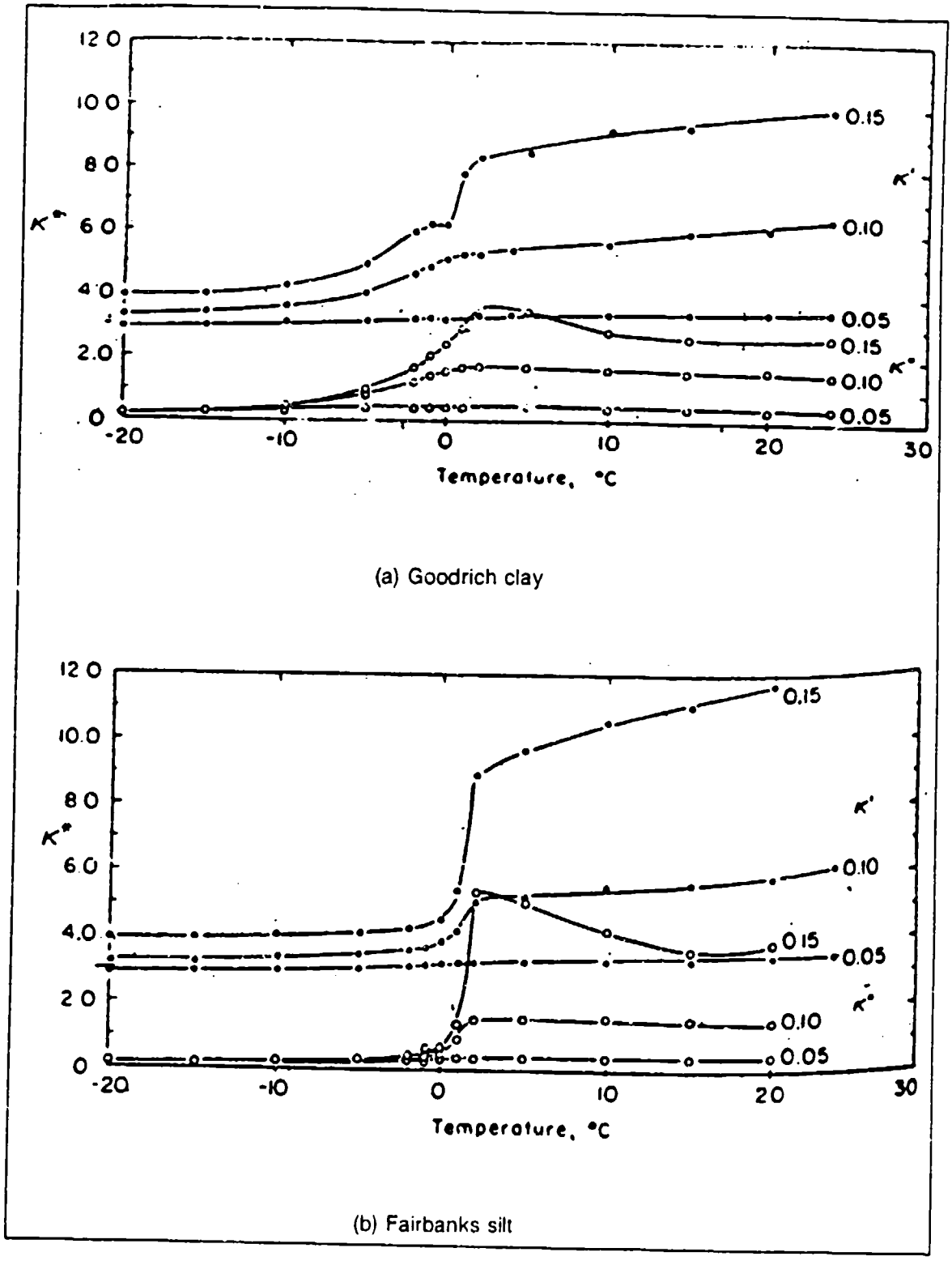

Figure 22. Dielectric constant of soils versus temperature at three volumetric moisture contents (from Hoekstra and Delaney (1974))

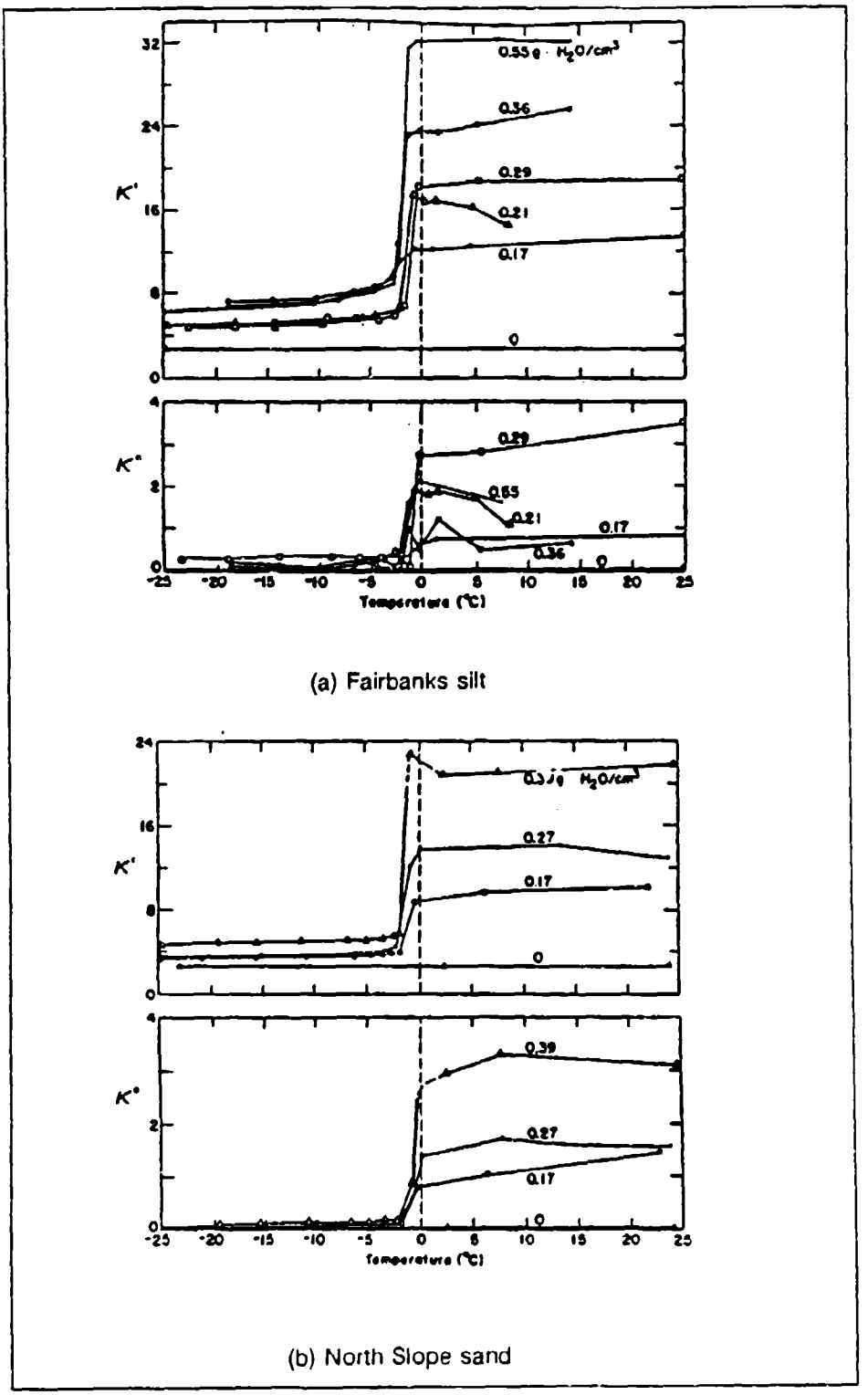

Figure 23. Dielectric constant of soils versus temperature at several volumetric moisture contents and a frequency of 0.5 GHz (from Delaney and Arcone (1982))

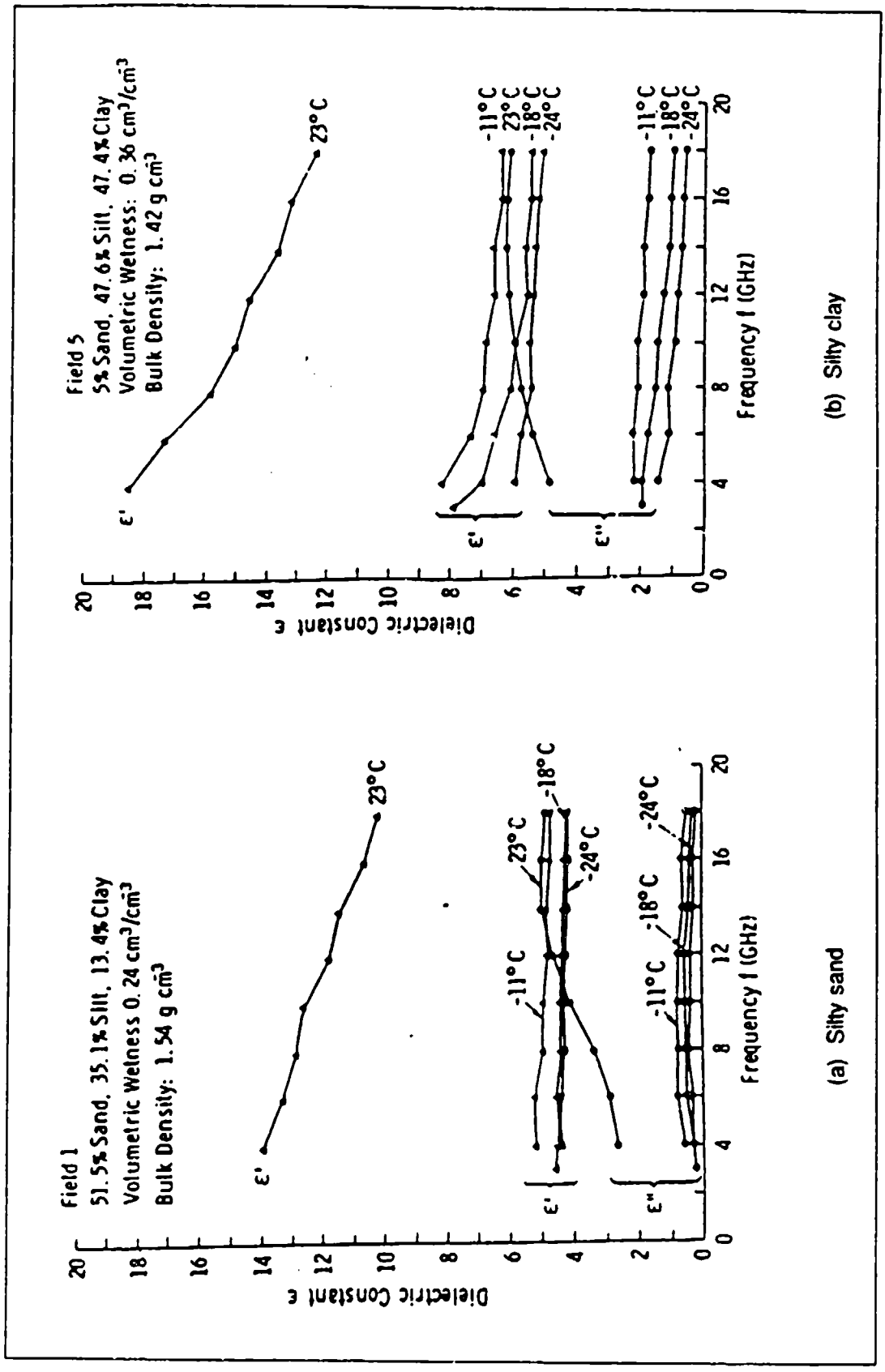

Figure 24. Dielectric constant for two soils as a function of frequency and temperature (from Hallikainen et al. (1985))

Hydrogen bonding

The most easily supportable picture of soil-water bonding is that of hydrogen bonding, which, as discussed previously, is the sharing of a proton by two electronegative atoms. Mitchell (1976) points out that soil particle surfaces are usually composed of either a layer of oxygen atoms or a layer of hydroxyl units. He argues that the shared proton is supplied by the water molecule if the surface layer is oxygen atoms, while the hydroxyl supplies the proton in the other situation. In either case, activation energy measurements do provide some supporting evidence of this mechanism. Newman (1987) further explains that unsatisfied bonds at the edges of clay particles present further bonding opportunities to the water molecules depending on the pH of the fluids in the moist soil.

van der Waal's forces

A second proposed mechanism for soil-water bonding is that of electrostatic attraction combined with the dipole nature of the water molecule to cause several layers of molecules to migrate to the negatively charged surfaces of the soil particles. In clayey soils with platelet surfaces nearly parallel, creating microscopic dielectric-filled capacitive elements through the van der Waal attraction mechanism is possible if one also has cations available to complete the dipole path as shown in Figure 25.

Hydration of exchangeable cations

A third soil-water bonding mechanism is a parasitic one in which cations are attracted to the negatively charged particle surfaces. Newman (1987) views this as the primary water adsorption mechanism in swelling clays. This mechanism assumes that the cations take their water of hydration along with them for the ride. Naturally, one must have cations available in solution for this model to have any validity, and the concentration of cations determines the amount of water that can be bonded. Dobson et al. (1985) was motivated by such a mechanism to model the contribution of bound water in a four-component dielectric mixing model. In reality, a double-layer model was used for ion distribution near clay particle surfaces to modify bulk conductivity for free water losses and simply assumed values of the complex dielectric constant for bound water.

Osmosis

The fourth mechanism (and that least supported by data) is that due to osmotic forces. Again assuming that there are a large number of cations in solution and that their attraction to the negatively charged particle surfaces is stronger than the attraction of the dipole water molecules to the surfaces, this model predicts that there will be a higher concentration of cations closer to the particle surfaces. The existence of another concentration of cations on a

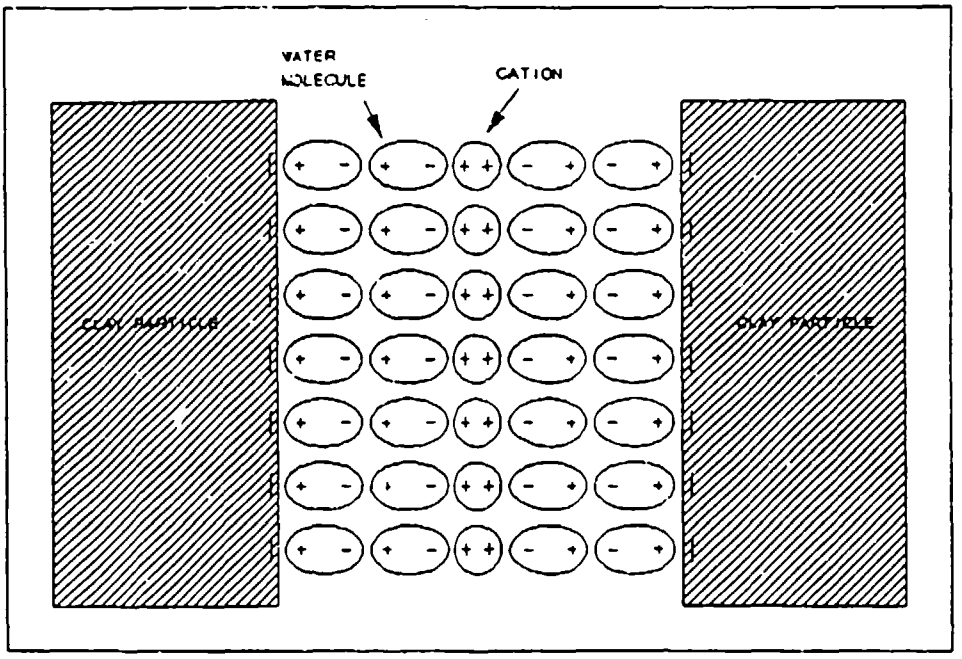

Figure 25. Microscopic capacitive elements in clayey soils

nearby surface then results in a volume of lower particle concentration between the surfaces and the resulting migration of water molecules to that volume.

Whatever the mechanism is, water is attracted to soil particles, particularly clay particles, as proven by the extraordinary pressures required to drain soil samples. In the immediate vicinity of the soil particle surface, the concentration of water molecules should be higher than in the bulk or free water occupying the void spaces (Martin 1960). Thus, one has to believe, even if the bonding mechanism was that of hydrogen bonds, that bound water should exhibit a different dielectric response than free water in the soil matrix.

Radio Frequency Loss Mechanisms

Clearly, water in contact with soil particles must behave differently (electrically) from free water. This shows up very dramatically at radio frequencies through a variety of loss mechanisms that do not exist for the dry minerals or for pure, liquid water. Not only does the water bind to the soil particle surfaces, but also salts are dissolved to produce a source of conducting ions (Mitchell 1974). As already mentioned, microscopic capacitive elements can be created simply from the platelet-like structure of clay particles. These and other phenomena lead to a number of loss mechanisms in moist soils within the radio frequency range that are discussed in the following paragraphs.

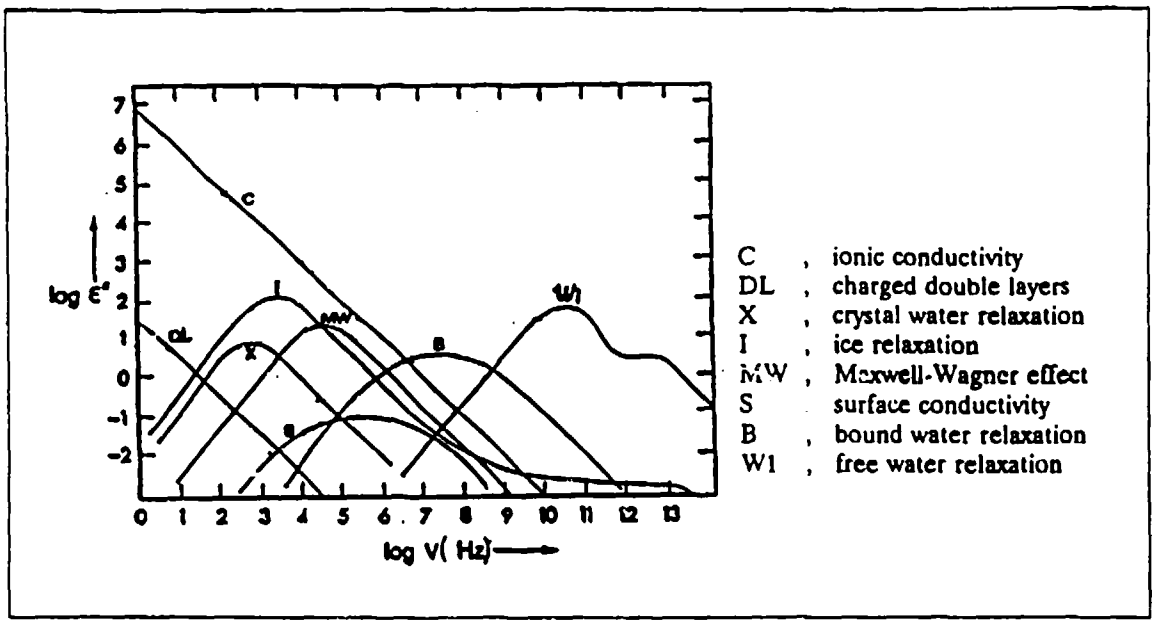

Figure 26. Dielectric loss mechanisms for heterogeneous moist materials (from Hasted (1973))

Hasted (1973) presented a particularly useful schematic (Figure 26) for the relative magnitude and frequency range of application of each of what are believed to be the major contributors to dielectric loss in heterogeneous moist materials. The absolute magnitudes of these effects should not be regarded as applying to any particular material. A very brief description of several of these mechanisms follows. More detailed expositions may be found in other sources (Campbell 1988; Hasted 1973; Mitchell 1976).

Free water relaxation

The inability of free water dipolar molecules to keep up with an applied alternating field has already been discussed in Chapter 2. Dipole relaxation in free water is the dominant loss mechanism at microwave frequencies.

Bound water relaxation

Experimental evidence exists (Muir 1954; Hoekstra and Delaney 1974) that indicates a lowering of the critical dipole relaxation frequency in water that is bound to solid particle surfaces. One can think of this physically in terms of the simple mechanical analog described in Chapter 2 and imagine that, for all other factors kept constant, an increase in the viscosity coefficient will result in an increase in the relaxation time or a lowering of the relaxation frequency. Hall and Rose (1978) proposed bound water relaxation as the dominant loss mechanism in carefully prepared kaolinite clays in the 10- to 100-kHz range of the spectrum, but their conclusions seem to contradict the observations of others and the implications of Figure 26.

Maxwell-Wagner effect

Another loss mechanism often referred to in the literature as the dominant mechanism at radio frequencies is one termed the Maxwell-Wagner effect (Campbell 1988; Bidadi, Schroeder, and Pinnavaia 1988). It originates in the experimental observation that there is dispersion in a suspension of conducting particles in nonconducting dielectric media much like that observed in a parallel-plate capacitor filled with two different dielectrics. The Maxwell-Wagner effect is seen as an accumulation of charge at the interface of dissimilar materials during the flow of current through heterogeneous material due to a discontinuity in dielectric constant values. This charge buildup is time dependent and results in dispersion as the frequency of the alternating current increases to a point where the buildup and relaxation cannot keep up.

When modeled as series capacitors, one having zero conductivity and the other a nonzero conductivity leading to a dielectric loss through Equation 10 (assuming the polarization loss is zero), the Maxwell-Wagner effect can be described by Debye-like relationships (Hasted 1973; Campbell 1988). For example, for equal thickness capacitors, the relaxation time expression is found to be as follows:

$$\tau = \frac{\varepsilon_1 + \varepsilon_2}{4\pi\sigma_1} \tag{31}$$

Thus the relaxation frequency is seen to get smaller as conductivity gets smaller.

One application of the Maxwell-Wagner model (Bidadi, Schroeder, and Pinnavaia 1988) had water as the conductive medium and the clay platelets as the nonconductive medium. The high capacitance of the closely separated platelets was used to argue for the observed enhancement of clay-water permittivity above the level for pure water.

Surface conductivity

Another radio frequency loss mechanism in moist heterogeneous materials is that of surface conductivity. A possible scenario for this loss is a rapid intermolecular proton exchange within the bound water layer on soil particles (Hoekstra and Doyle 1971; Fripiat et al. 1965; von Hippel 1988). One application of this model (Schwan et al. 1962) led to the calculation of a Debye-like relaxation time

$$\tau = \frac{\varepsilon_a}{4\pi\sigma_a} \tag{32}$$

where ε_a and σ_a refer to the permittivity and conductivity of the aqueous solution in which nonconducting particles were immersed. Again, as with the Maxwell-Wagner effect, reducing the conductivity of the aqueous solution reduces the relaxation frequency.

Charged double layers

If one accepts that cations can be attracted to negatively charged soil particle surfaces, then one can possibly think of the cations surrounding the charged particle like an electron cloud surrounding a nucleus. The charged double layer loss mechanism then has a parallel in the concept of atomic polarizability. As the electric field oscillates, so too does the ion cloud about the particle. As frequency goes up, the ability of the cloud to distort goes down with the resulting lowering of the dielectric loss

Ionic conductivity

The most dominant loss mechanism in moist heterogeneous materials at low frequencies is that due to ionic conductivity, the $4\pi\sigma/\omega$ term in Equation (10). Of course, this conductivity is brought about by dissolving salts in the soil and providing a path through the pore spaces for the transport of electrical energy to take place. As a result, low-frequency ionic conductivity in moist soils would have to be related in some way to the degree of saturation or how the pore spaces fill with water.

Activation Energy Data

In the earlier description of the structure of water found in Chapter 2 and under the section entitled Microwave Frequency Loss Mechanisms, arguments were made relating the frequency of peak loss in a Debye-type dielectric relaxation process to the activation energy associated with that process. The slope of a semilogarithmic plot of that relaxation frequency versus the inverse of the absolute temperature is proportional to the activation energy.

Hoekstra and Doyle (1971) argued that linear plots of the log of the dielectric loss term versus the inverse of absolute temperature can also be obtained when the variation in dielectric loss with temperature is caused by changes in the thermal energy of a charge carrier. In fact, the dynamical theory of sorption (Hasted 1973) relates the time of residence of a water molecule on a

surface to the heat of adsorption by the same kind of exponential relationship as used for the earlier activation energy development. Certainly, if loss is inversely proportional to this residence time by virtue of the molecules being free to reorient in the alternating electric field, then Hoekstra's and Doyle's arguments are valid. Thus, if the dielectric loss at any given frequency increases with sample temperature, the semilogarithmic plot mentioned above can lead to an estimate of the energy required to bring about such a change. This change, in turn, may help identify the loss mechansims.

In their 1971 paper, Hoekstra and Doyle did, in fact, measure a linear relationship between the natural logarithm of loss terms and the inverse of absolute temperature for Na-montmorillonite samples. Their results are reproduced in Figure 27 (a) for a frequency of 9.8 GHz and in Figure 27 (b) for a frequency of 0.1 MHz. The activation energy associated with the low-frequency measurements was about 12 kcal/mole, while that associated with the high-frequency measurements was about 6 kcal/mole as long as the temperature exceeded -52 °C. The high-frequency results are consistent with the free water dielectric relaxation mechanism discussed earlier and attributed to the breaking of hydrogen bonds. However, the low-frequency measurements indicate another mechanism for energy dissipation, most likely free charge carriers coupled with Maxwell-Wagner effects.

Campbell (1988) used the same approach as did Hoekstra and Doyle to estimate the activation energy in soils above freezing temperatures. Data he measured at 1 MHz are reproduced in Figure 28. Campbell calculated an activation energy of about 7 kcal/mole and argued that the dominant loss mechanism at this frequency was the Maxwell-Wagner effect.

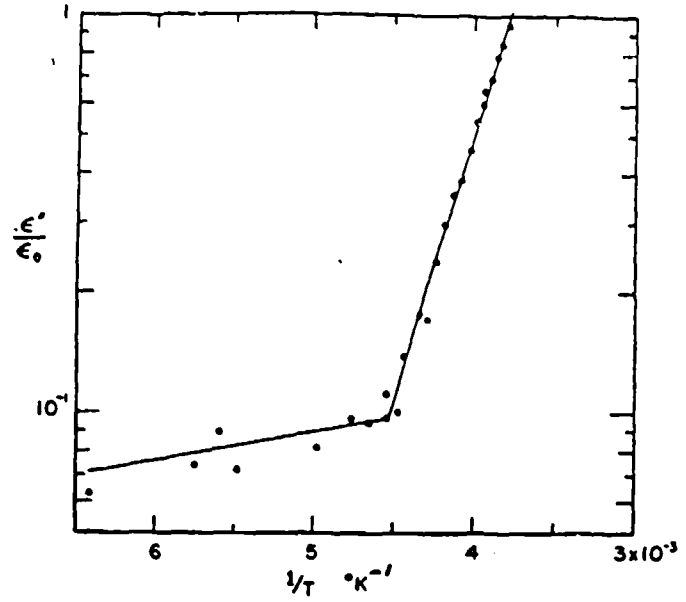

(a) 9.8 GHz, 0.69 g/g water content

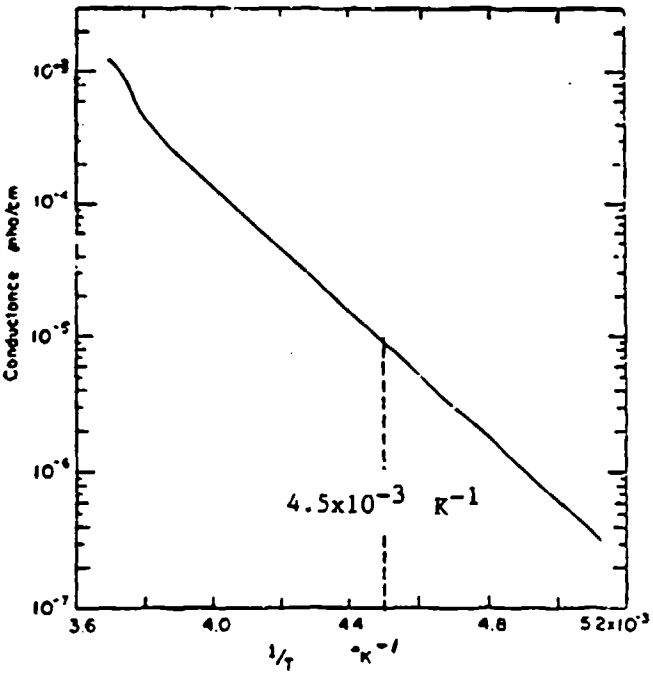

(b) 0.1 MHz, 0.65 g/g water content

Figure 27. Dielectric loss and conductance in Na-montmorillonite as a function of temperature (from Hoekstra and Doyle (1971))

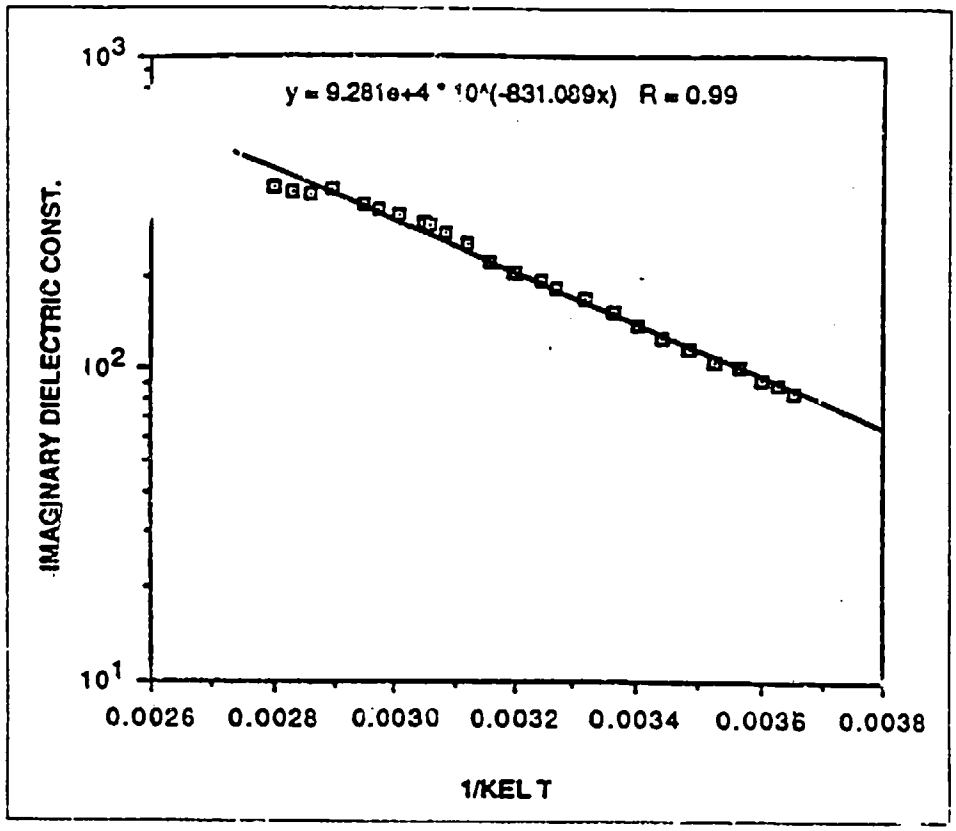

Figure 28. Dielectric losses at 1 MHz (from Campbell (1988))

4 Models for Soil Electrical Behavior

Moist soils are a heterogeneous mixture of mineral particles, water, air, and possibly any number of organic substances. The mineral particles cover a broad range of sizes, varying from as small as a few microns to several centimeters. Water is not pure and, as discussed in the previous section, in combination with the structural features of the mineral particles, can show anomalous dielectric behavior at radio frequencies unlike that of pure water. Nevertheless, the only practical approach to predicting soil response to either physical or electrical driving forces is that a real soil must be modeled as a continuum with homogeneous properties.

As with the review of related electrical property measurements in the previous chapter, a review of electrical property models for soils and water would be remiss without a summary table (Table 2) of significant contributions. Many of the entries in the table will be expounded on in succeeding sections.

Mixing Models

The most common approach to modeling the dielectric response of moist soils that attempts to draw upon a combination of the physical structure of the soil and experimental observations of the electrical response of laboratory samples is that of mixture theory in which the effective dielectric constant for the material takes the functional form

$$\varepsilon_m(f) = \varepsilon_m\left[\varepsilon_1(f), \varepsilon_2(f), \ldots, \varepsilon_n(f)\right] \tag{33}$$

Table 2
Electrical Property Models

Author(s)	Year	Material(s)	Frequency(ies)	Description
Debye	1929	Liquids	----	Classical anomalous-dispersion model with single-peak loss frequency (or relaxation time)
Cole, Cole	1941	Liquids, solids	-----	Modification to Debye's model to account for a distribution of relaxation times
Malmberg, Maryott	1956	Water	<1 MHz	Polynomial function relating permittivity to temperature
Reynolds, Hough	1957	Heterogeneous mixtures	-----	Mixture model incorporating ratio of field strength within particles to the macroscopic average
Looyenga	1965	Heterogeneous mixtures	----	Symmetrical weighted mixture formula
de Loor	1968	Heterogeneous mixtures	-----	Begins to focus on water
Stogryn	1971	Saline water	----	Debye model with empirical relationships for static permittivity and relaxation time
Ray	1972	Ice, water	----	Cole-Cole model plus DC conductivity and temperature dependence
Arulanandun, Smith	1973	Clays	2-60 MHz	Equivalent circuit applications
Olhoeft, Strangway	1975	Lunar soils	>100 MHz	Permittivity is a nonlinear function of density
Klein, Swift	1977	Sea water	1.4, 2.65 GHz	Similar to Stogryn
Wang, Schmugge	1980	Clays, sands	1.4, 5 GHz	Mixture model that accounts for moisture content, a transition moisture content, and soil porosity

(Continued)

Table 2 (Concluded)

Author(s)	Year	Material(s)	Frequency(ies)	Description
Troitskii, Stepanov	1980	Soils	0.6, 1.0, 10 MHz	Dependency of permittivity on specific surface and moisture at fixed frequencies
Shutko, Reutov	1982	Soils	1-3 GHz	Surveyed existing models to obtain best fits under selected conditions
Katz, Thompson	1985	Sandstones	—	Electrical conductivity modeled with fractal geometry concepts
Manabe, Liebe, Hufford	1987	Water	<100 MHz	Single Debye relaxation model with temperature dependence
Ulaby, El-Rayes	1987	Vegetation	0.2-20 GHz	Mixture model distinguishing free and bound water
Sapoval, Chazalviel, Peyriere	1988	Theoretical	—	An attempt to relate the observed response of porous electrodes to a fractal description of its surface
Dissado, Hill	1989	Theoretical	—	Fractal-dependent fractal dimensions of electrodes

where

$\varepsilon_m(f)$ = frequency-dependent dielectric constant of the mixture

$\varepsilon_i(f)$ = frequency-dependent dielectric constant of the ith component of the mixture

In general, the mixture dielectric should lie somewhere between that of a parallel plate capacitor that is filled with a mix of fibers extending from one plate to the other and that of a capacitor filled with sheets of material whose interfaces are parallel to the plates (Hasted 1973). The former is called parallel mixing, and the latter is called series mixing. For example, if one took the soil to consist of air, water, and some homogeneous soil mineral, the two mixing models would take the form

PARALLEL MIXING

$$\varepsilon_m = W_a\varepsilon_a + W_w\varepsilon_w + W_s\varepsilon_s \tag{34}$$

SERIES MIXING

$$\frac{1}{\varepsilon_m} = \frac{W_a}{\varepsilon_a} + \frac{W_w}{\varepsilon_w} + \frac{W_s}{\varepsilon_s} \tag{35}$$

where the subscripts are self-explanatory and the W_i represent weighting factors. The weighting factors are most commonly taken to be the volume fraction occupied by that substance.

One reference to an early generalization of the mixture model for three components was given by Ansoult, deBacker, and DeClercq (1984) as

$$\varepsilon_m^k = \varepsilon_a^k W_a + \varepsilon_w^k W_w + \varepsilon_s^k W_s \tag{36}$$

In this case, $k = +1$ represents parallel mixing, and $k = -1$ represents series mixing.

From an even more physical basis, many researchers have developed dielectric constant mixture models that consider the effects of local electric fields on the induced internal fields of specially shaped homogeneous dielectric particles. Reynolds and Hough (1957) argued that a general formulation for a three-component system could be written as either

$$\varepsilon_m = \varepsilon_1\delta_1 f_1 + \varepsilon_2\delta_2 f_2 + \varepsilon_3\delta_3 f_3 \tag{37}$$

or

$$(\varepsilon_m - \varepsilon_1)\delta_1 f_1 + (\varepsilon_m - \varepsilon_2)\delta_2 f_2 + (\varepsilon_m - \varepsilon_3)\delta_3 f_3 = 0 \tag{38}$$

where the δ_i are the volume fractions of material "i" and the f_i are the local field ratios; that is, the ratio of the field within the dielectric component to the average field in the sample. From Stratton (1941), a homogeneous electric field induces a field inside a spheroid in such a way that

$$f_i = \sum_{j=1}^{3} \frac{\cos^2\alpha_j}{1 + A_j\left[\left(\frac{\varepsilon_i}{\varepsilon^*}\right) - 1\right]} \tag{39}$$

where

α_j = angles between the field and the axes of the spheroid

A_j = depolarization factors related to the shape of the spheroid

ε^* = dielectric constant of the homogeneous material into which the spheroid is inserted

deLoor (1968) published the same result, but less general in the sense that he assumed a random orientation of spheroids for which $\cos^2\alpha_j = 1/3$.

One of the more well-known mixture formulae is that associated with Boettcher which, for a two-component mixture, can be written as

$$\frac{\varepsilon_m - \varepsilon_2}{3\varepsilon_m} = \delta_1 \frac{(\varepsilon_1 - \varepsilon_2)}{(\varepsilon_1 + 2\varepsilon_m)} \tag{40}$$

which comes from Equations 37 and 39 by setting A_j = 1/3 (spheres) and $\varepsilon^* = \varepsilon_m$. In this formula, ε_1 is the dielectric constant of the particles and ε_2 is the dielectric constant for the host medium.

Another popular formula comes from Equations 38 and 39 and $\varepsilon^* = \varepsilon_2$, A_j = 1/3 (spheres). This yields Rayleigh's formula

$$\frac{\varepsilon_m-\varepsilon_2}{\varepsilon_m+2\varepsilon_2} = \delta_1\frac{(\varepsilon_1-\varepsilon_2)}{(\varepsilon_1+2\varepsilon_2)} \tag{41}$$

Bruggeman took the differential form of Rayleigh's formula and integrated it between the limits of ε_2 and ε_m to arrive at the formula

$$\varepsilon_m = \varepsilon_1 - (\varepsilon_1-\varepsilon_2)(1-\delta_i)\left(\frac{\varepsilon_m}{\varepsilon_2}\right)^{\frac{1}{3}} \tag{42}$$

Looyenga (1965) converted Boettcher's formula into a differential equation on volume fraction δ_i and integrated between the limits of 0 and 1 to give the symmetrical form (similar to Equation 36)

$$\varepsilon_m^{\frac{1}{3}} = \delta_1\varepsilon_1^{\frac{1}{3}} + \delta_2\varepsilon_2^{\frac{1}{3}} \tag{43}$$

Birchak et al. (1974) utilized a symmetrical form much like Equation 43 except that the powers were taken to be 1/2 instead of 1/3.

$$\varepsilon_m^{\frac{1}{2}} = \delta_1\varepsilon_1^{\frac{1}{2}} + \delta_2\varepsilon_2^{\frac{1}{2}} \tag{44}$$

One positive feature of the mixture models is that they all come from the same origin; namely, consideration of the average electric field and electric displacement in a mixture of otherwise homogeneous materials in which the variables are physically measurable quantities of volume fractions and the dielectric constants of the components. Thus there is much physics involved in developing these formulae. The approximations involved in obtaining different formulae include the particle shapes and orientation distribution and what value gets assigned to the host medium dielectric constant when computing the field ratios.

All of these mixture formulae, as well as many others (Reynolds and Hough 1957) have been applied to particular data sets with satisfactory results. However, saying that one formula applies to all situations and materials would be impossible.

The converse is also true; i.e., one cannot expect all of these formulae to fit a limited set of data. Wang and Smugge (1980) exercised several

two-component mixture models (probably resulting in slight overestimates at low-moisture contents due to ignoring air voids) to calculate the real part of the complex dielectric constant as a function of moisture content and to compare the span of model predictions with real data collected at 1.4 GHz. Figure 29 shows the results of those calculations. Curve 3 is the bounding simple parallel mixing formula (Equation 34); curve 1 is Rayleigh's formula (Equation 41); curve 2 is Boettcher's formula (Equation 40); and curve 4, which gives the best fit, is Birchak's model (Equation 44). Looyenga's results (Equation 43) have also been added as "L" symbols.

Campbell (1988) has demonstrated that the dielectric response of real materials is bounded by the series and parallel models. It is not surprising that Looyenga's model for spherical particles is a good fit to much of the data (Hasted 1973), as it clearly lies between these limits. Dobson et al. (1985) has carried mixture models to the four-component level by introducing different parameters for soil particles, air, free water, and water tightly bound to the soil particles.

Equivalent Circuits

Thinking of mixtures in terms of their electrical analogs is often advantageous, particularly when one wants to consider different electrical paths through the medium and some semiempirical way to account for the weighting of those paths. The following paragraphs take a careful look at equivalent circuits for both individual components of mixtures and the mixtures themselves. They range from quite simple models to quite complex circuits. However, with today's readily available computational power, exercising these models is very straightforward.

Homogeneous materials

The complex dielectric constant and conductivity of a linear material relate an applied electric field to current flow within the material through Ampere's law (Equation 10). Current flow in the material can be modeled by a two-terminal network of lumped circuit elements. Furthermore, because real materials do exhibit both energy storage (capacitive) and energy-loss (free charge movement and dielectric relaxation) mechanisms, imagining that simple equivalent circuits will have to include both capacitive and resistive elements is natural. The following paragraphs describe models of the shunt response of two-terminal equivalent circuits that represent the flow of current (both conduction and displacement) between the inner and outer conducting surfaces of a coaxial device and through the dielectric mixture being measured. The series response, or current flow along the inner and outer conducting surfaces, which would be represented by series inductive and resistive elements, is not modeled.

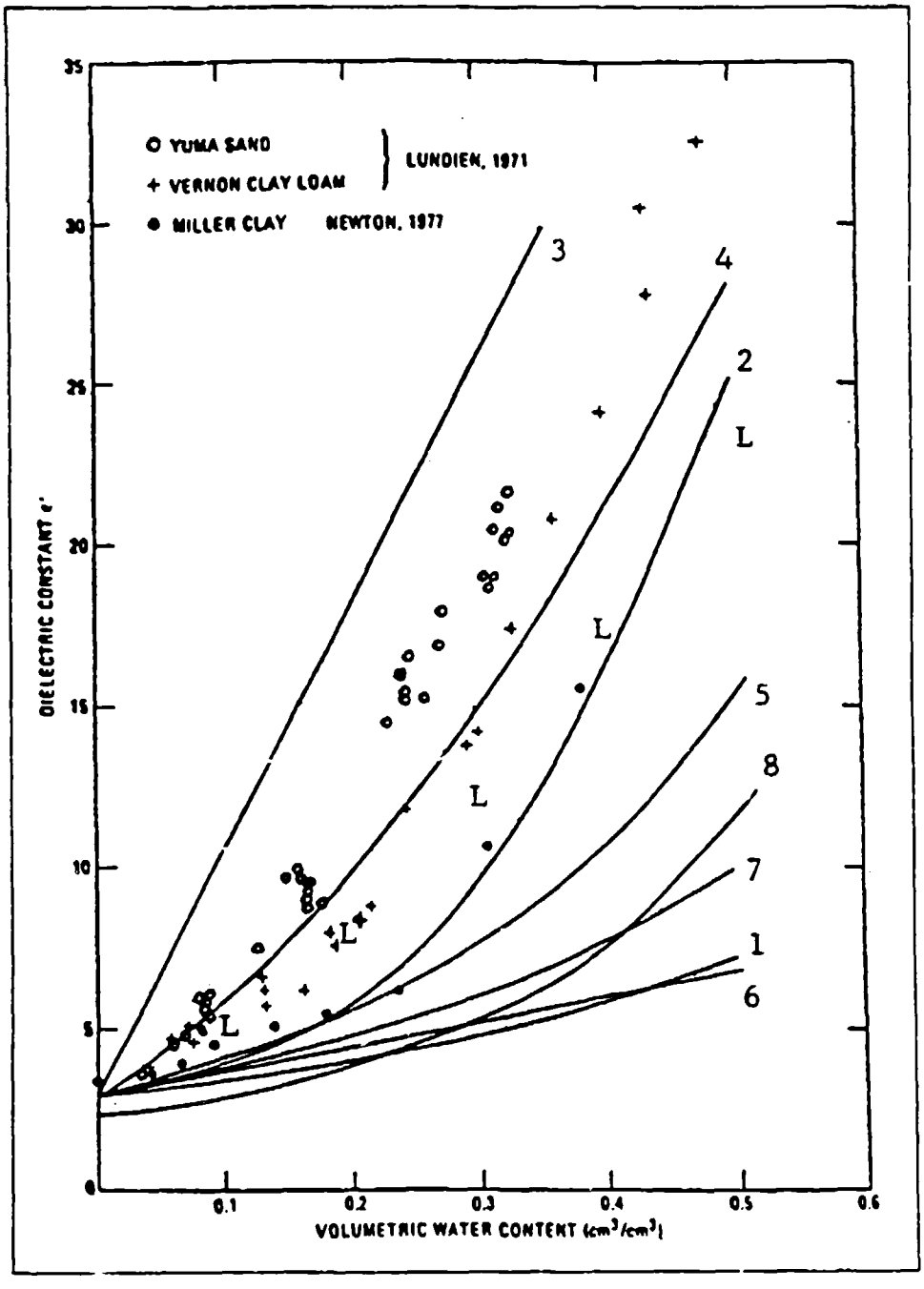

Figure 29. Several mixing formulas plotted against real data (from Wang and Smugge (1980))

As examples of simple equivalent circuits, one should consider the two circuits shown in Figure 30, one having constant value elements in series and the other with elements in parallel. Drawing upon the very useful concept of equivalent capacitances for each of the elements in these and the following circuits($C_R = i/\omega R$; $C_L = -1/\omega^2 L$), the frequency-dependent dielectric response of the circuits in Figure 30 can be shown to be

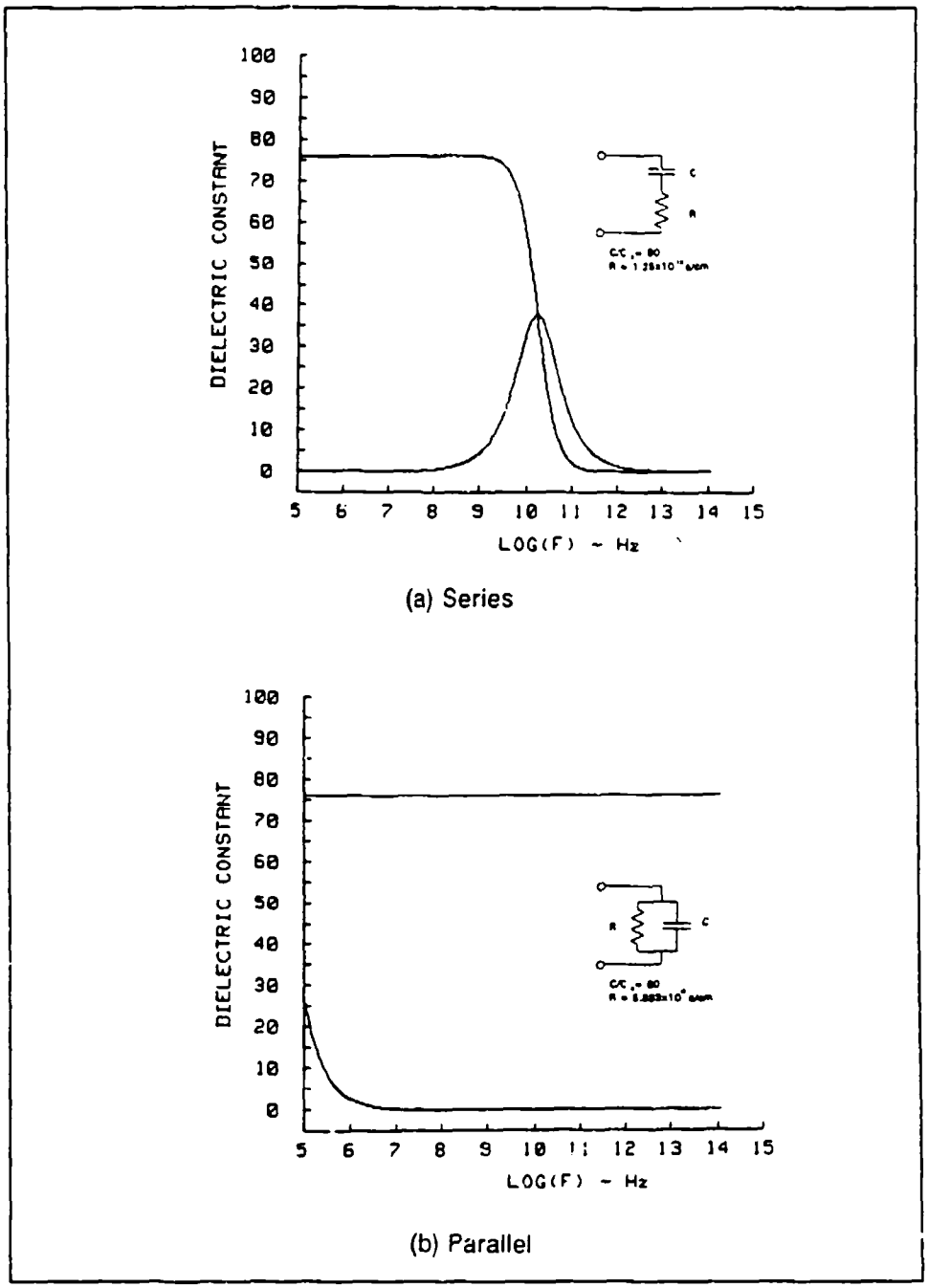

Figure 30. Simple equivalent circuits (after von Hippel (1954))

SIMPLE SERIES MODEL

$$\varepsilon' = \frac{C}{C_0\left[1+(\omega RC)^2\right]} \tag{45}$$

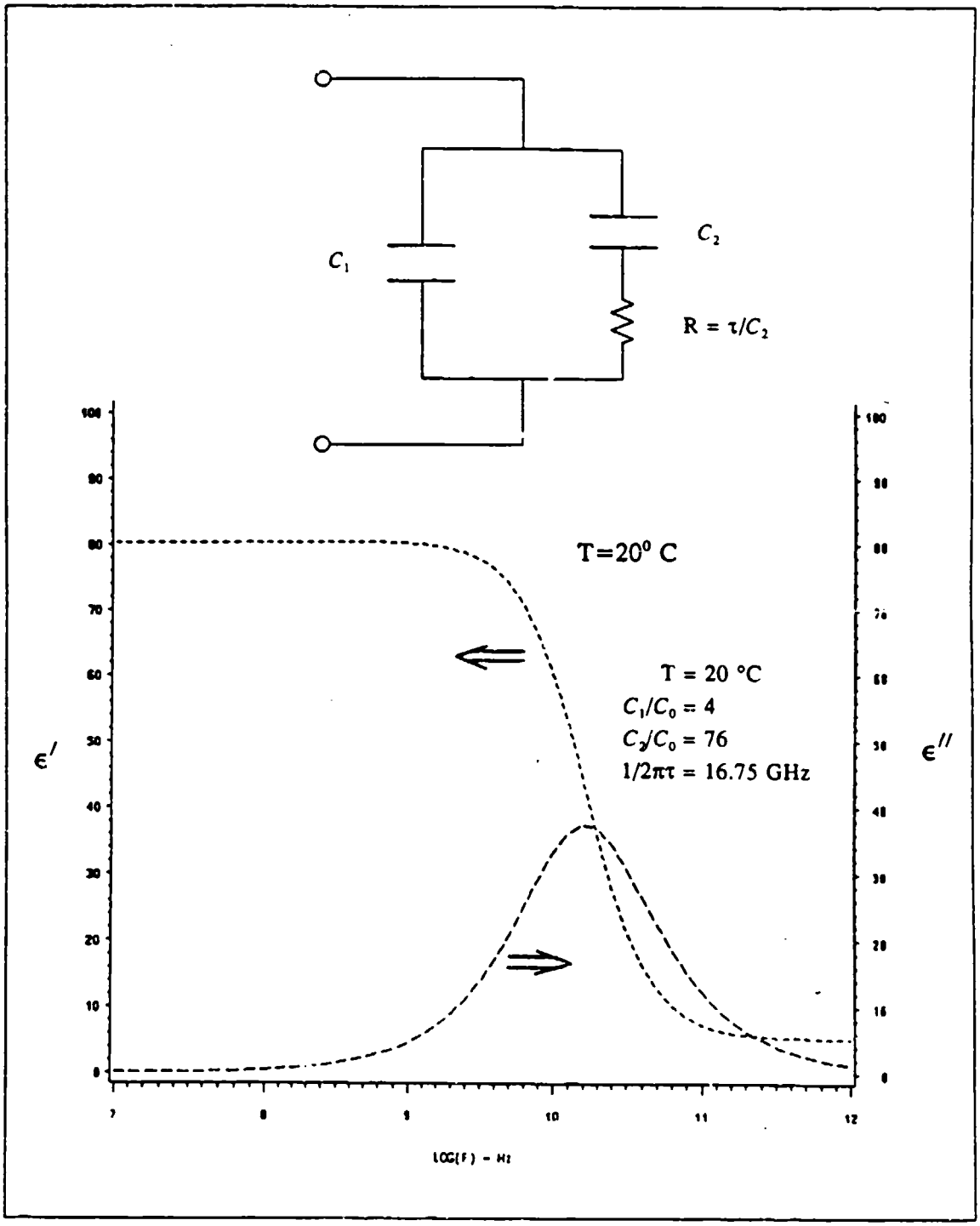

Figure 31. Debye equivalent circuit and its response

$$\varepsilon'' = \frac{\omega R C^2}{C_0 \left[1 + (\omega R C)^2\right]}$$

when C_0 represents the vacuum capacitance.

SIMPLE PARALLEL MODEL

$$\varepsilon' = \frac{C}{C_0} \tag{46}$$

$$\varepsilon'' = \frac{1}{C_0 \omega R}$$

The physical interpretation of the parameters contained in these equations is that the capacitor accounts for the dielectric polarization of the material and the resistor is representative of ionic conduction or other losses that decrease with increasing frequency. Both parameters are adjustable to provide the best fit of the amplitude and phase response of the material as it is measured over a broad range of frequencies.

However, neither of these circuits adequately model the high-frequency behavior of water with regard to the real part of the dielectric constant. The parallel model, when placed in series with another parallel model, has been used to model the Maxwell-Wagner losses in saturated soils (Smith 1971; Bidadi, Schroeder, and Pinnavaia 1988).

As reported in an earlier section, Cole and Cole (1941) used equivalent circuits to describe both the ideal Debye relaxation model and their own interpretation of real data. To help make this section of the study self-contained, their circuits are reproduced in Figures 31 and 32.

The corresponding governing equations for the Debye and Cole-Cole models are

DEBYE MODEL

$$\varepsilon' = \frac{C_1}{C_0} + \frac{C_2}{C_0\left[1 + (\omega R C_2)^2\right]} \tag{47}$$

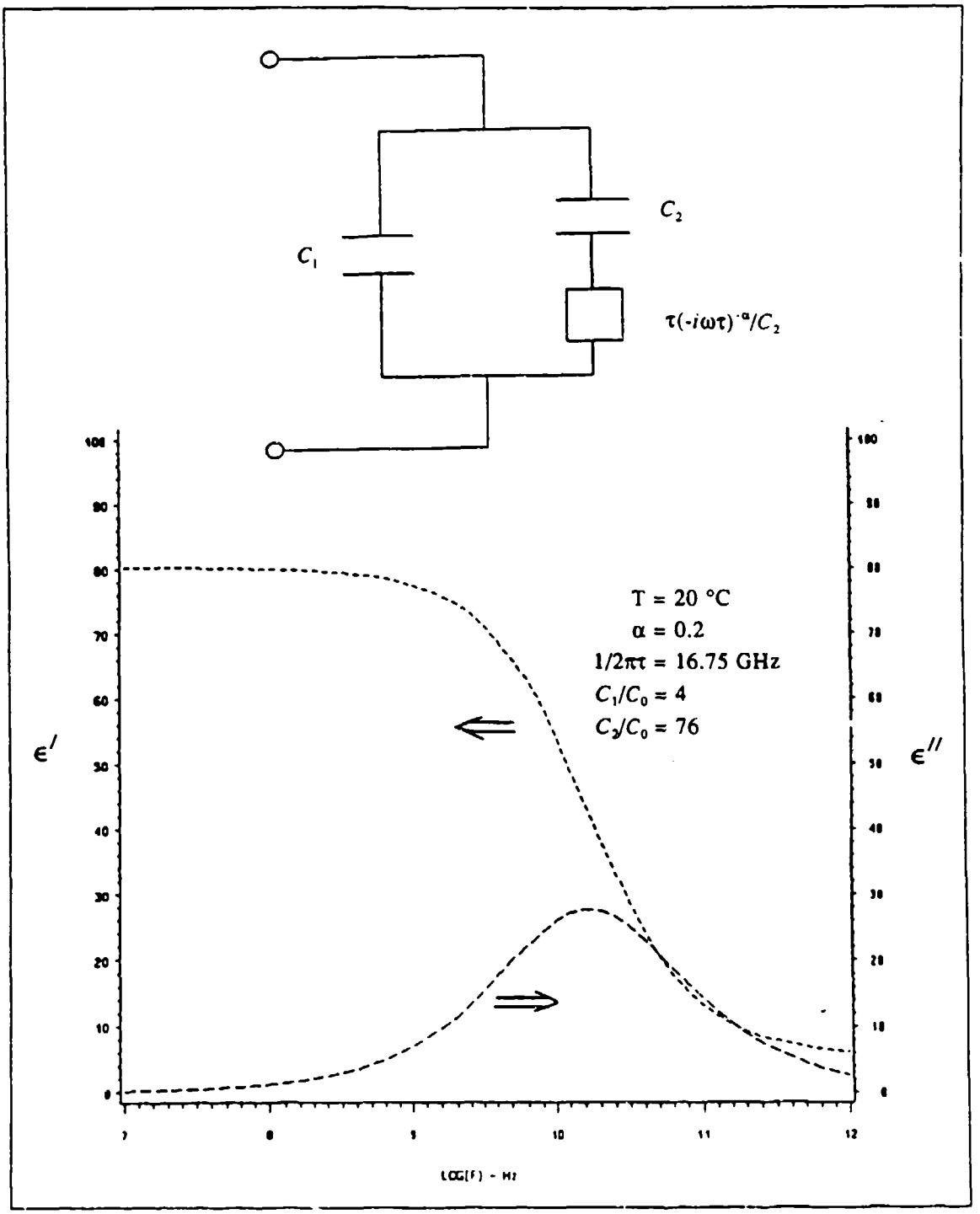

Figure 32. Cole-Cole equivalent circuit and its response

$$\varepsilon'' = \frac{\omega R C_2^2}{C_0\left[1+(\omega R C_2)^2\right]}$$

COLE-COLE MODEL

$$\varepsilon' = \frac{C_1}{C_0} + \frac{C_2}{C_0}\,\frac{\left[1 + (\omega\tau_0)^{1-\alpha}\sin\frac{\alpha\pi}{2}\right]}{\left[1 + 2(\omega\tau_0)^{1-\alpha}\sin\frac{\alpha\pi}{2} + (\omega\tau_0)^{2(1-\alpha)}\right]} \qquad (48)$$

$$\varepsilon'' = \frac{C_2}{C_0}\,\frac{\left[(\omega\tau_0)^{1-\alpha}\cos\frac{\alpha\pi}{2}\right]}{\left[1 + 2(\omega\tau_0)^{1-\alpha}\sin\frac{\alpha\pi}{2} + (\omega\tau_0)^{2(1-\alpha)}\right]}$$

where $1/\tau_0$ is the radial frequency at the peak loss.

Approximating the dielectric response of impure water through the use of equivalent circuits is even possible. von Hippel (1954) used the circuit shown on Figure 33 as an approximation to the frequency response of water exhibiting low-frequency ionic conductivity. The frequency response of the dielectric constant in von Hippel's water model is governed by the following set of equations.

VON HIPPEL'S WATER MODEL (with ionic conductivity)

$$\varepsilon' = \frac{C}{C_0\left[1 + (\omega R_2 C)^2\right]} \qquad (49)$$

$$\varepsilon'' = \frac{\left[1 + (\omega R_2 C)^2 + \omega^2 R_1 R_2 C^2\right]}{C_0 \omega R_1\left[1 + (\omega R_2 C)^2\right]}$$

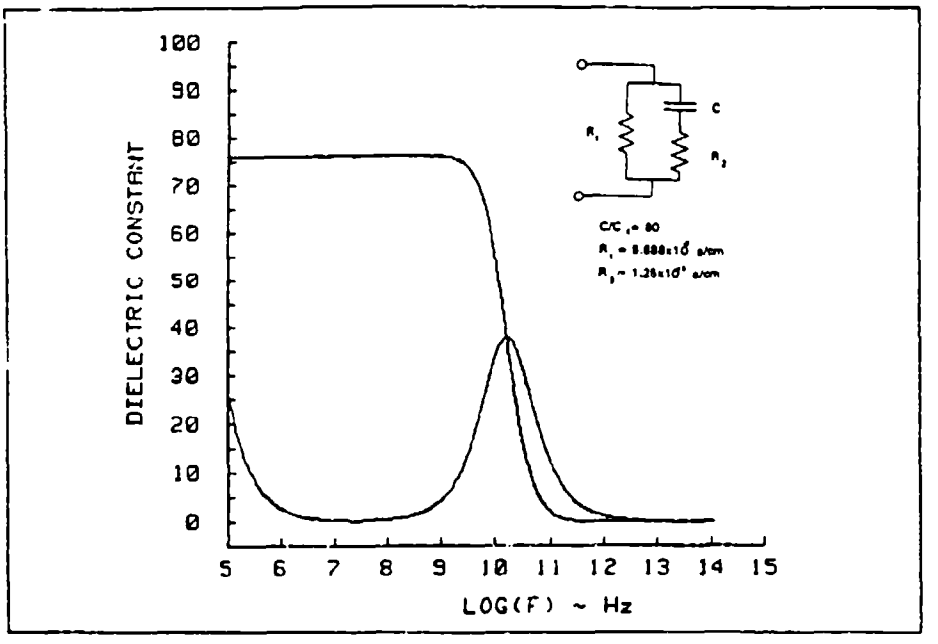

Figure 33. Equivalent circuit for impure water (after von Hippel (1954))

In fact, there is no reason not to include another parallel capacitor to von Hippel's water model to account for the high-frequency permittivity, ending up with a four-element model shown in Figure 34 for which the governing equations are

$$\varepsilon' = \frac{C_1}{C_0} + \frac{C_2}{C_0\left[1 + (\omega R_2 C_2)^2\right]} \tag{50}$$

$$\varepsilon'' = \frac{\left[1 + (\omega R_2 C_2)^2 + \omega^2 R_1 R_2 C_2^2\right]}{C_0 \omega R_1 \left[1 + (\omega R_2 C_2)^2\right]}$$

Mixtures

It certainly seems reasonable to use combinations of homogeneous material equivalent circuits to model the frequency dependent dielectric response of mixtures such as moist soils. In fact, such models would be particularly useful for studying the effects of water content in nonsaturated soils if there could be a sensible weighting of the equivalent circuit elements to account for varying moisture contents.

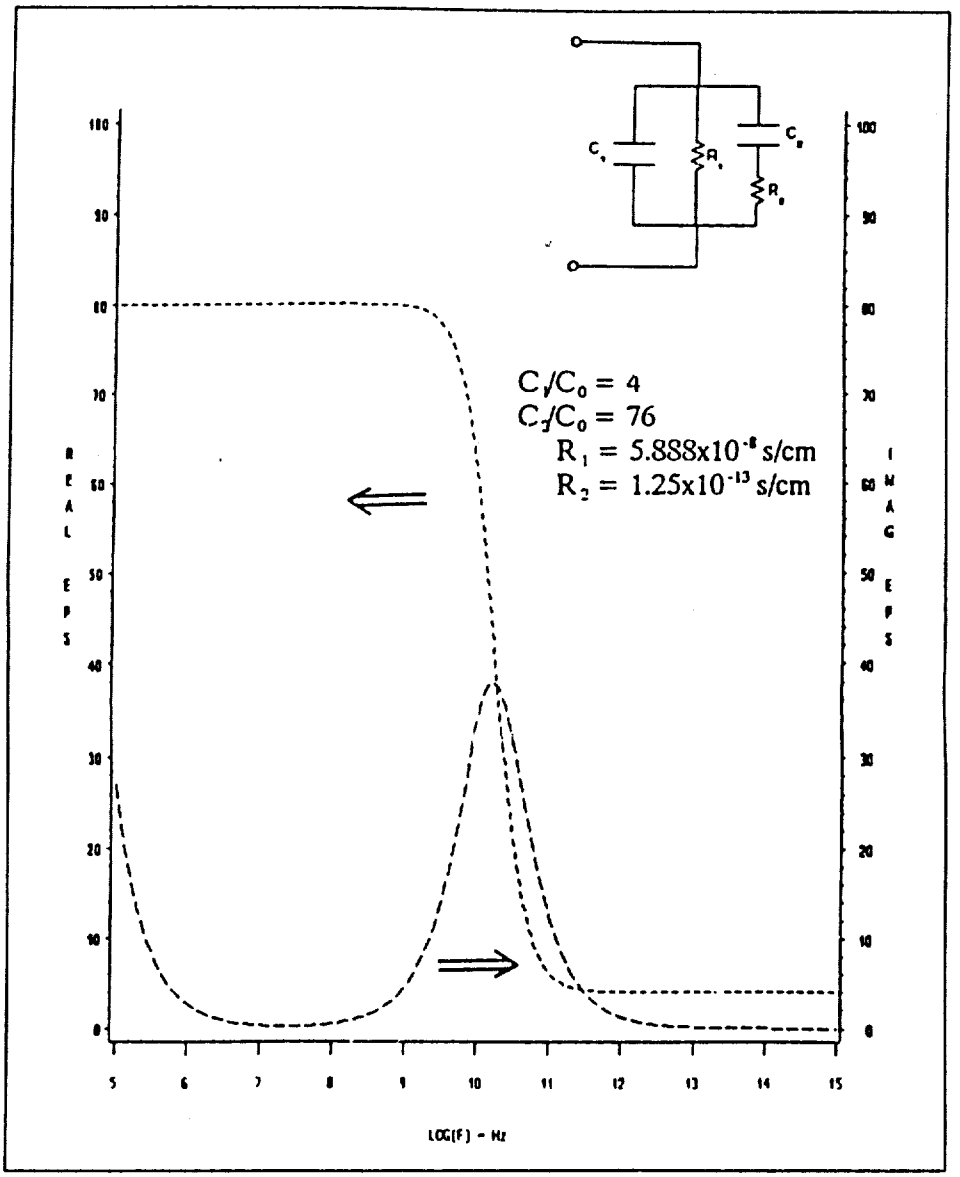

Figure 34. Water model including DC conductivity and optical permittivity

Campbell (1988) demonstrated quite clearly that if one considers the behavior of the real part of the complex dielectric constant as a function of water content for soils, it falls between the limits for a three-component system (soil, water, and air) created by assuming, from one viewpoint, that the three components can be represented by equivalent capacitances in series and, from another viewpoint, by equivalent capacitances in parallel.

Bidadi, Schroeder, and Pinnavaia (1988) extended this concept a bit further to successfully model the complex dielectric response of clay films as a Maxwell-Wagner mechanism using the equivalent circuit shown in Figure 35.

The upper frequency limit of their study was only about 100 MHz. Their reasoning for choosing such an arrangement of elements is the following. They wanted to model the physical situation of easy conducting paths through the clay interstices that could be interrupted by thin insulating barriers (clay platelets, for example), this being their interpretation of the Maxwell-Wagner effect. Small values of R_1 and large values of C_1 allow for easy current flow, while large values of R_2 and small values of C_2 account for the barriers. A similar model was proposed by Eicke et al. (1986) in which the barriers (actually, the solvent) were taken as lossless ($R_2 = 0$).

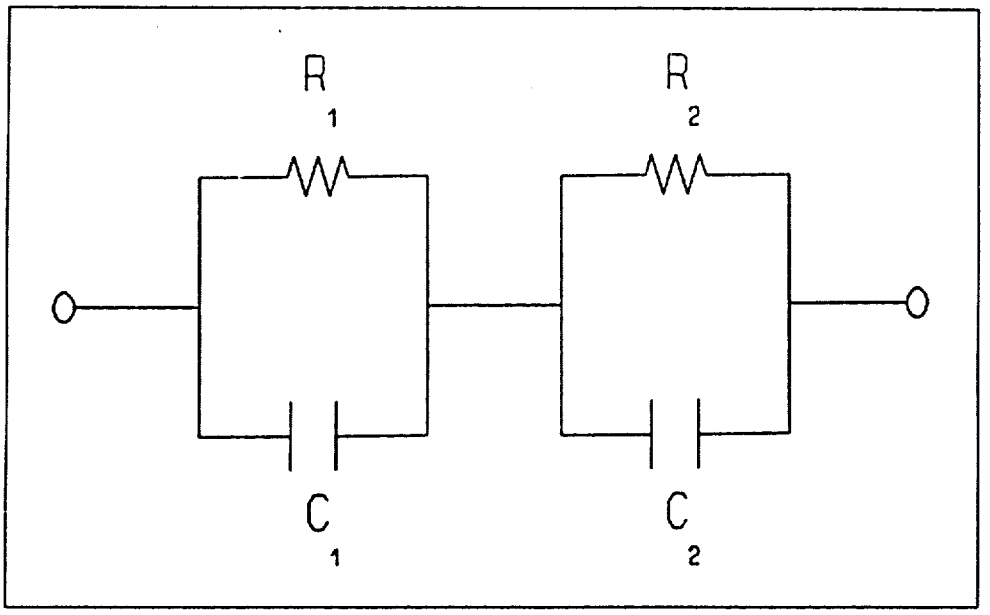

Figure 35. Equivalent circuit for clay film studies (adapted from Bidadi, Schroeder, and Pinnavaia (1988))

Backing up further in time, Sachs and Spiegler (1964) and, later, Smith (1971) applied even more complicated equivalent circuits to the study of the complex dielectric response of saturated materials. Theirs was a very physically satisfying approach to the problem in which they assumed a combination of equivalent circuits in series representing a discontinuous electrical path through the soil-water system (Bidadi's reasoning for interrupted current flow) and of equivalent circuit elements in parallel representing continuous paths for effective current flow. The resulting combined circuit is shown in Figure 36 and was applied to data that did not exceed 100 MHz.

The geometrical parameters a, b, c, and d were empirically established by Sachs and Spiegler for their work by obtaining a best fit to low-frequency conductivity data. One has to believe, however, that these parameters must be related to physical quantities. For example, it seems likely that d could be associated with porosity. For saturated media, the higher the porosity, the less chance exists for series-like interruptions in effective current flow. Likewise, b should be related to dry density. The greater the sample dry density,

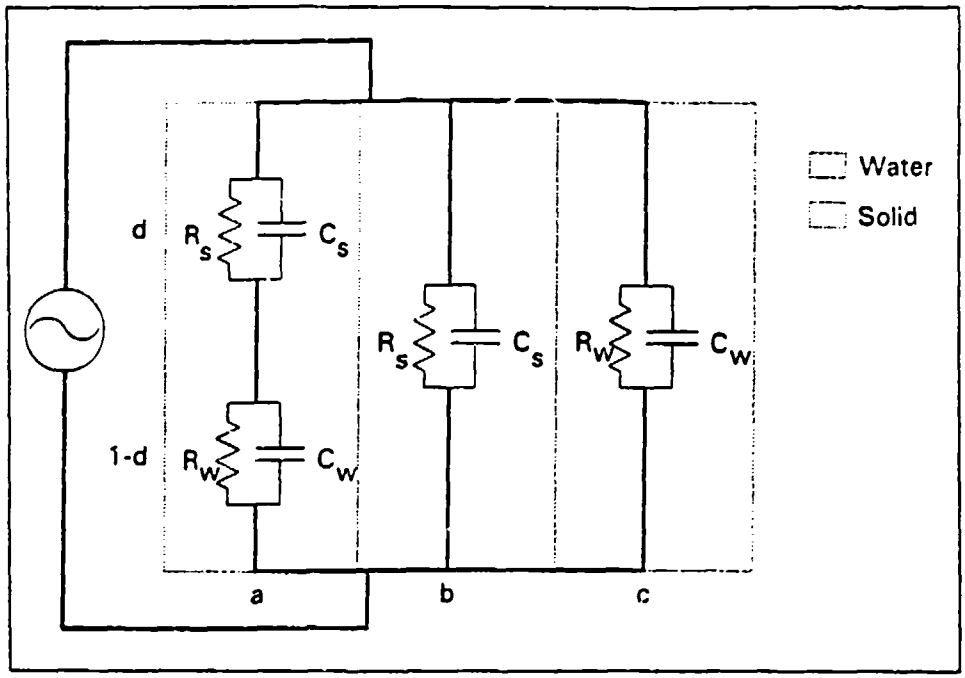

Figure 36. Equivalent circuit model for saturated media (adopted from Sachs and Spiegler (1964) and Smith (1971))

the more opportunity there is for conductive paths through the soil matrix. And finally, c should somehow relate to free water content in the soil sample. The greater the amount of free water, the greater would be the opportunity for current to flow through, unimpeded by the solid matrix. The governing equations for the circuit representation in Figure 36 are

THE THREE-PATH EQUIVALENT CIRCUIT

$$\varepsilon' = \frac{a(N_1D_1 + N_2D_2)}{C_0(D_1^2 + D_2^2)} + \frac{bC_s}{C_0} + \frac{cC_w}{C_0} \qquad (51)$$

$$\varepsilon'' = \frac{a(N_2D_1 - N_1D_2)}{C_0(D_1^2 + D_2^2)} + \frac{b}{C_0\omega R_s} + \frac{c}{C_0\omega R_w}$$

where

$$N_1 = \omega^2 R_s R_w C_s C_w - 1$$

$$N_2 = \omega \left(R_s C_s + R_w C_w\right)$$

$$D_1 = \omega^2 R_s R_w \left[(1-d)C_s + dC_w\right]$$

$$D_2 = \omega \left[dR_s + (1-d)R_w\right]$$

Including another set of equivalent circuits to those of Figure 36 to account for air in nonsaturated soils certainly seems reasonable. Perhaps even more simply, allow a + b + c < 1 and 1- d to be replaced by x - d where x < 1.

Furthermore, arranging a limited number of electrical circuit elements in such a way as to approximate almost any dielectric response in a single homogeneous material is undoubtedly possible. What is really needed is an equivalent circuit for which the elements not only allow a good reproduction of spectral response over a broad range of frequencies, but also have sensible physical meaning or whose values can be measured in the laboratory.

Percolation Transition or Long-Range Connectivity

As pointed out in Chapter 3, experimental data on moisture content variations in soils shows that the real part of the dielectric constant at low frequencies increases more rapidly with increasing moisture at higher levels of moisture content than it does at lower moisture levels. These data can be viewed as bilinear in moisture content, where below some critical value of moisture content, the rate of increase in dielectric constant is nearly constant. Above that critical value, the rate is again nearly constant but somewhat higher.

Wang and Smugge (1980) argued that this transition point was a function of soil texture; i.e., a function of the amount of sand and clay. They also related the wilting point of the soil (the volumetric water content under a pressure of 15 bars at standard temperature) to its texture and, in so doing, were able to show a strong correlation between the transition point and wilting point. In fact, Wang and Smugge went on to develop these observed soil texture effects into empirical relationships for the electrical properties of soils.

Campbell (1988) viewed this phenomenon by electrical analogy as a transition between series mixing (Equation 35) at lower water contents and parallel mixing (Equation 34) at moisture levels above the critical value. He borrowed from the percolation theory the concept of a percolation transition in moisture at which level one or more continuous, low resistance electrical paths through

the porous media suddenly appear. He referred to this transition as the appearance of "long-range connectivity."

Campbell attempted to create a computerized model of moist soil passing through the transition point using the grid shown in Figure 37. The grid was initially set up with a random distribution of soil and air squares to provide a given porosity. The air squares were then randomly replaced with water squares as water content was allowed to increase. A dielectric constant was then calculated for each column of soil, air, and water squares extending from one capacitor plate to the other by the series model (Equation 35), and finally, an effective dielectric constant for that moisture content was calculated as the average value for all of the columns.

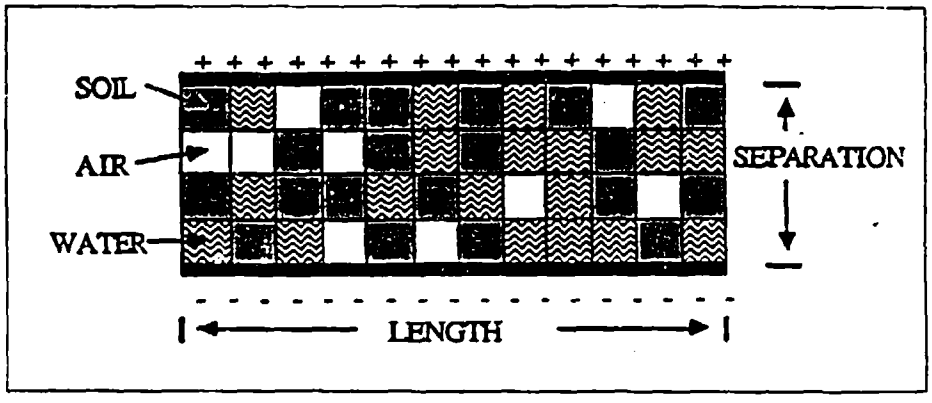

Figure 37. Campbell's (1988) percolation model grid for moist soil

While this model simulated the increasing rate of change in real dielectric constant with increasing water content, it did not, in fact, simulate long-range connectivity because it was only a one-dimensional model. Unless the dry soil grid contained several columns of only air spaces, simulating long-range connectivity was not possible. Campbell also pointed out that another shortcoming of this model was its inability to scale properly. Doubling capacitor dimensions gave a different result.

Fractal Models of Electrical Behavior

Modeling of electrodes

In recent years, fractals (see Appendix C for definitions) have been utilized to study the electrical behavior of fluid-saturated porous electrodes. The fundamental thought behind the use of fractal concepts is that the number of elements used to construct a fractal geometry scales as a power law of the element length or relative size (Mandelbrot 1983). It seems to have become fashionable to also talk about a fractal geometry as one for which "physical quantities scale as a power law of the length scale....on which they are

measured" (Brouers and Ramsamugh 1988). For example, if there is a region of the electromagnetic spectrum where conductivity of a sample of material is observed to vary as a power law in frequency (hence, wavelength), then that sample is thought to possess a fractal geometry. In fact, Brouers and Ramsamugh (1988) combined low-frequency permittivity and conductivity data for brine-saturated alumina ceramics with some statistical models to calculate fractal dimensions of 2.65 ± 0.10 for five different ceramic samples, independent of sample porosity.

As part of a study on the frequency response of porous battery electrodes, Sapoval, Chazalviel, and Peyriere (1988) also observed that the impedance of rough or porous electrodes often goes like a power law in frequency (constant phase angle behavior) and is, in fact, related to the fractal dimension of the electrode surface in some cases. The model they used to associate fractal dimension to electrode structure was that called a "finite modified Sierpinski electrode" as shown in Figure 38. The Sierpinski electrode is something like a one-dimensional Menger sponge that is discussed in Appendix C. Sapoval, Chazalviel, and Peyriere obtained an expression for the admittance of a single pore within the electrode and used the fact that the total pore admittance is the sum of the admittances of all the pores to analytically study the effect of fractal dimensions on the electrode response.

Dissado and Hill (1989) used the same model to simulate analytical response functions and to attempt to prove that there is one form of self-similarity at high frequencies (within individual fractal pores) and another at low frequencies (sum of all pores).

Fractal pore-filling model

Campbell (1988) observed that, up to the time of his publication, fractal concepts had been applied to the bound water and saturated regimes for porous media, but not to the broad regime of moisture contents below saturation. He was searching for a way to model the dielectric response of moist soils at moisture contents less than saturation and decided that it might be possible to do so using fractal techniques. His assumptions were as follows:

a. Water within pore spaces accumulates in uniformly sized fractal clusters.

b. The pore spaces are all of equal characteristic size l, which is equal to the average particle size of the soil.

c. The dielectric constant of the soil-water-air mixture increases with increasing moisture content in a series-mixing fashion until the size of the water clusters reaches the size limitation on pores at which time long-range water connectivity in the soil mixture is established; i.e., the percolation threshold is reached.

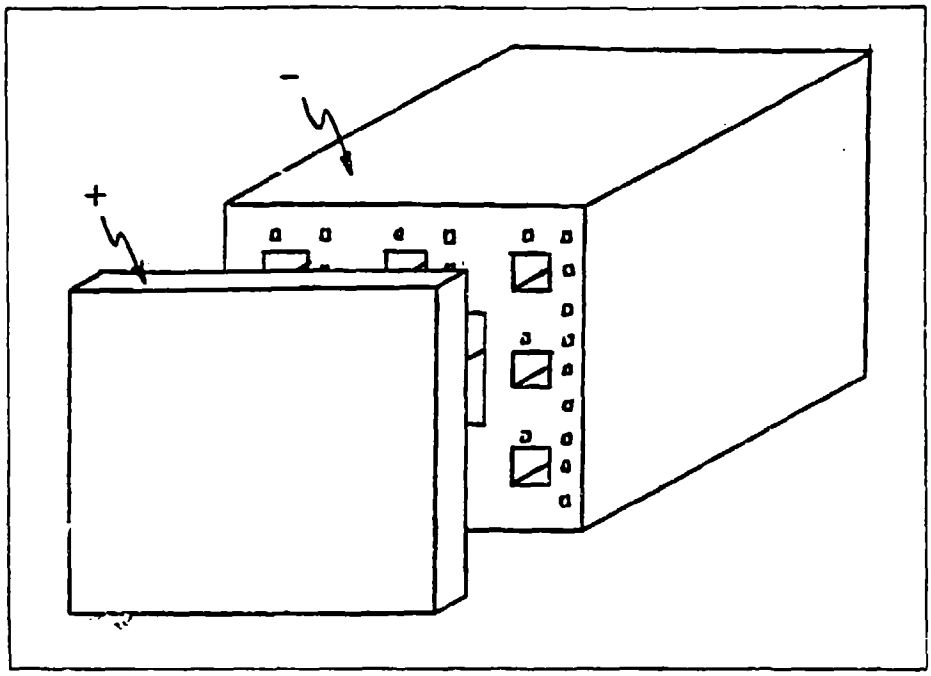

Figure 38. The "finite modified Sierpinski electrode" (adopted from Sapoval et al. (1988))

d. Once long-range connectivity is established, additional moisture enters in a nonfractal manner and the dielectric constant rises in a parallel-mixing fashion.

e. The soil is neither a clean gravel (which precludes water cluster spanning of the pore spaces) nor a pure clay (dominated by bound water effects).

The key assumptions made by Campbell that allowed a rather simple expression between critical water content (the moisture content at which long-range connectivity is established) and soil porosity to be developed were assumptions *a* and *b*. From *a*, Campbell wrote that the volume of water contained in a cluster of size r and fractal dimension D was

$$(cluster\ water\ volume) \propto r^D \tag{52}$$

Thus the volumetric water content also goes as r^D. Mandelbrot, himself, found no argument against the mass density relationship that stated that mass within a fractal cluster of size R went as (Mandelbrot 1983) and if one accepts that individual water molecules all have the same size and mass, then Equation 52 is believable.

$$(cluster\ mass) \propto R^{D} \tag{53}$$

At such time as the clusters just span the pores of size l to produce long-range connectivity, the volumetric water content can be written as

$$\theta_{critical} \propto l^{D} \tag{54}$$

Campbell took the soil sample porosity ϕ to be defined in three-space as

$$\phi \propto l^{3} \tag{55}$$

He finally concluded from the ratio of these last two quantities that

$$\frac{\theta_c}{\phi} \propto l^{(D-3)} \tag{56}$$

and that a log-log plot of θ_c/Φ versus l should be a straight line with slope equal to D-3. If there is no difference in how the fractal water clusters grow in different soils, then D is the same for any type of soil that fits within the bounds presented by assumption *e*. In fact, Campbell plotted critical water content data for five soils at a frequency of 50 MHz (shown in Figure 39) and found a fractal dimension of 2.4 that is similar to others' calculations of about 2.5 for aggregate clustering. He made no attempt, nor is there sufficient data, to draw any conclusions about the effects of soil texture or signal frequency on critical water content.

Campbell's fractal pore-filling model is very simplistic, but in his own words, "..the similar dielectric behavior of soils with huge ranges in particle size and shape of particles argues against a complicated model which considers many different soil parameters.." (Campbell 1988). He went on to admit that the weakest point in his model was, in fact, assumption *b*; i.e., that the characteristic pore size equals the median particle size of the soil.

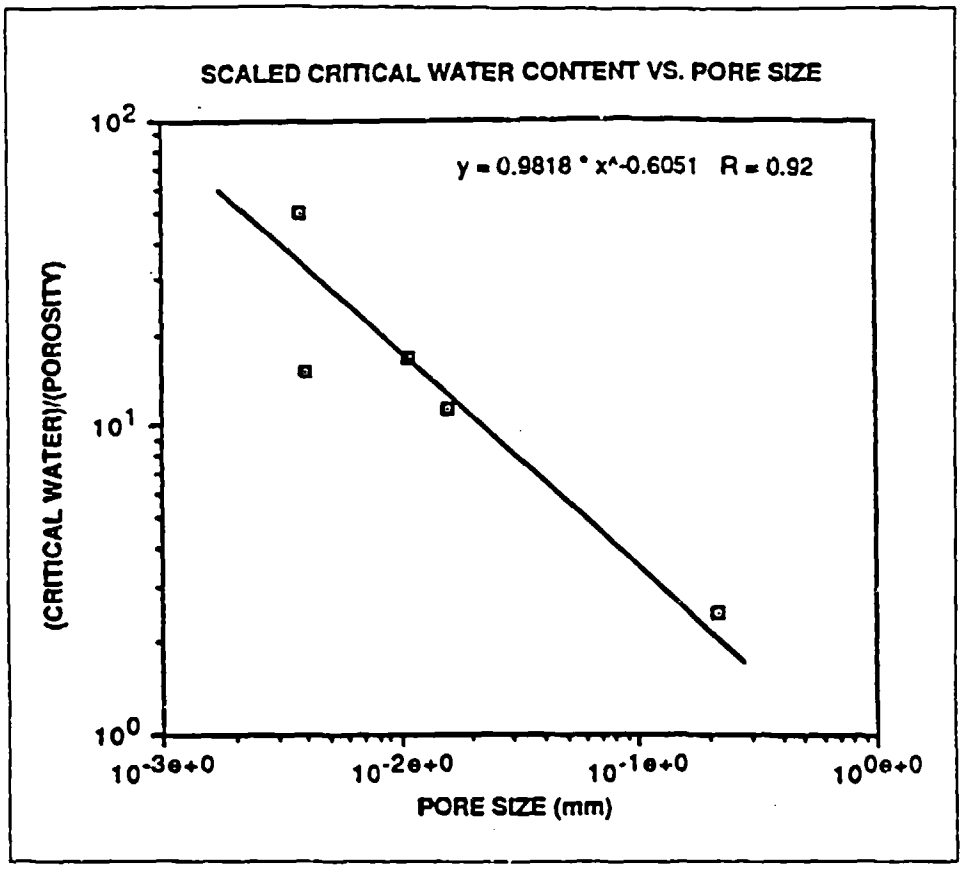

Figure 39. Scaled critical water content versus pore size (from Campbell (1988))

References

Albrecht, H. J. (1966). "Climatic influence upon skin depth in earth." *Proceedings of the IEEE (Correspondence).*

Ansoult, M., DeBacker, L. W., DeClercq, M. (1984). "Statistical relationship between apparent dielectric constant and water content in porous media," *Journal of the American Society of Soil Science* 48, 47-50.

Arulanandan, K., and Smith, S. S. (1973). "Electrical dispersion in relation to soil structure," ASCE, *Journal of the Soil Mechanics and Foundations Division* SM12, 1113-1133.

Ballard, R. F. (1983). "Cavity detection and delineation research; Report 5, Electromagnetic (radar) techniques applied to cavity detection," Technical Report GL-83-1, U.S. Army Engineer Waterways Experiment Station, Vicksburg, MS.

Berlin, G. L., Tarabzouni, M. A., Al-Naser, A. H., Sheikho, K. M., and Larson, R. W. (1986). "SIR-B subsurface imaging of a sand-buried landscape: Al Labbah Plateau, Saudi Arabia." *IEEE transactions on geoscience and remote sensing.* GE-24(4), 595-602.

Bidadi, H., Schroeder, P. A., and Pinnavaia, T. J. (1988). "Dielectric properties of montmorillonite clay films: Effects of water and layer charge reduction," *Journal of Physics and Chemistry of Solids* 49(12), 1435-1440.

Birchak, J. R., Gardner, C. G., Hipp, J. E., and Victor, J. M. (1974). "High dielectric constant microwave probes for sensing soil moisture." *Proceedings of the IEEE.* 62(1), 93-98.

Brouers, F., and Ramsamugh, A. (1988). "Percolation and anomalous conduction on fractals in fluid-saturated porous media," *Journal of Physics C: Solid State Physics* 21, 1839-1847.

Brunfeldt, D. R. (1987). "Theory and design of a field-portable dielectric measurement system." *Proceedings of IGARSS '87 Symposium.* Ann Arbor, MI, 559-563.

Campbell, J. E. (1988). "Dielectric properties of moist soils at RF and microwave frequencies," Ph.D. diss., Dartmouth College, Hanover, NH.

Campbell, M. J., and Ulrichs, J. (1969). "Electrical properties of rocks and their significance for lunar radar observations," *Journal of Geophysical Research* 74(25), 5867-5881.

Carrol, R. D., Eberle, W. R., and Cunningham, D. R. (1969). "Electrical properties of Earth at the EMP Simulator Site, Fort Huachuca, Arizona," U.S. Department of the Interior, Geological Survey, Special Projects Report 26.

Cole, K. S., and Cole, R. H. (1941). "Dispersion and absorption in dielectrics," *Journal of Chemical Physics* 9, 341-351.

Colwell, R. N., ed. (1983). *Manual of remote sensing*. 2nd ed., American Society of Photogrammetry, Falls Church, VA.

Cotton, F. A., and Wilkinson, G. (1972). *Advanced inorganic chemistry*. Interscience Publishers, New York.

Curtis, J. O. (1992). "Moisture and temperature effects on the microwave dielectric behavior of soils," Ph.D. diss., Dartmouth College, Hanover, NH.

Debye, P. (1929). *Polar molecules*. Dover Publications, Inc., New York.

Delaney, A. J., and Arcone, S. A. (1982). "Laboratory measurements of soil electric properties between 0.1 and 5 GHz," Report 82-10, U.S. Army Cold Regions Research and Engineering Laboratory, Hanover, NH.

de Loor, G. P. (1968). "Dielectric properties of heterogeneous mixtures containing water," *Journal of Microwave Power* 3(2), 67-73.

Dissado, L. A., and Hill, R. M. (1989). "The fractal nature of the cluster model dielectric response functions," *Journal of Applied Physics* 66(6), 2511-2524.

Dobson, M. C., Ulaby, F. T., Hallikainen, M. T., and El-Rayes, M. A. (1985). "Microwave dielectric behavior of wet soil - Part II: Dielectric mixing models." *IEEE transactions on geoscience and remote sensing*. GE-23(1).

Eicke, H., Geiger, S., Sauer, F. A., and Thomas, H. (1986). "Dielectric study of fractal clusters formed by aqueous nanodroplets in apolar media," *Berichte Bunsenges Physical Chemistry* 90, 872-876.

El-Rayes, M. A., and Ulaby, F. T. (1987a). "Microwave dielectric behavior of vegetation material," Radiation Laboratory, The University of Michigan, Repon 022132-4-T.

El-Rayes, M. A., and Ulaby, F. T. (1987b). "Microwave dielectric spectrum of vegetation - Part I: Experimental observations." *IEEE transactions on geoscience and remote sensing*. GE-25(5), 541-549.

Farr, T. G., Elachi, C., Hartl, P. and Chowdhury, K. (1986). "Microwave penetration and attenuation in desert soil." *IEEE transactions on geoscience and remote sensing*. GE-24(4), 590-594.

Feynman, R. P, Leighton, R. B., and Sands, M. (1964). "Mainly electromagnetism and matter." *The Feynman lectures on physics*. Vol II, Addison-Wesley, Reading, MA.

Friesen, W. I., and Mikula, R. J. (1987). "Fractal dimensions of coal particles," *Journal of Colloid and Interface Science* 120(1), 263-271.

Fripiat, J. J., Jelli, A., Poncelet, G., and Andre, J. (1965). "Thermodynamic properties of adsorbed water molecules and electrical conduction in montmorillonite and silicas," *Journal of Physical Chemistry* 69(7), 2185-2197.

Gabriel, C., Grant, E. H., and Young, I. R. (1986). "Use of time domain spectroscopy for measuring dielectric properties with a coaxial probe," *Journal of Physics, E: Scientific Instrumentation* 19, 843-846.

Grant, H. H., Buchanan, T. J., and Cook, H. F. (1957). "Dielectric behavior of water at microwave frequencies," *Journal of Chemical Physics* 26(1), 156-161.

Grimshaw, R. W. (1971). *The chemistry and physics of clays*. John Wiley and Sons, New York.

Hall, P. G., and Rose, M. A. (1978). "Dielectric properties of water adsorbed by kaolinite," *Journal of the Chemical Society of London, Faraday Transactions* I74, pp. 1221-1233.

Hallikainen, M. T., Ulaby, F. T., Dobson, M. C., El-Rayes, M. A., and Wu, L. (1985). "Microwave dielectric behavior of wet soil - Part I: Empirical models and experimental observations." *IEEE transactions on geoscience and remote sensing*. GE-23(1).

Hasted, J. B. (1973). *Aqueous dielectrics*. Chapman and Hall, London.

Hayre, H. S. (1970). "Geophysical dielectric constant determination." *IEEE transactions on geoscience electronics*. GE-8(4), 289-295.

Hippel, A. R., von. (1954). *Dielectrics and waves*. John Wiley and Sons, Inc., New York.

Hippel, A., von. (1988c). "The dielectric relaxation spectra of water, ice, and aqueous solutions, and their interpretation 3. Proton organization and proton transfer in ice." *IEEE transactions on electrical insulation*. 23(5), 825-840, 1st pub. 1967, MIT report.

Hoekstra, P., and Delaney, A. (1974). "Dielectric properties of soils at UHF and microwave frequencies," *Journal of Geophysical Research* 79(11), 1699-1708.

Hoekstra, P., and Doyle, W. T. (1971). "Dielectric relaxation of surface adsorbed water," *Journal of Colloid and Interface Science* 36(4), 513-521.

Jackson, J. D. (1975). *Classical electrodynamics*. John Wiley and Sons, New York.

Jakkula, P., Ylinen, P., and Tiuri, M. (1980). "Measurement of ice and frost thickness with an FM-CW radar." *Proceedings of the 10th European microwave conference*. Warszawa, Poland, 584-587.

John, B. (1992). "Soil moisture detection with airborne passive and active microwave sensors," *International Journal of Remote Sensing* 13(3), 481-491.

Kaatze, U. (1986). "The dielectric spectrum of water in the microwave and near-millimetre wavelength region," *Chemical Physics Letters* 132(3), 291-293.

Katz, A. J., and Thompson, A. H. (1985). "Fractal sandstone pores: Implications for conductivity and pore formation," *Physical Review Letters* 54(12), 1325-1328.

Klein, L. A., and Swift, C. T. (1977). "An improved model for the dielectric constant of sea water at microwave frequencies." *IEEE transactions on antennas and propagation*. AP-25(1), 104-111.

Krepfl, M., Moore, C., and Lee, W. (1989). "A quantitative description of soil microstructure using fractals, Volume I of II, Research Results," Report WL-TR-89-48, Vol. 1, Weapons Laboratory, Kirtland AFB, New Mexico.

Lane, J. A., and Saxton, J. A. (1952a). "Dielectric dispersion in pure polar liquids at very high radio-frequencies. I. Measurements on water, methyl and ethyl alcohols," *Proceedings of the Royal Society*. A213, 400-408.

Lane, J. A., and Saxton, J. A. (1952b). "Dielectric dispersion in pure polar liquids at very high radio frequencies III. The effect of electrolytes in solution." *Proceedings of the Royal Society*. 214 A, 531-545.

Looyenga, H. (1965). "Dielectric constants of heterogeneous mixtures," *Physica* 31, 401-406.

Lundien, J. R. (1966). "Terrain analysis by electromagnetic means; Report 2, Radar responses to laboratory prepared soil samples," Technical Report 3-693, U.S. Army Engineer Waterways Experiment Station, Vicksburg, MS.

_____. (1971). "Terrain analysis by electromagnetic means; Report 5, Laboratory measurement of electromagnetic propagation," Technical Report 3-693, U.S. Army Engineer Waterways Experiment Station, Vicksburg, MS.

_____. (1972). "Determining presence, thickness, and electrical properties of stratified media using swept-frequency radar," Technical Report M-72-4, U.S. Army Engineer Waterways Experiment Station, Vicksburg, MS.

Madden, T. R. (1974). "Near surface electrical properties of rocks as a guide to mechanical properties," Report AFCRL-TR-75-0179, Air Force Cambridge Research Laboratories, Hanscom, AFB, MA.

Malmberg, C. G., and Maryott, A. A. (1956). "Dielectric constant of water from 0° to 100° C," *Journal of Research of the National Bureau of Standards* 56(1), 1-8.

Mandelbrot, B. B. (1983). *The fractal geometry of nature*. W. H. Freeman and Company, New York.

Martin, R. T. (1960). "Adsorbed water on clay: A Review." *Clays and clay minerals, proceedings of the ninth national clay conference*. Purdue University.

McCauley, J. F., Breed, C. S., Schaber, G. G., McHugh, W. P., Issawi, B., Haynes, C. V., Grolier, M. J., and el Kilani, A. (1986). "Paleodrainages of the Eastern Sahara - The Radar Rivers Revisited (SIR-A/B Implications for a Mid-Tertiary Trans-African Drainage System." *IEEE transactions on geoscience and remote sensing*. GE-24(4), 624-648.

Mitchell, J. K. (1976). "Soil water." *Fundamentals of soil behavior*. Chapter 7, John Wiley and Sons, Inc., New York.

Moore, C. A., and Krepfl, M. (1991). "Using fractals to model soil fabric," *Geotechnique* 41(1), 123-134.

Moore, D. M. and Reynolds, R. C. (1989). *X-Ray diffraction and the identification and analysis of clay minerals*. Oxford University Press, New York.

Muir, J. (1954). "Dielectric loss in water films adsorbed by some silicate clay minerals," Chemical Society of London, *Faraday Transactions* 50, 249-254.

Nelson, S. O. (1972). "A system for measuring dielectric properties at frequencies from 8.2 to 12.4 GHz." *Transactions of the ASAE*. 15(6), 1094-1098.

_____. (1973). "Microwave dielectric properties of grain and seed." *Transactions of the ASAE*. 16(5), 902-905.

_____. (1983). "Dielectric properties of some fresh fruits and vegetables at frequencies of 2.45 to 22 GHz." *Transactions of the ASAE*. 26(2), 613-616.

Nelson, S. O., Lindroth, D. P., and Blake, R. L (1989). "Dielectric properties of selected minerals at 1 to 22 GHz," *Geophysics* 54(10), 1344-1349.

Newman, A. C. D., ed. (1987). "The interaction of water with clay mineral surfaces." *Chemistry of clays and clay minerals*. Chapter 5, Mineralogical Society Monograph No. 6, John Wiley and Sons, New York.

Olhoeft, G. R. (1977). "Electrical properties of natural clay permafrost," *Canadian Journal of Earth Sciences* 14(1), 16-24.

_____. (1983). "Impulse radar studies of near surface geological structure." *Proceedings of the conference on lunar and planetary science X*. Houston, TX, 943-945.

Olhoeft, G. R., Frisillo, A. L., and Strangway, D. W. (1974). "Electric properties of Lunar Sample 15301,38," *Journal of Geophysical Research* 79(11), 1599-1604.

Olphen, H., van. (1963). *An introduction to clay colloid chemistry*. John Wiley Interscience Publishers, New York.

O'Neill, K., and Arcone, S. A. (1991). "Investigations of freshwater and ice surveying using short-pulse radar," CRREL Report 91-15, U.S. Army Engineer Cold Regions Research and Engineering Laboratory, Hanover, NH.

Parchomchuk, P., Wallender, W. W., and King, R. J. (1990). "Calibration of a waveguide sensor for measuring soil moisture." *IEEE transactions on geoscience and remote sensing*. 28(5), 873-878.

Pissis, P. (1985). "A study of sorbed water on cellulose by the thermally stimulated depolarization technique," *Journal of Physics D: Applied Physics* 18, 1897-1908.

Ray, P. S. (1972). "Broadband complex refractive indices of ice and water," *Applied Optics* 11(8), 1836-1844.

Reitz, J. R., Milford, F. J., and Christy, R. W. (1980). *Foundations of electromagnetic theory*. Addison-Wesley Publishing Co., Reading, MA.

Reynolds, J. A., and Hough, J. M. (1957). "Formulae for dielectric constant of mixtures." *Proceedings of the Physical Society of London.* 70B(45), Part 8, 769-775.

Sachs, S. B., and Spiegler, K. S. (1964). "Radiofrequency measurements of porous conductive plugs. Ion-exchange resin solution systems," *Journal of Physical Chemistry* 68(5), 1214-1222.

Saint-Amant, M., and Strangway, D. W. (1970). "Dielectric properties of dry, geologic materials," *Geophysics* 35(4), 624-645.

Sapoval, B., Chazalviel, J. N., and Peyriere, J. (1988). "Electrical response of fractal and porous interfaces," *Physical Review A* 38(11), 5867-5887.

Schaber, G. G., McCauley, J. F., Breed, C. S., and Olhoeft, G. R. (1986). "Shuttle imaging radar: Physical controls on signal penetration and subsurface scattering in the Eastern Sahara." *IEEE transactions on geoscience and remote sensing.* GE-24(4), 603-623.

Schwan, H. P., Schwarz, G., Maczuk, J., Pauly, H. (1962). "The low frequency dielectric dispersion of colloidal particles in electrolyte solution," *Journal of Physical Chemistry* 66, 2626-2635.

Shutko, A. M., and Reutov, E. M. (1982). "Mixture formulas applied in estimation of dielectric and radiative characteristics of soils and grounds at microwave frequencies." *IEEE transactions on geoscience and remote sensing.* GE-20(1), 29-32.

Smith, S. S. (1971). "Soil characterization by radio frequency electrical dispersion," Ph.D. diss., University of California at Davis.

Stewart, M. T. (1982). "Evaluation of electromagnetic methods for rapid mapping of salt-water interfaces in coastal aquifers," *Ground Water* 20(5), 538-545.

Stogryn, A. (1971). "Equations for calculating the dielectric constant of saline water." *IEEE transactions on microwave theory and techniques.* 733-736.

Strangway, D. W., Chapman, W. B., Olhoeft, G. R., and Carnes, J. (1972). "Electrical properties of lunar soil dependence on frequency, temperature and moisture," *Earth and Planetary Science Letters* 16, 275-281.

Stratton, J. A. (1941). *Electromagnetic theory.* McGraw-Hill Book Co., New York.

Swanson, R., Zoughi, R., Moore, R. K., Dellwig, L. F., and Soofi, A. K. (1988). "Backscatter and dielectric measurements from rocks of South-Eastern Utah at C-, X-, and K_u- Bands," *International Journal of Remote Sensing* 9(4), 625-639.

Telford, W. M., Geldart, L. P., Sheriff, R. E., and Keys, D. A. (1984). "Electrical properties of rocks." *Applied geophysics*. Chapter 5, Cambridge University Press.

Thomas, A. M. (1966). "In Situ measurement of moisture in soil and similar substances by 'fringe' capacitance," *Journal of Scientific Instruments* 43, 21-27.

Topp, G. C., Davis, J. L., Annan, A. P. (1980). "Electromagnetic determination of soil water content: Measurements in coaxial transmission lines," *Water Resources Research* 16(3), 574-582.

Troitskii, N. B., and Stepanov, L. N. (1980). "Dependence of dielectric constant of soil on its specific surface," *Soviet Agricultural Sciences* 7, 63-66.

Ulaby, F. T., Bengal, T. H., Dobson, M. C., East, J. R., Garvin, J. B., and Evans, D. L. (1990). "Microwave dielectric properties of dry rocks." *IEEE transactions on geoscience and remote sensing*. 28(3), 325-336.

Ulaby, F. T., Cihlar, J., and Moore, R. K. (1974). "Active microwave measurement of soil water content," *Remote Sensing of Environment* 3, 185-203.

Ulaby, F. T., and El-Rayes, M. (1986). "Microwave dielectric spectrum of vegetation material." *Proceedings of IGARSS' 86 symposium*, Zurich, 8-11 Sept. 1103-1106.

_____. (1987). "Microwave dielectric spectrum of vegetation - Part II: Dual-dispersion model." *IEEE transactions on geoscience and remote sensing*. GE-25(5), 550-557.

Waite, W. P., Sadeghi, A. M., Scott, H. D. (1984). "Microwave bistatic reflectivity dependence on the moisture content and matric potential of bare soil." *IEEE transactions on geoscience and remote sensing*. GE-22(4), 394-405.

Wang, J. R., and Schmugge, T. J. (1980). "An empirical model for the complex dielectric permittivity of soils as a function of water content." *IEEE transactions on geoscience and remote sensing*. GE-18(4), 288-295.

Wegmuller, Urs. (1990). "The effect of freezing and thawing on the microwave signatures of bare soil," *Remote Sensing of the Environment* 33, 123-135.

Wright, D. L., Olhoeft, G. R., and Watts, R. D. (1984). "Ground-penetrating radar studies on Cape Cod." *Proceedings of NWWA/EPA conference on surface and borehole geophysical methods in ground water investigations.* San Antonio, TX, 666-681.

Appendix A
Skin Depth Calculations

Obviously, skin depth effects preclude the utility of practical electromagnetic devices to penetrate to distances comparable with acoustic devices, but nevertheless, low-frequency devices have some utility (Berlin et al. 1986; Farr et al. 1986; Schaber et al. 1986).[1] As a means of quantifying the penetration of electromagnetic waves into earth media in terms of the complex dielectric constant of the media, one should consider the following arguments. The one-dimensional propagation of an electromagnetic wave into some medium can be described by an amplitude function such as

$$e^{i(kx-\omega t)} \tag{A1}$$

where

i = symbol designating the imaginary quantity $\sqrt{-1}$

k = complex wave number

x = distance

ω = radial frequency

t = time

Furthermore, let

$$k \equiv \beta + i\,\frac{\alpha}{2} \tag{A2}$$

[1] References cited in this appendix are located at the end of the main text.

where

β = phase constant and governs how a lossless medium propagates a wave

α = the attenuation factor and controls how the amplitude of the wave decreases with distance traveled through the medium.

Then the amplitude of the wave is as follows:

$$e^{-(\beta x - \omega t)} e^{-\left(\frac{\alpha}{2}\right)x} \tag{A3}$$

i.e., a traveling wave combined with an attenuation factor.

If skin depth is defined as that distance over which the wave amplitude decreases by a factor of $1/e$, then the skin depth δ is

$$\delta \equiv \frac{2}{\alpha} \tag{A4}$$

But the wave number can also be written

$$k = \frac{\omega}{v} = \frac{\omega N}{c} \tag{A5}$$

where

v = phase velocity in the medium

N = complex index of refraction
= $n' + in''$

c = the speed of light

Thus

$$\delta = \frac{2}{\alpha} = \frac{c}{\omega n''} \tag{A6}$$

or the skin depth is inversely proportional to the imaginary part of the complex index of refraction.

However, this study focuses on the complex dielectric constant ε as the measure of soil electrical characteristics.

$$\varepsilon = \varepsilon' + i\varepsilon'' \equiv N^2 \tag{A7}$$

Following several substitutions and simplifications, one can show that

$$\delta = \frac{\lambda_0}{2\pi}\left[\frac{\varepsilon'\left(\sqrt{1+(\varepsilon''/\varepsilon')^2}-1\right)}{2}\right]^{-\frac{1}{2}} \tag{A8}$$

where λ_0 is the free-space wavelength. A visualization of this equation for the range of values of permittivity ε' and loss tangent $\varepsilon''/\varepsilon'$ normally found in soils is provided in Figure A1. This figure does not represent any new science, as the same information has been presented in other forms (von Hippel 1954). It is, however, a more condensed way of visualizing the skin depth that has not been observed elsewhere in the literature. Figure A1 is valid for any interpretation of loss tangent; i.e., whether one is speaking of a loss mechanism due to actual charge migration or one due to dielectric relaxation.

Another useful skin depth relationship found in the literature is the nomograph generated by Albrecht (1966) and reproduced on Figure A2. Albrecht first developed an empirical relationship that associated ground conductivity to gravimetric moisture content and ground temperature at low frequencies. He then related skin depth to wavelength and conductivity by the usual equation for highly conductive materials (assumes that the conductivity phenomenon dominates the loss mechanism in soils at low frequencies):

$$\delta = \sqrt{\frac{\lambda_o}{\pi\mu c\sigma}} \tag{A9}$$

where the units used are MKS, and the skin depth is in meters and the ground conductivity is in units of mho/meter. The magnetic permeability was taken to be $4\pi X10^{-7}$ Henrys/meter. The way to use this nomograph is to select a moisture content and move on a horizontal line to the appropriate temperature curve. Then move on a vertical line to the appropriate frequency curve. From that point, a horizontal line to the right-hand scale reveals the desired

value of skin depth. There is no way to relate Albrecht's results to those of Figure A1, because it begins with an unknown empirical relationship among Vmoisture, temperature, and conductivity.

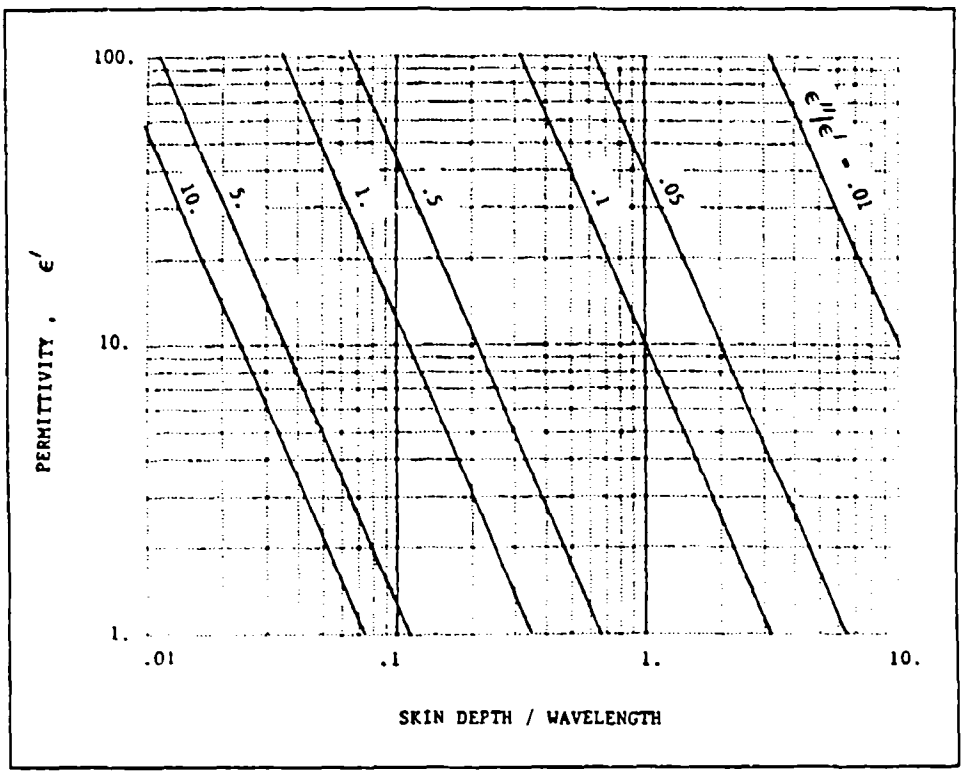

Figure A1. Skin depth as a function of wavelength, permittivity, and loss tangent

Hoekstra and Delaney (1974) also published some useful data on plane wave attenuation in moist soils at higher frequencies. These data are shown in Figure A3. They concluded that attenuation was relatively independent of soil fabric and that either passive or active microwave sensors could obtain a measureable response from only about the first 5 cm of ground below the surface.

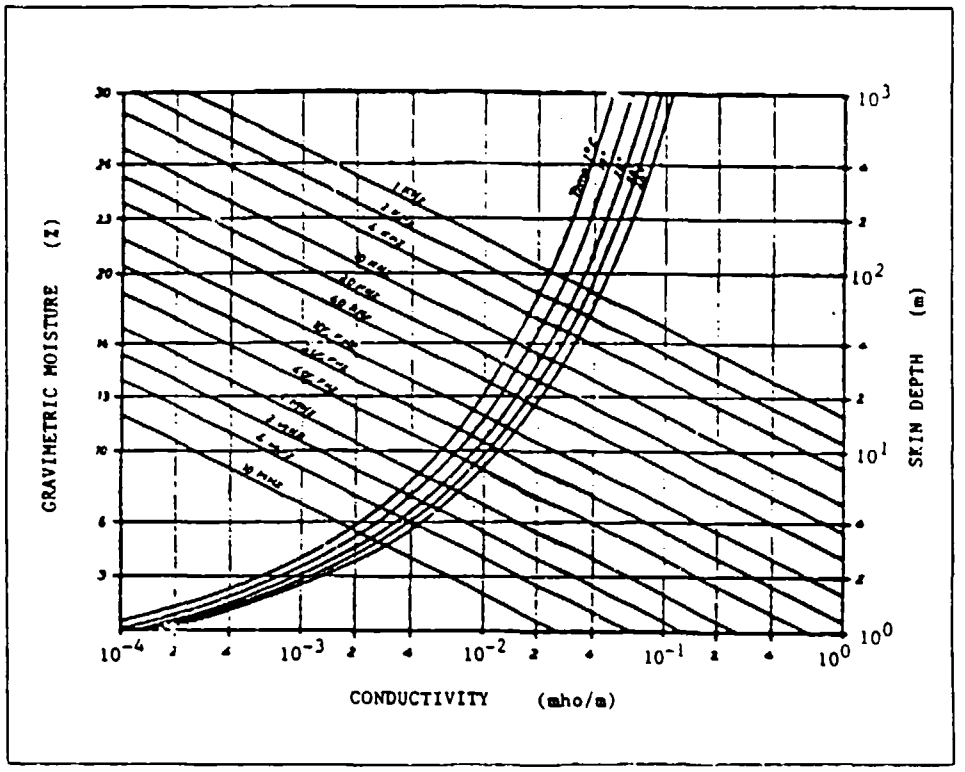

Figure A2. Skin depth nomograph (from Albrecht (1966))

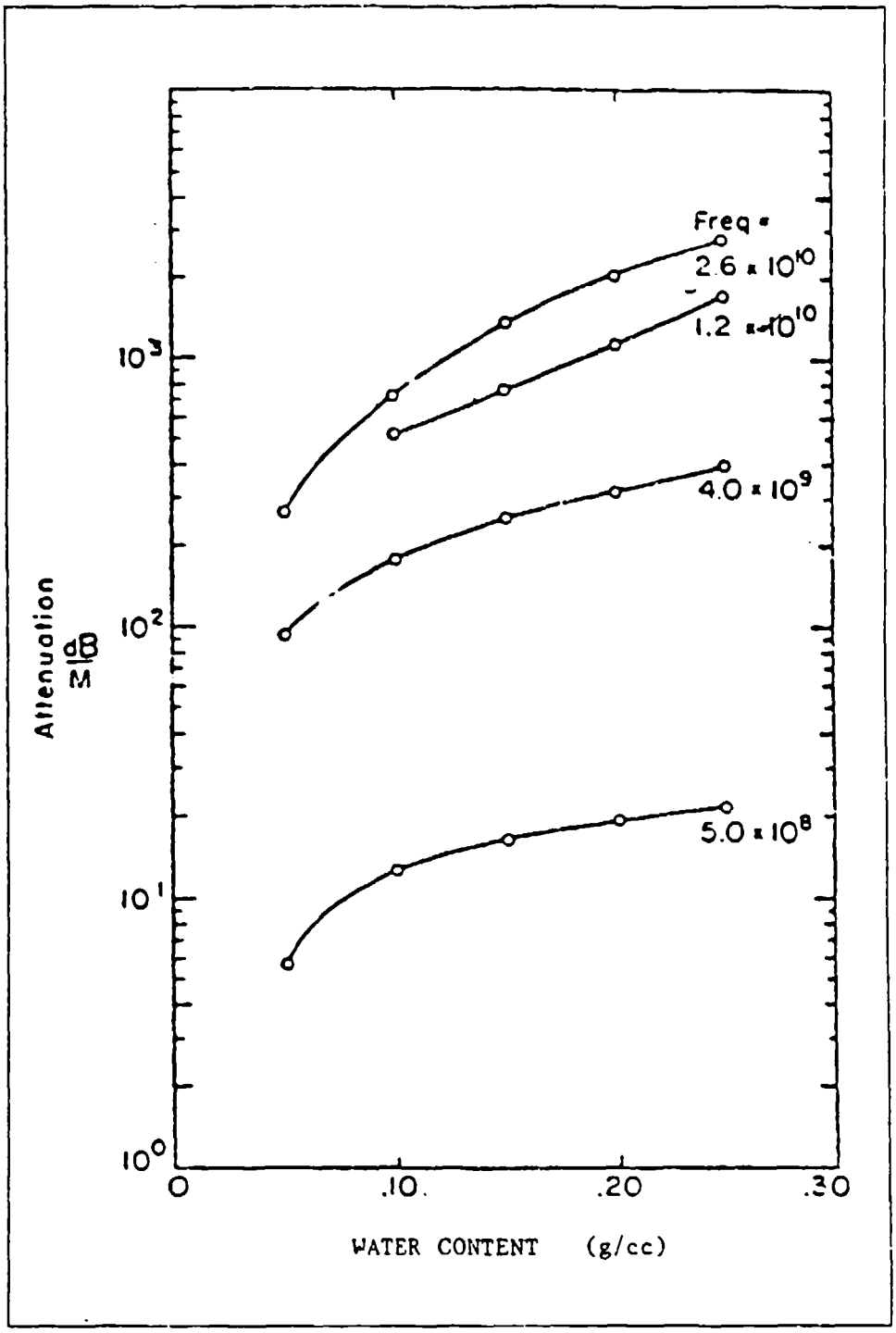

Figure A3. Attenuation in moist soils (from Hoekstra and Delaney (1974))

Appendix B
Reflection and Refraction at Plane Interfaces

Remote sensing of the environment usually involves the interaction of electromagnetic energy waves with solid media at some air-media interface. For example, an active radar transmits waves toward a surface (usually at some oblique angle) and measures what is reflected back toward itself (backscatter) or toward some other receiver (bistatic reflection). Passive devices receive energy emitted by the surface (and the atmosphere within the antenna's beamwidth) due to internal sources as well as what is reflected from natural sources such as the sun, the atmosphere, and surrounding terrain.

An idealization of the wave interaction phenomenon is shown in Figure B1 where an incident plane wave, defined by its wave vector $\vec{k}_I$, gives rise to a reflected wave $\vec{k}_R$ and a refracted (or transmitted) wave $\vec{k}_T$. (Nearly every textbook on electromagnetic theory has a development on reflected and refracted plane waves. What follows was taken primarily from Jackson (1975)[1] with a slight change in notation. Units are centimeter-gram-second.) The wave vectors are related to the dielectric properties of both media by

$$|\vec{k}_I| = |\vec{k}_R| = k = \frac{\omega N_1}{c} = \frac{\omega\sqrt{\mu_1\varepsilon_1}}{c} \tag{B1}$$

$$|\vec{k}_T| = k_T = \frac{\omega N_2}{c} = \frac{\omega\sqrt{\mu_2\varepsilon_2}}{c} \tag{B2}$$

[1] References cited in this appendix are located at the end of the main text.

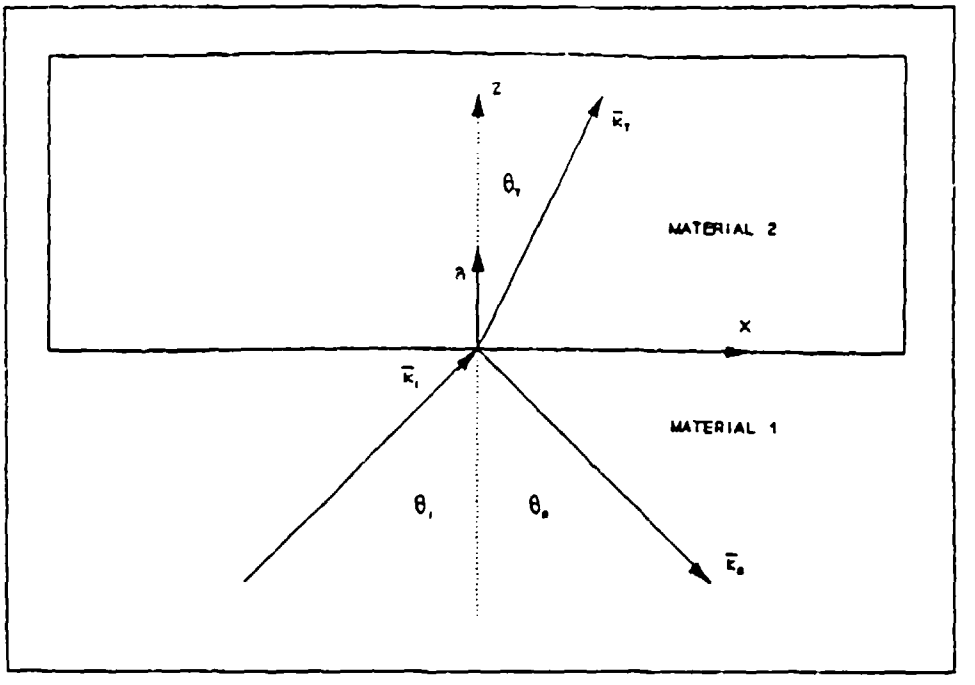

Figure B1. Wave vectors at a plane interface

where

ω = radial frequency

c = speed of light in a vacuum (3×10^8 m/sec)

μ = magnetic permeability (hereafter taken to be unity)

ε = complex dielectric constant

N = complex index of refraction

The plane of incidence is taken to be that plane formed by the $\vec{k}_i$ and $\hat{n}$ vectors; i.e., the plane of the paper.

Under these ideal conditions of plane waves at a smooth interface, one can write the following expressions for the three sets of electromagnetic energy fields.

INCIDENT

$$\vec{E}_i = \vec{E}_{i_0} e^{i\left(\vec{k}_i \cdot \vec{r} - \omega t\right)} \tag{B3}$$

$$\vec{B}_I = \sqrt{\mu_1 \varepsilon_1}\ \frac{\vec{k}_I \times \vec{E}_I}{k} = \frac{c}{\omega}\ \vec{k}_I \times \vec{E}_I \tag{B4}$$

REFRACTED (TRANSMITTED)

$$\vec{E}_T = \vec{E}_{T_0} e^{i\left(\vec{k}_T \cdot \vec{x} - \omega t\right)} \tag{B5}$$

$$\vec{B}_T = \sqrt{\mu_2 \varepsilon_2}\ \frac{\vec{k}_T \times \vec{E}_T}{k_T} = \frac{\omega}{c}\ \vec{k}_T \times \vec{E}_T \tag{B6}$$

REFLECTED

$$\vec{E}_R = \vec{E}_{R_0} e^{i\left(\vec{k}_R \cdot \vec{x} - \omega t\right)} \tag{B7}$$

$$\vec{B}_R = \sqrt{\mu_1 \varepsilon_1}\ \frac{\vec{k}_R \times \vec{E}_R}{k} = \frac{c}{\omega}\ \vec{k}_R \times \vec{E}_R \tag{B8}$$

By insisting that the phase factors ($\vec{k} \cdot \vec{x}$ terms) are all equal at z = 0, one is led to Snell's law and the fact that $\theta_I = \theta_R$.

$$\frac{\sin\theta_I}{\sin\theta_T} = \frac{k_T}{k} = \sqrt{\frac{\mu_2 \varepsilon_2}{\mu_1 \varepsilon_1}} = \frac{N_2}{N} \tag{B9}$$

What one desires to have are expressions for the amplitudes of the reflected and refracted waves, for it is the wave amplitude (or voltage amplitude) that is measured by a receiver unit. Amplitude relationships can be found by applying the electromagnetic boundary conditions; namely, that the normal components of electric displacement $\vec{D}$ and magnetic induction $\vec{B}$ are continuous across the interface as are the tangential components of the electric field $\vec{E}$ and the magnetic field $\vec{H}$. These conditions may be written as follows:

$$\left[\varepsilon_1\left(\vec{E}_{I_o} + \vec{E}_{R_o}\right) - \varepsilon_2\vec{E}_{T_o}\right] \cdot \hat{n} = 0 \tag{B10}$$

$$\left[\vec{k}_I \times \vec{E}_{I_o} + \vec{k}_R \times \vec{E}_{R_o} - \vec{k}_T \times \vec{E}_{T_o}\right] \cdot \hat{n} = 0 \tag{B11}$$

$$\left[\vec{E}_{I_o} + \vec{E}_{R_o} - \vec{E}_{T_o}\right] \times \hat{n} = 0 \tag{B12}$$

$$\left[\frac{1}{\mu_1}\left(\vec{k}_I \times \vec{E}_{I_o} + \vec{k}_R \times \vec{E}_{R_o}\right) - \frac{1}{\mu_2}\left(\vec{k}_T \times \vec{E}_{T_o}\right)\right] \times \hat{n} = 0 \tag{B13}$$

The Fresnel Coefficients

At this point, two further idealizations are made before finally writing down the expressions for reflected and refracted wave amplitudes. One is to assume that the incident electric field vector is perpendicular to the plane of incidence (into the paper with respect to Figure B1), and the other is to assume it is parallel to the plane of incidence (lying within the paper with respect to Figure B1). In radar parlance, the terms are "horizontal polarization" and "vertical polarization," respectively.

Due to redundancies generated by Snell's law, one only needs the third and fourth boundary conditions expressed in Equations B12 and B13 to arrive at the final expressions for amplitude ratios, which are known as the Fresnel reflection coefficients.

HORIZONTAL POLARIZATION

$$\frac{E_{T_o}}{E_{I_o}} = \frac{2\cos\theta_I}{\cos\theta_I + \frac{\mu_1}{\mu_2}\sqrt{\frac{\mu_2\varepsilon_2}{\mu_1\varepsilon_1} - \sin^2\theta_I}} \tag{B14}$$

$$\frac{E_{R_\bullet}}{E_{I_\bullet}} = \frac{\cos\theta_I - \frac{\mu_1}{\mu_2}\sqrt{\frac{\mu_2\varepsilon_2}{\mu_1\varepsilon_1} - \sin^2\theta_I}}{\cos\theta_I + \frac{\mu_1}{\mu_2}\sqrt{\frac{\mu_2\varepsilon_2}{\mu_1\varepsilon_1} - \sin^2\theta_I}} \tag{B15}$$

VERTICAL POLARIZATION

$$\frac{E_{T_\bullet}}{E_{I_\bullet}} = \frac{2\cos\theta_I}{\sqrt{\frac{\mu_1\varepsilon_2}{\mu_2\varepsilon_1}}\cos\theta_I + \sqrt{1 - \frac{\mu_1\varepsilon_1}{\mu_2\varepsilon_2}\sin^2\theta_I}} \tag{B16}$$

$$\frac{E_{R_\bullet}}{E_{I_\bullet}} = \frac{\cos\theta_I - \sqrt{\frac{\mu_2\varepsilon_1}{\mu_1\varepsilon_2} - \left(\frac{\varepsilon_1}{\varepsilon_2}\right)^2\sin^2\theta_I}}{\cos\theta_I + \sqrt{\frac{\mu_2\varepsilon_1}{\mu_1\varepsilon_2} - \left(\frac{\varepsilon_1}{\varepsilon_2}\right)^2\sin^2\theta_I}} \tag{B17}$$

Reflection From Lossless Media

The previous equations apply to lossy as well as lossless media. For lossless media, the dielectric constant and index of refraction are real quantities. Refracted waves propagate without attenuation, and both refracted and reflected waves retain the polarization of the incident wave.

Of practical value to the remote sensing arena is the variation with incidence angle of the reflection coefficient in a lossless media. Because received power in a sensor goes as the square of the amplitude of the signal and is proportional to the radar cross sections of the object being illuminated, scientists and engineers have a simple model between electrical properties of the media and its response to electromagnetic energy. What is deduced from the sensor measurements and a knowledge of the surface slopes is an apparent dielectric constant or apparent permittivity of the medium.

Figure B2 is a representation of how the apparent permittivity of a medium affects the reflected amplitude ratio as a function of incidence angle for

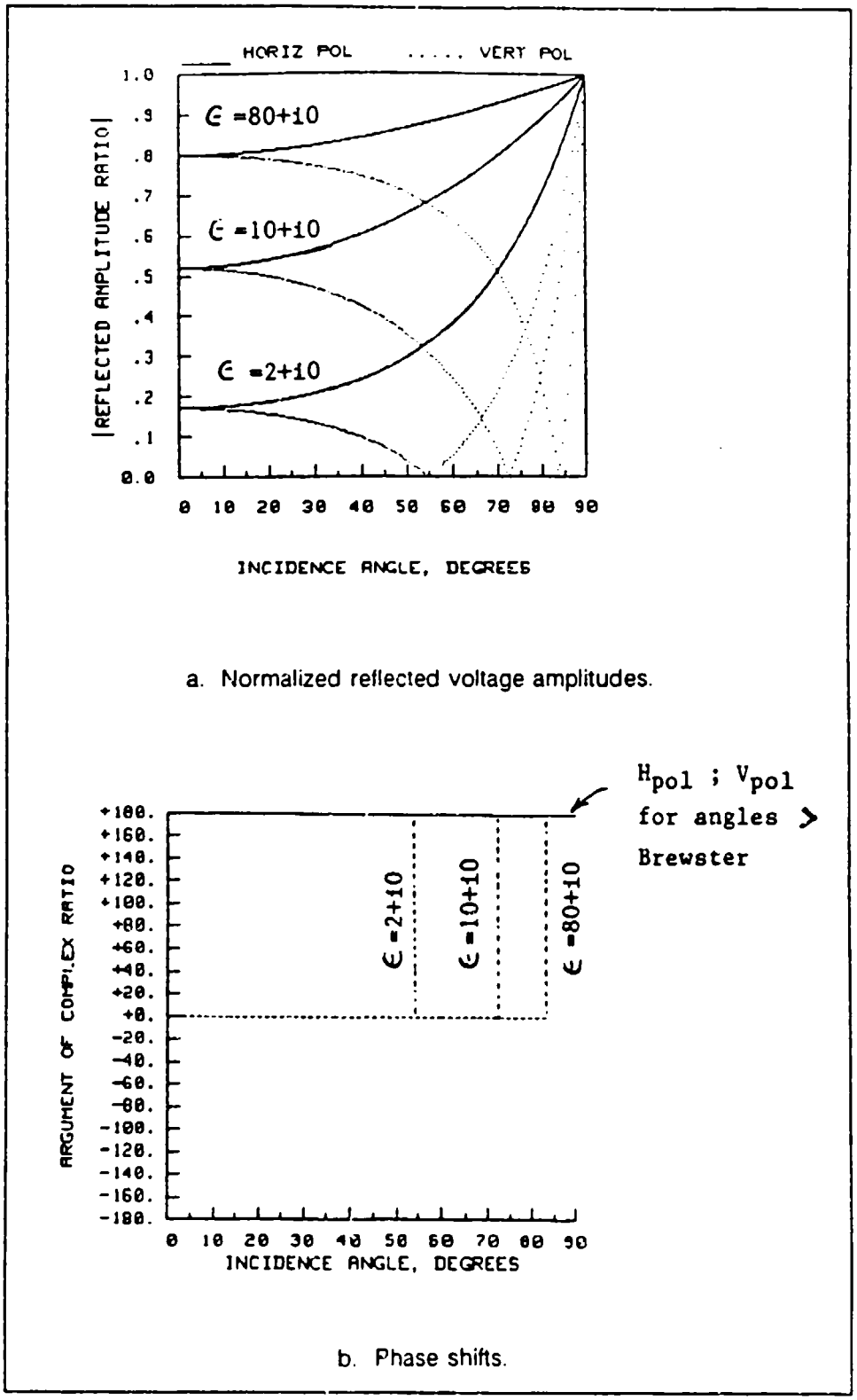

Figure B2. Reflection amplitudes and phase shifts for nonmagnetic lossless materials ($\mu_1 = \mu_2 = \varepsilon_1 = 1.0$)

nonmagnetic materials. The angle at which the reflected wave is totally eliminated in the vertical polarization case is referred to as the Brewster angle ($\tan\theta_B = N_2/N_1 = \sqrt{\varepsilon_2/\varepsilon_1}$). For angles less than the Brewster angle, the reflected wave suffers a phase reversal. The values of dielectric constant were chosen to span the range of values from dry soil to pure water.

Reflection From Lossy Media

Appendix A gave some indication of what happens to electromagnetic waves incident on a lossy media ($\varepsilon'' > 0$). The refracted, or transmitted, wave is attenuated. Furthermore, for oblique (non-zero) angles of incidence, surfaces of constant amplitude are no longer parallel to the surfaces of constant phase, resulting in what is referred to as an inhomogeneous wave (Stratton 1941). In fact, the index of refraction for lossy media becomes a function of the angle of incidence of the incoming wave. As lossiness goes up, the refracted wave vectors get closer and closer to normal to the interface.

Similarly, it is possible to rationalize the second expressions in Equations B7 and B8 to obtain ratios of reflected amplitudes to incident amplitudes. One representation of these relationships may be found in Stratton (1941). The effects of adding a loss term to the dielectric constant are to enhance reflectance and to reduce the destructive interference mechanism that causes the total loss of reflected energy at the Brewster angle. A visual comparison of the effects of loss factors in materials is shown in Figure B3.

It is not inconceivable that if one had good reflectance data at a single frequency over a large range of incidence angles (enough to include the minimum on the vertical polarization curve) and if the wavelength of the sensor could assume smooth interface conditions, then one could iteratively obtain a first approximation to the complex dielectric constant for the material near the surface.

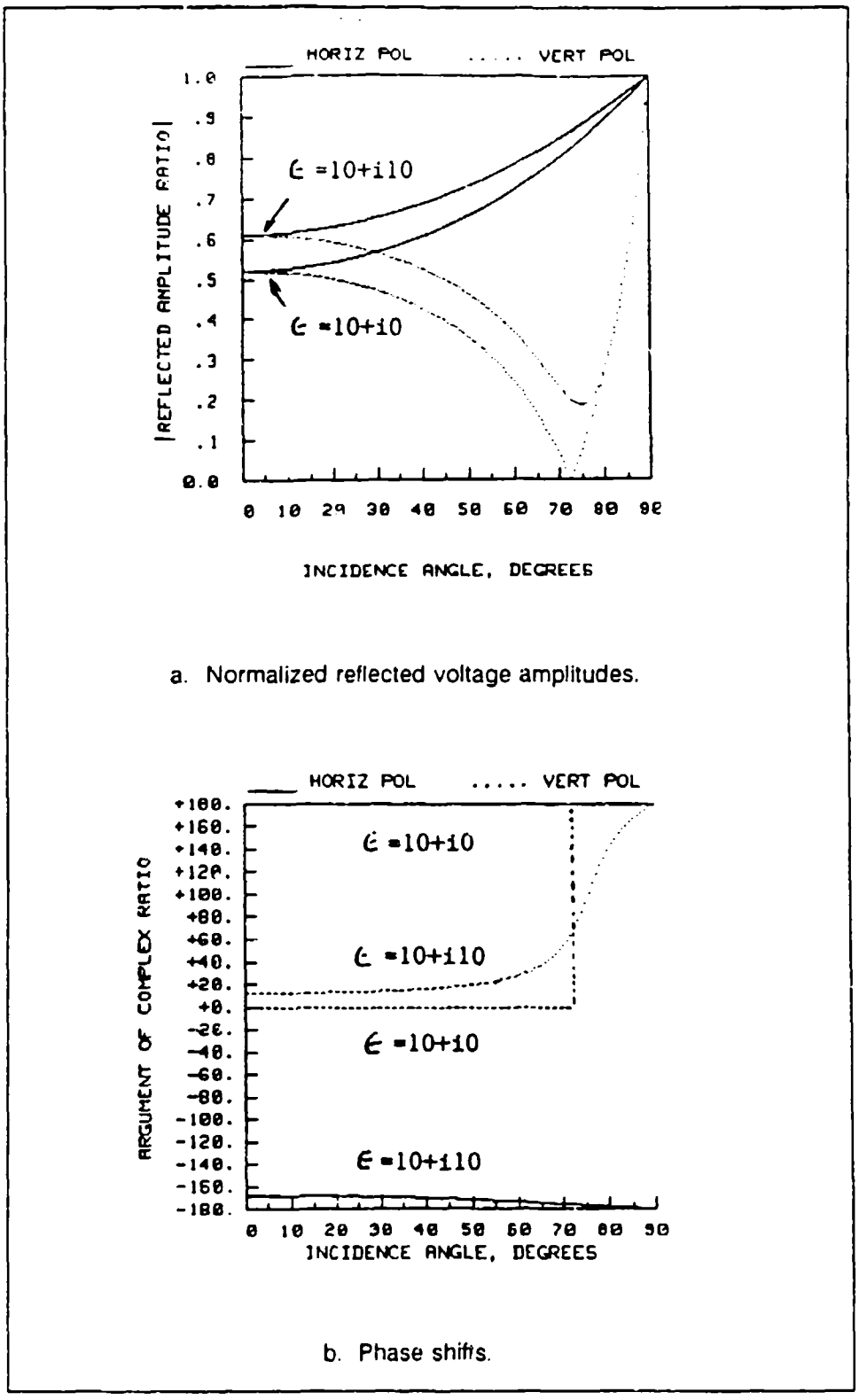

Figure B3. Reflection amplitudes and phase shifts for nonmagnetic lossy materials

Appendix C
Fractal Models of Soil Structure

Fractals

In recent years, some very interesting work has been done on the conductive behavior of porous media using the concept of self-similar geometries, or fractals, to model the behavior of certain physical quantities of that media. Mandelbrot, the guru of fractals, defines self-similar shapes as those in which a certain part of the shape can be broken up into N smaller parts, each looking like the original, but reduced in size by a fractional factor labeled r (Mandelbrot 1983).[1] The fractal dimension D of this self-similar shape can be written as

$$D = \frac{\log (N)}{\log \left(\frac{1}{r}\right)} \qquad (C1)$$

or

$$N r^{D} = 1 \qquad (C2)$$

Mandelbrot insisted that the exponent D be thought of as a dimension because it arose from a method of measuring the perimeter of an object having an irregular boundary.

Fractals are often used to generate complex, or textured, curves or surfaces from very simple initiator geometries. For example, consider Figure C1 in

[1] References cited in this appendix are located at the end of the main text.

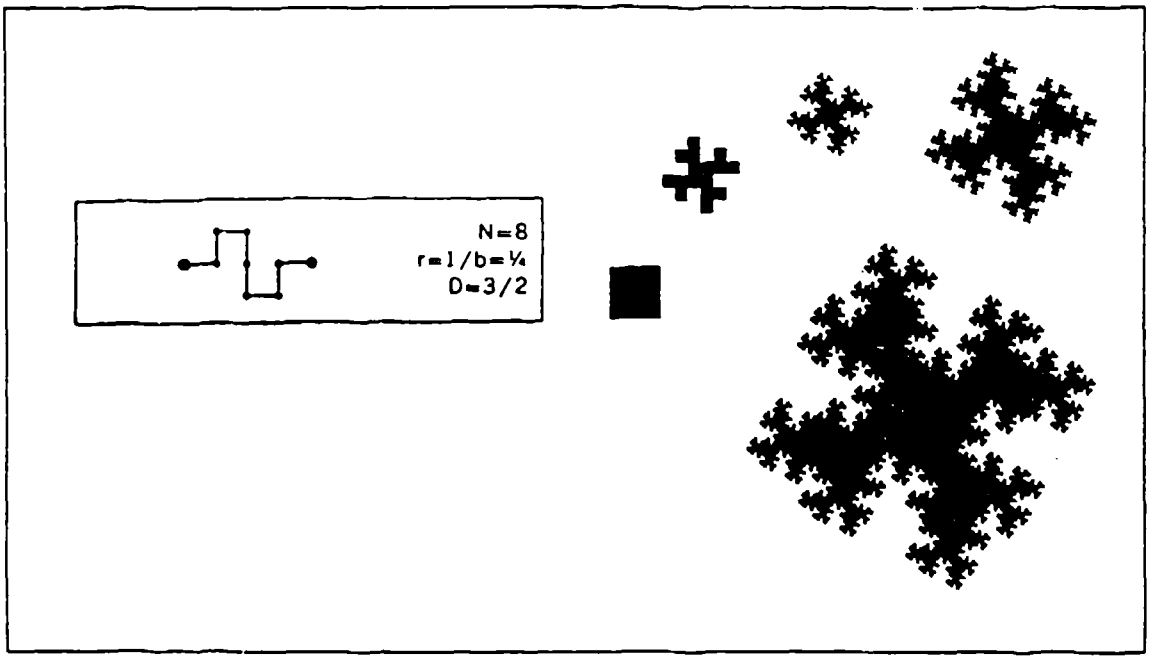

Figure C1. Fractal snowflake of dimension 1.5 (Mandelbrot 1983)

which the initiator (or the initial segment of the geometry that will be fractalized) is a solid square (precisely stated, each side of the square is an initiator), and the generator (or the desired geometry) is the broken line segment as shown. Moving clockwise from the initiator, the first two applications of the generator are shown at full scale, while the next two are enlarged to show the edge detail. Figure C2 shows another construction initiated with a solid square in which the generator results in the formation of both "lakes" and "islands."

Soil Structure

A third example of a fractal construction that is useful for studying porous media, and may be particularly useful for studying soil structure, is that shown in Figure C3 in which the initiator is a cube with square holes centered on each face and joining in the center. The generator is the same object but reduced by a factor of one-third. Therefore, in the first stage, the initiator is divided into 20 smaller cubes, resulting in a fractal dimension of 2.7268. Mandelbrot referred to this construction as a Menger sponge. Friesen and Mikula (1987) used the Menger sponge to model the fractal dimension of the surface area of coal in such a way that the slope of the isotherm (fractional volume change versus pressure for porosimetry measurements) plotted on a log-log scale is linearly related to the fractal dimension. At least one recent study attempted to measure the fractal dimensions of sandstone solid-void interfaces (Katz and Thompson 1985). Measured values of interface fractal

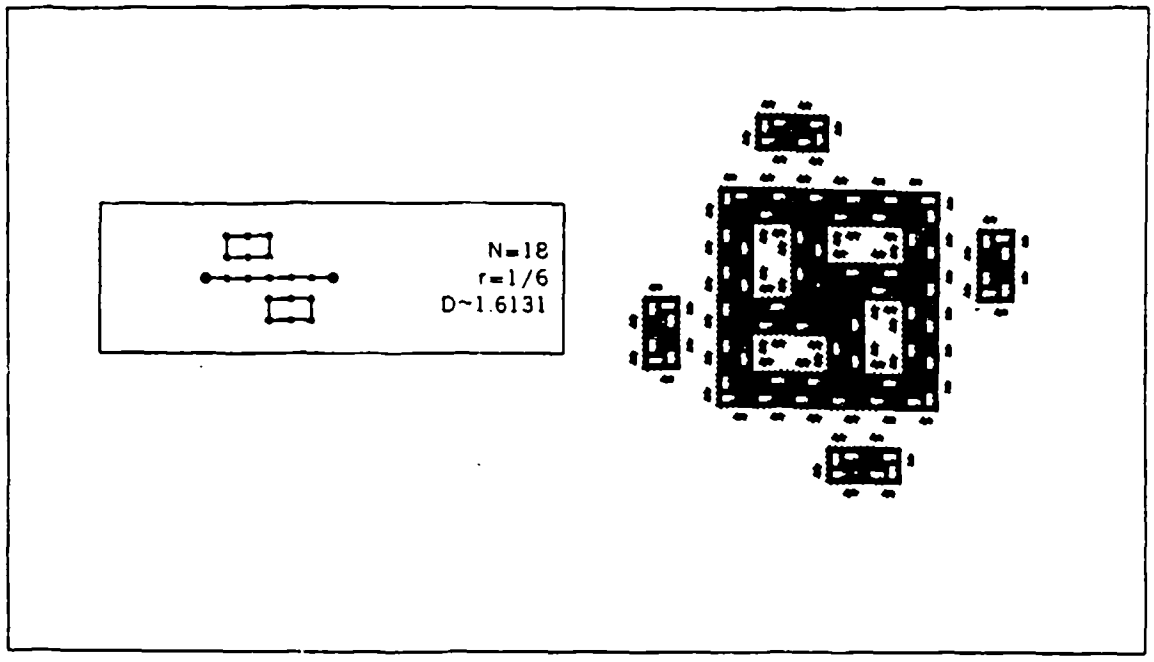

Figure C2. Fractal islands and lakes of dimension 1.6131 (from Mandelbrot (1983))

dimensions on five different samples using electron microscope techniques varied from 2.57 to 2.87.

Work has been done very recently on modeling the microstructure of soil using fractals (Krepfl, Moore, and Lee 1989; Moore and Krepfl 1991). A two-dimensional representation of a three-dimensional model using hexagonal-shaped flakes as the generator is shown in Figure C4. Such models may be useful as a representation of pure clays. This particular fractal structure is strongly reminiscent of microphotographs of the pure kaolinite mineral structure.

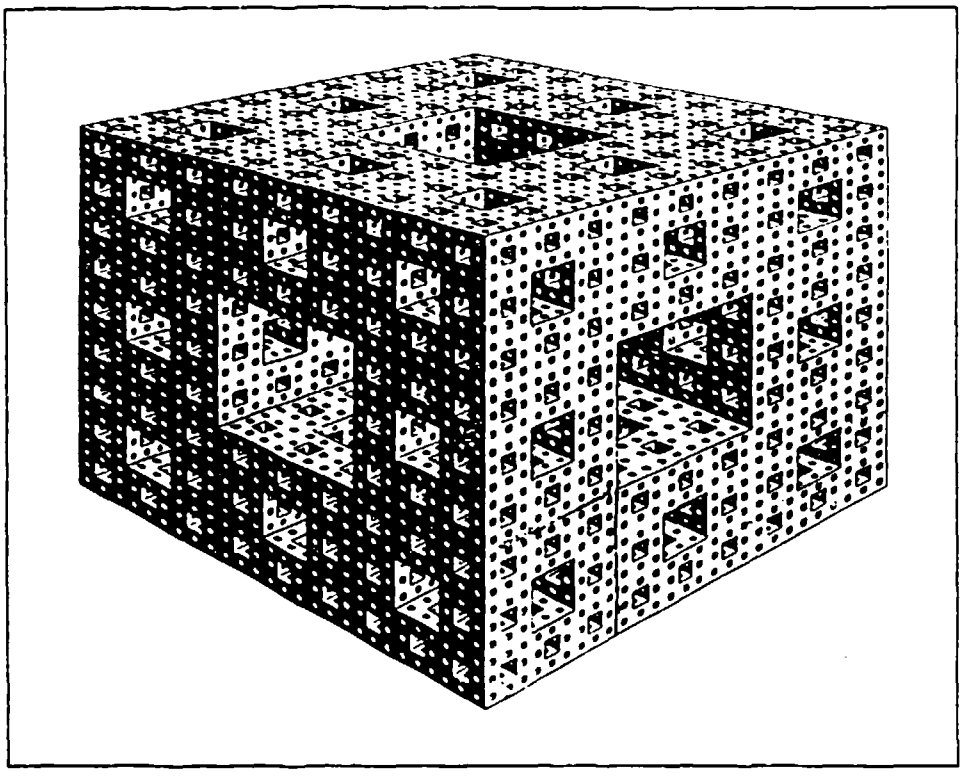

Figure C3. Menger sponge, fractal dimension 2 7268 (from Mandelbrot (1983))

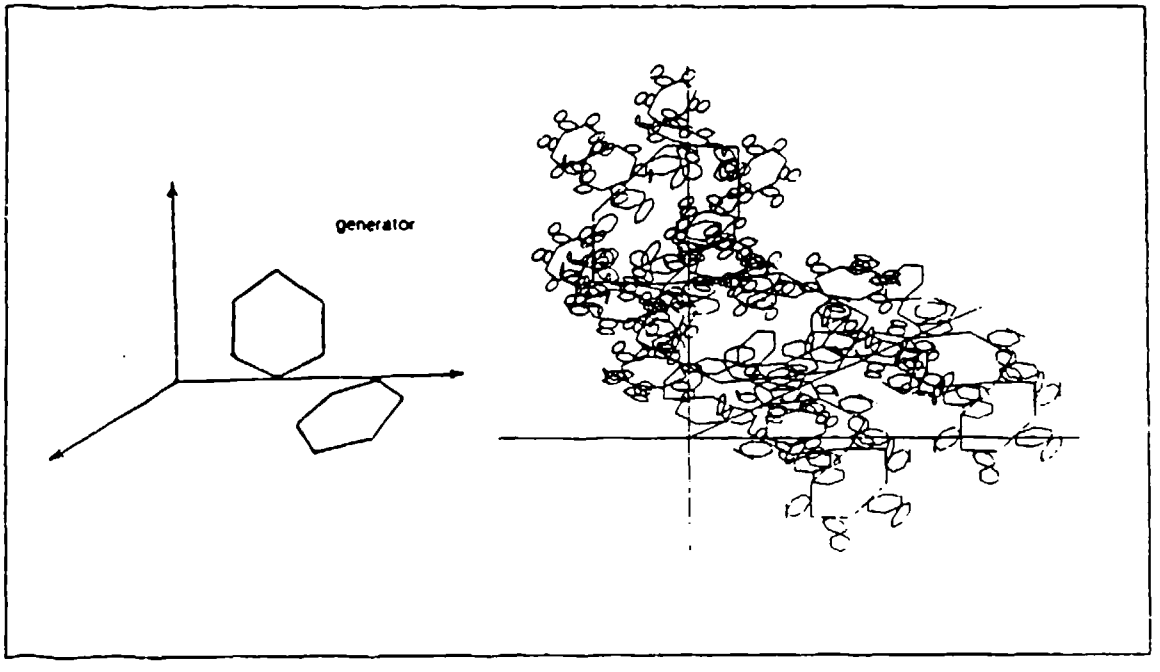

Figure C4. Fractal representation of soil fabric (from Moore and Krepfl (1991))

REPORT DOCUMENTATION PAGE

Form Approved
OMB No 0704-0188

1. AGENCY USE ONLY (Leave blank)	2. REPORT DATE	3. REPORT TYPE AND DATES COVERED
	December 1993	Report 1 of a series

4. TITLE AND SUBTITLE
Microwave Dielectric Behavior of Soils; Report 1, Summary of Related Research and Applications

5. FUNDING NUMBERS

6. AUTHOR(S)
John O. Curtis

7. PERFORMING ORGANIZATION NAME(S) AND ADDRESS(ES)
U.S. Army Engineer Waterways Experiment Station
Environmental Laboratory
3909 Halls Ferry Road, Vicksburg, MS 39180-6199

8. PERFORMING ORGANIZATION REPORT NUMBER
Technical Report
EL-93-25

9. SPONSORING/MONITORING AGENCY NAME(S) AND ADDRESS(ES)
U.S. Army Corps of Engineers, Washington, DC 20314-1000

10. SPONSORING/MONITORING AGENCY REPORT NUMBER

11. SUPPLEMENTARY NOTES
Available from National Technical Information Service, 5285 Port Royal Road, Springfield, VA 22161.

12a. DISTRIBUTION/AVAILABILITY STATEMENT
Approved for public release; distribution is unlimited.

12b. DISTRIBUTION CODE

13. ABSTRACT (Maximum 200 words)

As a precursor to developing a well-documented database of complex electrical properties of soils as a function of signal frequency, sample moisture, sample temperature, and soil type, a comprehensive study of existing data collection methodology and analytical modeling was undertaken. Of particular utility are chronological tables of experimental and analytical milestones as well as an extensive reference list. Several appendices are included that are helpful in understanding soil-electromagnetic wave interactions and new concepts in modeling soil structure.

14. SUBJECT TERMS
Complex dielectric constant; Microwave; Soil
Conductivity; Permittivity

15. NUMBER OF PAGES
116

16. PRICE CODE

17. SECURITY CLASSIFICATION OF REPORT	18. SECURITY CLASSIFICATION OF THIS PAGE	19. SECURITY CLASSIFICATION OF ABSTRACT	20. LIMITATION OF ABSTRACT
UNCLASSIFIED	UNCLASSIFIED		